University of Montana
ScholarWorks at University of Montana

Graduate Student Theses, Dissertations, & Professional Papers

Graduate School

2009

Biogenesis, Assembly and Intracellular Trafficking of Junin Arenavirus Envelope Glycoprotein Complex

Sudhakar Srinivasarao Agnihothram
The University of Montana

Follow this and additional works at: https://scholarworks.umt.edu/etd
Let us know how access to this document benefits you.

Recommended Citation
Agnihothram, Sudhakar Srinivasarao, "Biogenesis, Assembly and Intracellular Trafficking of Junin Arenavirus Envelope Glycoprotein Complex" (2009). *Graduate Student Theses, Dissertations, & Professional Papers*. 96.
https://scholarworks.umt.edu/etd/96

This Dissertation is brought to you for free and open access by the Graduate School at ScholarWorks at University of Montana. It has been accepted for inclusion in Graduate Student Theses, Dissertations, & Professional Papers by an authorized administrator of ScholarWorks at University of Montana. For more information, please contact scholarworks@mso.umt.edu.

BIOGENESIS, ASSEMBLY AND INTRACELLULAR TRAFFICKING OF JUNIN ARENAVIRUS ENVELOPE GLYCOPROTEIN COMPLEX

By

SUDHAKAR AGNIHOTHRAM

Masters of Engineering (Biotechnology), Birla Institute of Technology and Sciences, Pilani, India, 2002.

Dissertation

presented in partial fulfillment of the requirements
for the degree of

Doctor of Philosophy
in Molecular Biology

The University of Montana
Missoula, MT

Fall 2008

Approved by:

Dr. Perry Brown
Associate Provost, Graduate School

Dr. Jack H. Nunberg, Chair
Montana Biotechnology Center

Dr. J. Stephen Lodmell
Division of Biological Sciences

Dr. Mark L. Grimes
Division of Biological Sciences

Dr. Michele A. McGuirl
Division of Biological Sciences

Dr. David J. Poulsen
Department of Biomedical and Pharmaceutical Sciences

Biogenesis, Assembly and Intracellular Trafficking of Junin Arenavirus Envelope Glycoprotein Complex.

Chairperson: Jack H. Nunberg, Ph.D.

An unusual feature in the arenavirus envelope glycoprotein complex (GP-C) is the presence of a myristoylated stable signal peptide (SSP) in addition to the receptor binding subunit G1 and the transmembrane fusion subunit G2. Genetic studies were employed to understand the structure-function of the GP-C complex, with emphasis on elucidating the role of SSP in arenavirus life cycle. We present genetic evidence that support the inclusion of G2 as a member of Class I viral fusion protein, where membrane fusion is mediated by six-helix bundle structure as in HIV and Influenza viruses. Furthermore, we have identified crucial roles for SSP in the GP-C complex. In the mature glycoprotein complex, SSP assumes a bitopic membrane topology with both its N and C termini in the cytosol, and a short ectodomain loop. This membrane orientation allows it to mask the endogenous endoplasmic reticulum retrieval signals in the cytoplasmic tail of G2 thereby allowing the transit of fully assembled GP-C complex through the Golgi to the cell surface. SSP also interacts with the ectodomain of G2 on the outer surface of the membrane. This interaction is critical in modulating the pH at which the membrane fusion is activated. The SSP-G2 pocket has been identified as the target of newly discovered small-molecule inhibitors of arenaviral entry. Beyond its role in intracellular trafficking and pH-dependent membrane fusion of GP-C complex, SSP might be involved in virus assembly and budding. Studies employing immunogold electron microscopy indicated that GP-C complex clusters into microdomains of 120 nm size independent of other viral proteins. Clustering of GP-C into membrane microdomains is neither influenced by SSP myristoylation nor by the co-expression of the matrix protein Z. Regions of plasma membrane containing Z not co-localize with GP-C containing microdomains. Clustering of proteins or lipids on the plasma membrane may bring Z and GP-C together at the virus budding sites. Taken together, these data have contributed to the understanding of the unique subunit organization in GP-C complex and the mechanisms underlying efficient co-ordination of these subunits to execute significant functions in the arenavirus life cycle.

TABLE OF CONTENTS

LIST OF FIGURES

CHAPTER ONE

INTRODUCTION

1. Arenavirus disease and treatment

The Arenaviridae family encompasses a large group of enveloped negative-strand RNA viruses. The species in the arenaviridae family have co-evolved and diversified with their respective rodent host (33, 152). A majority of the arenavirus species are non-pathogenic to humans, but some viruses can be transmitted to humans to cause severe acute hemorrhagic fevers. Recurring outbreaks are common in regions of arenavirus endemicity, and therapeutic options to combat arenavirus infection are limited. Phylogenetic analyses divide the arenaviruses into the Old World (OW) species, such as Lassa fever virus (LASV) and Lymphocytic choriomeningitis viruses (LCMV), and the New World (NW) species, such as Junín virus (JUNV) and Machupo virus (MACV) . Up to 300,000 infections with Lassa fever (LASV) virus occur annually in Africa (122), and outbreaks of New World viruses in the Americas are sporadic but routine (122). Recently, infections by LCMV in transplant recipients have been reported (28). Prophylactic vaccines are not available and treatment options are limited. Ribavirin, a non-specific antiviral drug, is currently used with mixed results in patients (170). Early administration of human convalescent antiserum has been shown to be effective in case of Argentine hemorrhagic fever caused by Junín virus. In the absence of licensed prophylaxis or treatment, the hemorrhagic fever arenaviruses remain an urgent public health concern. Research over the past years has shed light on the notion that viral binding and entry is an attractive target for the development of antiviral therapeutics. Currently used inhibitors

and neutralizing antibodies demonstrate the clinical utility of targeting viral envelope glycoproteins in antiviral drug development (46, 73, 86, 127, 144, 165, 180, 182). Thus, understanding the structure and function of arenavirus envelope glycoprotein (GP-C) is critical for designing antiviral strategies that target arenavirus entry and prevent infection and my dissertation research has contributed several important findings in this regard.

2. Description of the virion and its life cycle

The arenavirus genome contains two single-stranded RNA molecules that encode for ambisense expression for four viral proteins (21, 34). The S RNA (~ 3.4 Kb) is transcribed to a genomic-sense mRNA which then is translated into envelope glycoprotein precursor, whereas the nucleoprotein is translated from the anti-genomic sense mRNA. Similarly, the LRNA (~ 7.2Kb) encodes for the matrix protein (Z) and the RNA dependent RNA polymerase (RDRP) (L) using the ambisense strategy. The L protein and the N protein encapsidate the genome, forming the Ribonucleoprotein core (RNP). The Z matrix protein is myristoylated and drives the budding of virus-like particles (VLPs) on its own (140). Myristolation of Z is essential for membrane association and formation of arenavirus VLPs (25, 142). The envelope glycoprotein exists as a tripartite complex containing the receptor binding subunit G1, transmembrane fusion subunit G2 and the stable signal peptide (SSP). The life-cycle of the virus is initiated by binding of G1 (receptor binding subunit) of GP-C to the receptor on the cell-surface. Transferrin receptor-1 is the receptor for the pathogenic NW arenaviruses, (147, 148) whereas the OW viruses utilize α-dystroglycan or an unknown receptor (58, 161).

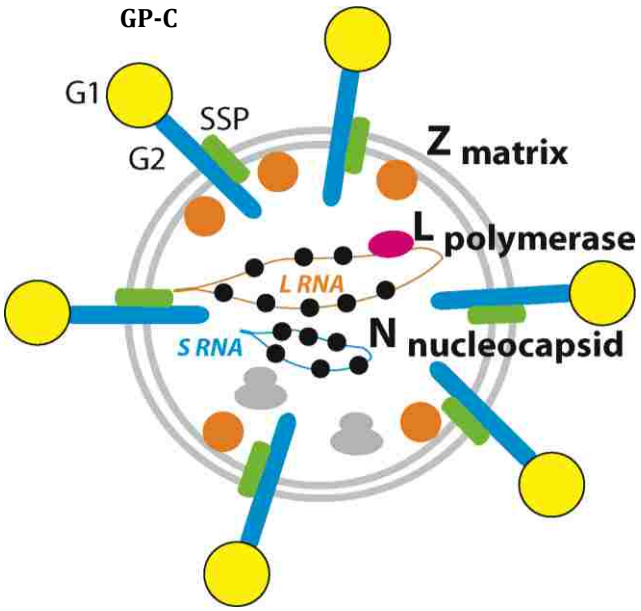

Figure 1. Schematic of an arenavirus virion.

The lipid envelope bilayer derived from the plasma membrane of the host cell is indicated as a grey circle. The envelope surrounds the ribonucleoprotein core, where the RNA is encapsidated by nucleoprotein (black circles) and the RNA-dependent RNA polymerase L (pink circle). The matrix protein Z (orange circles) is attached on the lower leaflet of the envelope and is in close apposition with the GP-C complex. The GP-C complex anchored in the lipid envelope forms the spike of the virion. The receptor binding subunit G1 (yellow circle) is exposed on the surface of the virion and mediates receptor recognition, binding and entry. The blue stalk below G1 that spans the lipid membrane represents transmembrane fusion subunit G2, which mediates the fusion of viral and endosomal membranes. The stable signal peptide (SSP) represented as a green stalk remains non-covalently associated with the G2 subunit.

Upon binding to the receptor, the virion is endocytosed and delivered to the late endosomal compartment, where fusion between the viral and endosomal membrane is activated by acidic pH (15, 26, 43). The OW viruses including LCMV and LFV utilize a novel cholesterol-dependent pathway which is independent of clathrin, caveolin, and lipid rafts (146, 151). The NW Junín virus is endocytosed via a clathrin-dependent pathway where the virions get trafficked to late endosome (116). Following endocytosis, the virion is subjected to progressive acidification of the endosomal compartment where the membrane-fusion activity of GP-C is activated by low pH (42, 43). GP-C belongs to Class-I viral fusion proteins ((57, 183) and described in detail in **Chapter 2**)) wherein membrane fusion is mediated by a stable six-helix bundle structure, formed by the structural reorganization of the transmembrane fusion subunit either upon receptor binding (as in retro- and paramyxoviruses) or by low pH in the endosome (as in orthomyxoviruses). Membrane fusion leads to deposition of the viral core in the cytoplasm, initiating virus replication and transcription (15, 27, 42, 43). Arenavirus particles assemble and bud at the plasma membrane and the current paradigm suggests that the matrix protein Z might mediate the interaction between the envelope glycoprotein complex (GP-C) and the RNP core, on the cytoplasmic face to facilitate arenavirus morphogenesis.

3. Envelope glycoproteins and their significance

The envelope glycoproteins are anchored on the lipid bilayer derived from the host cell during virus budding, and they play a major role in the life cycle of enveloped viruses. Several important stages in the virus life cycle including receptor recognition and binding, entry into the host cell, and fusion of viral and host cell membrane to facilitate

infection, are dictated by the viral envelope glycoproteins. They also play a crucial role in virus assembly and budding by interacting with host cell proteins (31) and other viral structural proteins. Because of their widespread roles in the virus life cycle, envelope glycoproteins are important from the perspective of antiviral therapeutics. In particular, the involvement of envelope glycoproteins in receptor binding and membrane fusion make them significant targets of neutralizing antibodies or small molecule inhibitors designed to prevent viral entry. Strategies along this line have shown some promise in preventing virus infection in many enveloped viruses including HIV and Influenza (8, 138).

3. a. Classes of viral fusion proteins

Based on the structural features, the envelope glycoproteins have been grouped into three major classes in the context of mediating membrane fusion.

1. Class I fusion proteins e.g., Orthomyxovirus - Influenza HA2, Retroviridae (85) - HIV-1 gp41, and Coronaviridae - Mouse hepatitis virus S2 proteins (85).

2. Class II fusion proteins e.g. Flaviviruses - E protein of Dengue virus, Togaviridae - E1 protein of Semliki forest virus (84).

3. Class III fusion proteins e.g. G protein of Vesicular Stomatitis Virus (VSV)

In Class I fusion proteins, membrane fusion is promoted by the α-helical core of a trimer-of-hairpins structure formed by the refolding of N- and C-terminal heptad-repeating hydrophobic residues, either upon activation by receptor binding at neutral pH (e.g., HIV-1), or by exposure to the acidic pH in the endosome (e.g., Influenza). The viral and the

cellular membrane are brought into opposition by the formation of this stable six-helix bundle structure, which also provides the driving energy for membrane fusion.

Below is an illustration of proposed sequence of membrane fusion in Influenza haemagglutinin, which represents a well studied model for class I viral fusion proteins. This figure and the figure legend are adopted from a review article "Viral membrane fusion" by Stephen C Harrison, Nature Structural and Molecular Biology, Vol 15 (7) 2008. The figure provides a visual understanding of the sequence of conformational changes that are proposed to happen in Class I viral fusion proteins, and enables the reader to appreciate the rationale behind the genetic studies described in chapter 2. The illustration also provides a platform to correlate how the results of the experiments described in chapter 2 may be significant in the process of membrane fusion in arenaviruses.

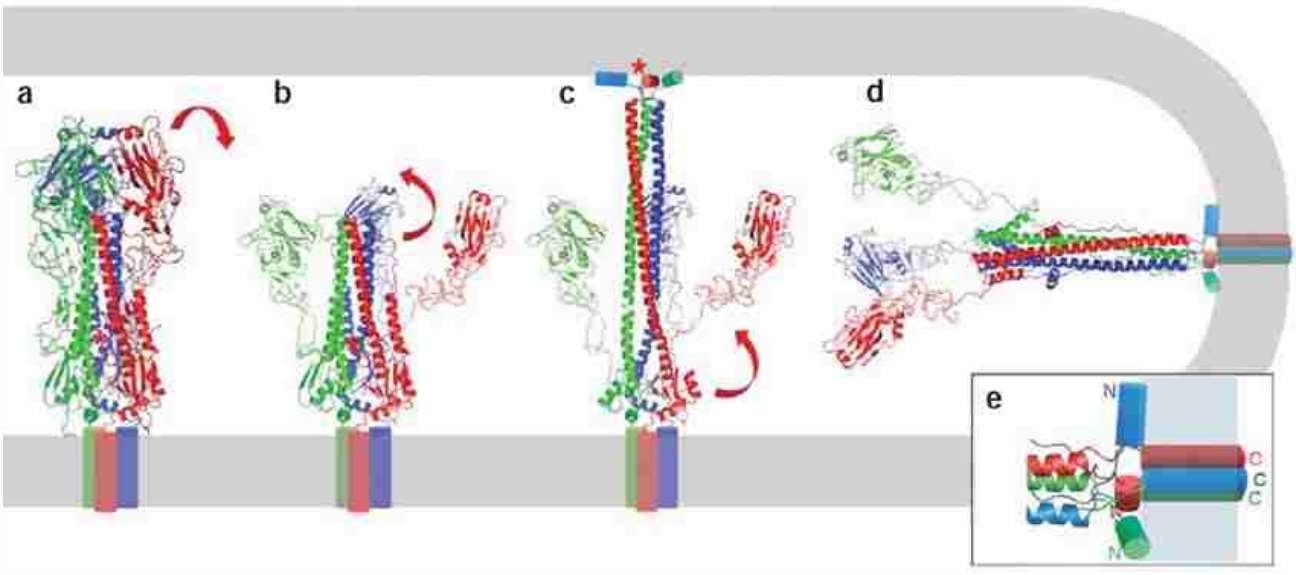

Figure 2. Influenza virus hemagglutinin: proposed sequence of fusogenic conformational changes.

(**a**) The pre-fusion conformation. Each subunit is shown in a different color. The binding site for the receptor, sialic acid, is at the top of each subunit, but contact with a receptor molecule is not shown. Red asterisk, the sequestered fusion peptide of the red subunit, at the N terminus of HA2. (**b**) HA1 dissociates from its tightly docked position in response to proton binding. Each HA1 remains flexibly tethered to the corresponding HA2 by a disulfide bond (near the bottom of the ectodomain, in the orientation shown here). (**c**) The extended intermediate. The loop between the shorter and longer helices in HA2 (for example, the two red helices and the loop connecting them, in **b**) becomes a helix, thereby translocating the fusion peptide toward the target membrane. The fusion peptides (asterisk) are shown interacting as amphipathic helices with the target bilayer. The loop-to-helix transition creates a long, three-chain coiled coil at the core of the trimer. (**d**)

Collapse of the extended intermediate to generate the post-fusion conformation. The lower parts of the protein (as seen in the orientation in **c**) fold back along the outside of the three-chain coiled coil. The collapse is complete only when the two membranes have fused completely. The post-fusion conformation is shown in a 'horizontal' orientation. (**e**) Detail illustrating some features of the membrane-proximal region of influenza virus HA2 after fusion is complete. The N termini of the coiled-coil helices are capped by contacts with amino acid residues in the link between the fusion peptide and the coiled coil, as well as with residues near the C terminus of the ectodomain, proximal to the transmembrane helices. This cap locks into place all the membrane-proximal components of the structure (32). The fusion peptides at the N termini of three HA2 chains are shown as cylinders (possible amphipathic helices) lying partly immersed in the outer leaflet of the membrane bilayer, as suggested by NMR and EPR studies (75). The transmembrane segments, likely to be α-helices, are also shown as cylinders. The relationships in this drawing among the fusion peptides and the transmembrane helices, chosen to illustrate the scale of the structures and the approximate distances between them, are purely schematic, as there is no single structure yet determined experimentally that contains all the elements included here. Only the crystallographically determined components are in ribbon representation.

In Class II proteins, membrane fusion is promoted by the formation of trimer-of-hairpins structure composed of stable β-sheet structure, as in E protein of flaviviruses and E1 protein of the Semliki forest virus, an alphavirus (84, 85). Protonation in the endosomal compartment leads to oligomeric rearrangement in Class II fusion proteins (5, 176, 177). This is followed by the conversion of metastable prefusion dimer to a more stable

homotrimer (72, 162) which is inserted into the target membrane leading to membrane fusion (61, 62).

Examples of Class III fusion proteins are the envelope proteins of Rhabdovirus, e.g., Vesicular stomatitis virus and Rabies virus, where the homotrimeric membrane fusion protein G mediates fusion in a low-pH-dependent reaction. The hydrophobic region of the fusion protein G is inserted in the membrane and subsequent conformational changes drive the fusion of viral and endosomal membrane (68). Proteolytic processing of the fusion protein G is not required for membrane fusion and G is not synthesized along with a companion protein. Moreover, the conformational changes induced by low pH are reversible in G. Both of these features are not characteristic of either the Class I or Class II fusion proteins (85) and there are no structural similarities of G with Class I and II proteins, making it a member of a distinct third class of viral fusion proteins.

3. b. Assembly and intracellular trafficking of envelope glycoproteins

Characterization of biogenesis, assembly and intracellular trafficking of an envelope glycoprotein is an integral component in understanding its role in the viral life cycle. These studies not only aid in the identification of subunit organization in the envelope glycoprotein complex but also provide insight on how these individual subunits coordinate together to control the function of glycoprotein complex. Viruses encode specific determinants in their glycoproteins that enable them to interact with the host factors and mediate intracellular trafficking and assembly. Identifying these host factors will further broaden our understanding on how viruses evolve to utilize these regulatory mechanisms to their advantage. For instance, the cytoplasmic tail of the spike protein of

the severe acute respiratory syndrome coronavirus (SARSCoV) contains a novel dibasic motif (119). This motif was found to interact with the host coatomer protein 1(COP1) and prevent the trafficking of the spike protein through the Golgi to retain it in the endoplasmic reticulum (ER)-Golgi intermediate (ERGIC) compartment, which is the site of coronavirus assembly and budding (24). On the contrary, in bunyaviruses the Gc envelope glycoprotein is retained in the endoplasmic reticulum (ER) by means of a basic amino acid cluster (74) and the association with the Gn glycoprotein enables the trafficking of the Gn-Gc complex to the Golgi compartment, where the progeny virions assemble and virus budding occurs (69, 74, 157). These observations highlight the use of cellular ER-Golgi trafficking machinery to control the assembly and transport of multimeric glycoprotein complexes during the virus life cycle. Knowledge gained from such studies broadens our understanding of molecular mechanisms involved in these processes and can help develop targets for antiviral therapy as shown in the inhibition of rubella virus release by inhibitors of exocytic pathway (145).

3. c. Membrane orientation in transmembrane envelope glycoproteins

Analyzing the topology of a transmembrane protein is essential to determine its organization across the lipid bilayer and utilize this information to decipher its function. Viruses are frugal in the use of their genetic material and hence encode proteins that are multifunctional. In viral proteins, every individual subunit serves a particular function and the topology of the protein might play a significant role in coordinating these functions efficiently. Thus, gaining information about the membrane topology of an envelope glycoprotein complex will help us to identify the function of individual subunits, since execution of a particular function demands a specific intracellular

localization. For instance, a proteoloytic processing step like a signal peptidase cleavage in a protein occurs in the ER lumen, whereas fatty acid modification of the same protein happens in the cytosol. These processes are essential for intracellular trafficking and membrane attachment of an envelope glycoprotein respectively, and regions of the protein that are located in the appropriate cellular localizations will serve as targets for these modifications. Studies that have established the polytopic membrane topology of hepatitis envelope glycoproteins E1 and E2 have been instrumental in explaining the multifunctional property of this protein including ER retention, signal sequence function, membrane anchoring and E1-E2 heterodimerizaion (134). These observations also assist in identifying the host factors that might interact with the glycoproteins to promote their functions. A recent report by Awe et al., has indicated the role of mammalian BiP in the translocation of hepatitis B envelope glycoprotein across the ER membrane (7).

3. d. Role of glycoproteins in assembly and budding of progeny virions

After gaining detailed information on essential biological processes such as biogenesis, assembly and intracellular trafficking of an envelope glycoprotein and identifying its membrane topology, the next obvious research question would be to apply these facts to investigate the role of envelope glycoprotein in the virus life cycle. As discussed earlier, envelope glycoproteins play a significant role in several stages of viral lifecycle including receptor binding and membrane fusion, virus assembly and budding. Knowledge gained about the biochemical aspects of an envelope glycoprotein would be vital in deciphering its membrane fusion mechanism. Another significant step in the virus life cycle is the assembly and budding of progeny virions from the cell. Assembly refers to the localization of all the viral components at a specific intracellular compartment, where

interactions between the viral proteins then mediate virus assembly and budding. In enveloped viruses, structural proteins of the virus play a significant role in promoting assembly and budding. In particular, the membrane-associated matrix protein serves as the driving force for virion assembly and budding (29), and interactions of the matrix protein with the envelope protein and the ribonucleoprotein core are critical in the budding of progeny virions (29). Determinants for membrane targeting for the matrix and envelope proteins are dictated by the amino acid clusters, or could arise as a result of post translational modification such as acylation. Viruses bud from various intracellular compartments such as the membranes of ER, and Golgi e.g., Mouse hepatitis virus and Hepatitis virus B, or from the plasma membrane e.g., Human Immunodeficiency virus-1 (HIV-1), Simian virus 5 (SV5). Several viruses that bud from the plasma membrane employ lipid raft microdomains that serve as platforms for interaction between the structural proteins of virus to mediate assembly and budding (10, (166). Association of the envelope glycoproteins with lipid rafts is dictated by the palmitoylation as in the case of HIV (12) and amino acid clusters in the cytoplasmic domain as in the case of Influenza virus (4). Similarly membrane association of the matrix protein can be mediated by myristoylation cooperating with a cluster of basic amino acid residues as in the case of Gag protein of HIV (4), or a stretch of α-helical hydrophobic residues as in the case of M1 protein of Influenza virus (66). Evaluating the role of the envelope glycoprotein in the virus life cycle involves identification of the determinants that might be involved in membrane targeting, interaction with other viral structural proteins and thereby mediating virus assembly and budding. These studies will benefit the design of antiviral strategies

from the perspective of blocking virus assembly, release and infection as shown in the case of HIV (102).

4. The unique tripartite organization of GP-C

Prior to the start of my dissertation research, the following facts were established about the arenavirus GP-C, which served as a useful tool in pursuing hypothesis-driven research aimed at understanding many crucial aspects of GP-C biology. Arenavirus GP-C is translated from a genomic-sense mRNA to generate a precursor polypeptide (Fig. 3) containing a signal peptide to target the nascent protein to endoplasmic reticulum (ER), where it is cleaved by cellular signal peptidase (SPase) (13, 117). In contrast to conventional signal peptides, arenavirus GP-C signal peptide is unusually long and stably included in the mature GP-C complex (52, 62, 188). The signal peptide is myristoylated at the N-terminus (63), which might have implications in membrane trafficking of GP-C. Following cleavage of the signal peptide (SSP), the precursor is anchored into the membrane via a C-terminal transmembrane domain with classical type I (N_{exo}/C_{cyto}) topology and glycosylated (20). Subsequent cleavage of the precursor at a highly conserved motif by cellular proprotein convertase subtilisin/kexin isozyme-1, also known as SKI-1/S1P (19, 53) in the cis/medial-Golgi compartment yields the receptor binding (G1) and transmembrane fusion subunit G2 (10, 90, 99). Proteolytic maturation is required for its membrane fusion activity (188).

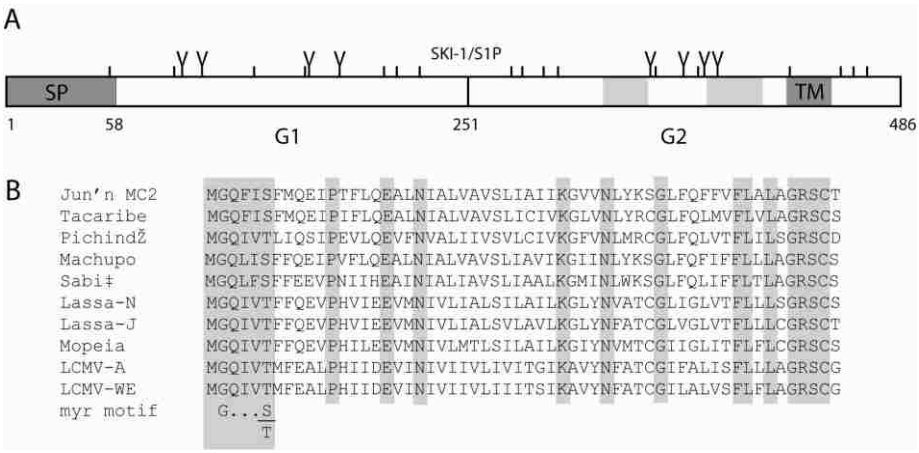

Figure 3. Schematic representation of the Junín virus GP-C glycoprotein and signal peptide (SSP).

(A) The Junín virus MC2 GP-C glycoprotein is depicted. Amino acids are numbered from the initiating methionine, and cysteine residues (|) and potential glycosylation sites (Y) are marked. The SP cleavage site (after amino acid 58) and the SKI-1/S1P cleavage site (after amino acid 251) and the resulting SP, G1 and G2 subunits are indicated. Within G2, the C-terminal transmembrane domain (TM) is shown, as are heptad-repeat regions (light gray shading) that may be involved in membrane fusion. The N termini of the arenavirus G1 and G2 glycoproteins have been previously determined experimentally (20, 22, 50, 99). (B) A comparison of the signal peptides of New World (Junín MC2 [accession no. D10072]), Tacaribe [accession no. M20304], Pichindé [accession no. M16735], Machupo [accession no. AY129248], and Sabiá [accession no. U41071] and Old World (Lassa-Nigeria [Lassa-N, accession no. X52400]), Lassa-Josiah [Lassa-J, accession no. M15076], Mopeia [accession no. M33879], LCMV-Armstrong [LCMV-A, accession no. M20869] and LCMV-WE [accession no. M22138] arenaviruses is shown. Identically conserved regions are highlighted, as is the conserved myristoylation (myr) motif G-X_3-S/T (150).

5. Significance of the research project

Arenavirus GP-C differs from other viral glycoproteins in that the mature GP-C complex retains SSP in addition to G1 and G2 subunits. My research project has employed genetic studies to understand the structure-function of GP-C complex, with special emphasis on investigating the role of the unique SSP subunit in the assembly, biogenesis and intracellular trafficking of GP-C complex. The following paragraphs are a narrative of research questions addressed in individual chapters. They provide the reader with an idea of how the findings described in the individual chapters collectively gain us an understanding of subunit organization of GP-C complex and its significance in the virus life cycle.

Studies described in Chapter 2 provide evidence that GP-C belongs to a member of Class - I viral fusion proteins (64) such as in retroviruses (e.g., HIV), orthomyxoviruses (e.g., Influenza virus), and filoviruses (e.g., Ebola virus). Membrane fusion in these envelope proteins is promoted by refolding of the N- and C-terminal heptad-repeat regions upon activation of the glycoprotein complex by receptor binding or exposure to low pH, to a form the α-helical core of a trimer-of-hairpins structure. Alanine scanning mutagenesis identified four positions in the N-terminal heptad repeat (**I333, L336, I347 and L350),** and two in C-terminal heptad repeat (**R392 and W395)** that contribute specifically in promoting pH-dependent membrane fusion by the Junín virus GP-C.

Chapter 3 illustrates the quality control mechanism evolved in arenavirus GP-C, where SSP masks the endogenous endoplasmic reticulum (ER) retention/retrieval signals in the cytoplasmic tail of G2 to ensure that the fully assembled GP-C complex is transported through the Golgi to cell surface for virion assembly. In the absence of SSP, G1-G2

precursor localizes to the ER and is not subjected to the proteolytic maturation by SKI-1/S1P protease in the Golgi. ER retention of the G1-G2 precursor is mediated by two dibasic ER retrieval (ERR) motifs in the cytoplasmic domain of G2. Association of SSP with transmembrane and cytoplasmic domains of G2 masks these endogenous signals and enables transport of fully assembled GP-C complex to the cell surface for virion assembly. Although this assembly-dependent control of intracellular trafficking has been reported in many cellular heteromultimeric protein complexes (41, 83, 101, 114) and other viral glycoproteins, this study was the first to report the involvement of a signal peptide in a quality control mechanism for protein folding and assembly. These findings also pointed out that SSP might play other important functions in the compartments beyond Golgi and at the plasma membrane, which might be critical for arenavirus life cycle.

Membrane orientation of SSP in the mature GP-C complex is critical for understanding the role of SSP in the GP-C complex. Chapter 4 demonstrates the membrane topology of SSP in the mature glycoprotein complex and reports the genetic determinants in SSP that determine its membrane orientation. Results described in Chapter 4 indicate that SSP assumes a bitopic membrane topology in the GP-C complex, with N and C termini in the cytosol and a central region forming a short ectodomain loop. These findings help to decipher a functional model for GP-C complex which is consistent with the results described in Chapter 3, that SSP interacts with the cytoplasmic tail of G2 to control intracellular trafficking of GP-C. The model also agrees with the other observations made in our laboratory, that interactions at the SSP-G2 interface on the outer surface of the membrane modulate the pH at which the membrane fusion is activated (187). Our model

of bitopic topology of SSP differs from the previously described reports for SSP of OW arenaviruses (51), and provide proof-of-concept for the function of GP-C complex of the NW arenaviruses. Furthermore, this model serves as a solid basis to understand the mechanism of action of small-molecule inhibitors of pH dependent membrane fusion and entry of NW hemorrhagic fever viruses (184). These studies suggest that the unique cytoplasmic face of GP-C, including the myristoylated SSP and the cytoplasmic tail of G2, plays a critical role in structure and function of GP-C complex. The observations also raise a possibility that the distinct subunit organization of GP-C complex might have implications in several stages of arenavirus life cycle including assembly and budding, which is examined in Chapter 5.

The hypothesis that myristoylation-dependent co-trafficking of GP-C and the matrix protein Z facilitates arenavirus assembly and budding, is investigated in Chapter 5. Studies employing Immunogold electron microscopy (IEM) and clustering analysis (18) indicate that GP-C is organized into membrane microdomains on the plasma membrane. SSP myristoylation does not impact the clustering of GP-C. Moreover, results from co-localization analysis point out that Z is not localized to GP-C containing microdomains. Taken together, these observations suggest a phenomenon that although GP-C and Z are not localized in the same microdomains, their interaction could be mediated by the clustering of proteins or lipids on the plasma membrane, leading to the formation of virus budding sites. A similar mechanism has recently been described in vesicular stomatitis virus (VSV) (167). These studies offer new insights on membrane organization of GP-C and Z that might underlie arenavirus assembly and budding. Employing the IEM system to analyze the GP-C mutants that exhibited interesting phenotypes in intracellular

trafficking (described in Chapter 3) would enable the dissection of the genetic determinants in GP-C essential for its organization into membrane microdomains.

Chapter 5 also describes the use of a reverse-genetic system (RGS) to study the role of GP-C in arenavirus morphogenesis and infectivity. In the reverse genetic system, all the four viral proteins (GP-C, Z, L and N) are expressed from the plasmids along with the minigenome that contains the luciferase reporter gene (MGLuc) in an antisense orientation with essential genetic elements for replication and transcription. Expression of the viral proteins and the minigenome leads to the generation of virus-like particles (VLPs) containing the RNP core with MGLuc. The VLPs are then transduced on to the target cells which express N and L to support the replication and transcription of the minigenome and thus the expression of luciferase reporter. Infectivity is then measured by quantitating the light units generated upon cleavage of a chemiluminiscent luciferase substrate. The RGS established for the OW LCMV (59) was adapted, and reproducible results were obtained as reported (60). JUNV-GP-C was shown to substitute LCMV GP-C in packaging the ribonucleoprotein core (RNP) of LCMV which includes a minigenome containing the luciferase reporter gene in an antisense orientation (MG-Luc). Furthermore, JUNV GP-C was efficient in transducing the luciferase signal to target cells, which is a measure of infectivity of the budding virus-like particles (VLPs). Proteolytic processing of JUNV GP-C was found to be essential for infectivity. This system will be utilized for future studies to investigate the genetic determinants in GP-C that are essential for its incorporation and arenavirus infectivity.

My dissertation research has contributed to gaining a detailed knowledge of the structure-function of GP-C complex. Genetic evidence suggesting the classification of GP-C as a

Class I fusion protein (57, 183), and the findings that identified the membrane organization of SSP (2) and its unique role in the assembly and intracellular trafficking of GP-C complex , are crucial in deciphering the function of GP-C complex. These studies also point out towards a working-model of GP-C complex, which benefits our understanding of the mechanism of action of newly discovered arenavirus entry inhibitors (94). Studies elucidating the membrane organization of GP-C and Z shed light on the process of arenavirus assembly and budding, a mechanism not described previously. Finally, the establishment of RGS to study the role of GP-C in arenavirus assembly and budding offers a great platform to identify determinants in GP-C, which are vital in arenavirus life cycle.

CHAPTER TWO

GENETIC ANALYSIS OF ARENAVIRUS ENVELOPE GLYCOPROTEIN-MEDIATED MEMBRANE FUSION

1. Abstract

The transmembrane fusion subunit G2 of GP-C includes two heptad-repeat regions of hydrophobic amino acid residues that are proposed to form a six helix bundle structure required for membrane fusion activity of Class I viral fusion proteins. Alanine-scanning mutagenesis was utilized to identify the role of these heptad-repeating regions, and in particular the significance of putative interhelical *a* and *d* position side chains was examined. All the mutant glycoproteins were expressed and transported to the cell surface. All but two mutants showed proteolytic cleavage by SKI-I/S1P and among the adequately cleaved mutants, four positions in the N-terminal heptad-repeat (I333, L336, I347 and L350**)** and two positions in the C-terminal heptad-repeat R392 and W395 were found to be critical determinants in mediating pH dependent membrane fusion. These findings indicate that arenavirus membrane fusion is likely mediated by the formation of α-helical coiled-coil structures, and support the inclusion of arenavirus GP-C among Class I viral fusion proteins as in HIV and Influenza viruses.

Studies described in this chapter were published in Virology and the citation is given below. I performed the genetic analysis for C-terminal heptad-repeating residues and Joanne York did the studies on N-terminal heptad-repeating residues.

York, J., S. S. Agnihothram, V. Romanowski, and J. H. Nunberg. 2005. Genetic analysis of heptad-repeat regions in the G2 fusion subunit of the Junín arenavirus envelope glycoprotein. Virology **343:**267-79.

2. Introduction

Arenaviruses are endemic in rodent populations worldwide and are transmitted to humans by exposure to infected animals. Infection by Old World arenaviruses such as Lassa virus, or New World species such as the South American group including Junín, Machupo and Guanarito viruses, are responsible for recurring and emerging outbreaks of viral hemorrhagic fevers with high mortality.

The mature envelope glycoprotein complex of the arenavirus consists of three noncovalently associated subunits derived from the GP-C precursor: a stable, myristoylated 58 amino-acid signal peptide (SSP), the receptor-binding G1 subunit and the transmembrane G2 fusion protein. Cleavage to generate SSP is likely mediated by the cellular signal peptidase and subsequent cleavage of the precursor to yield the mature G1 and G2 subunits is mediated by the cellular SKI-1/S1P protease. Proteolytic maturation is essential for pH-dependent membrane fusion.

Sequence analysis of the G2 ectodomain of Lassa virus and Lymphocytic choriomeningitis virus (LCMV) has revealed two heptad-repeat regions predicted to form amphipathic helices (35). This feature is commonly found among Class I viral fusion proteins such as those belonging to retroviruses, orthomyxoviruses, paramyxoviruses, filoviruses and coronaviruses.

The widely accepted model for membrane fusion by Class I viral envelope glycoproteins includes a series of conformational changes, initiated either upon receptor binding or exposure to low pH in the endosome. In the structural reorganization of the fusion subunit, the hydrophobic fusion peptide at the N-terminus is inserted into the cellular

membrane to form a protein bridge between the viral and cellular membranes. Subsequent collapse of the heptad-repeat regions forms a highly stable structure comprising a six-helix bundle.

This six-helix core involves a central coiled coil, formed by a trimer of N-terminal heptad-repeat regions surrounded by three anti-parallel helices of the C-terminal heptad repeats which bind to conserved hydrophobic grooves on the coiled-coil surface. Formation of this thermodynamically favored six-helix bundle brings the viral and cellular membranes into apposition and is thought to provide the driving energy to initiate membrane fusion. We hypothesized that the N- and C-terminal heptad repeating hydrophobic residues in the G2 ectodomain may be involved in fornation of six-helix bundle structure thereby mediating pH-dependent membrane fusion of GP-C. Here, we applied genetic methods to test this model of membrane fusion in the New World Junin arenavirus GP-C.

3. Results

Heptad-repeat regions are highly conserved among the arenavirus GP-C envelope glycoproteins

Sequence analysis of the ectodomain of the G2 subunit of Junin virus revealed heptad repeats of hydrophobic residues on the N and C terminus, which is characteristic of Class I virus fusion proteins as in HIV and Influenza viruses. To determine whether this sequence is conserved across all the arenaviruses, the amino acid sequences of heptad repeats were aligned between Old and New world arenaviruses, which demonstrated a high degree of conservation within the family, as shown below (Fig. 4, bottom panel).

The degree of hydrophobicity was maximized at interhelical *a* and *d* positions (Fig. 5) as shown in red circles, while assigning a register to proposed helical coiled coil of the heptad repeats (i.e. positions *a* through *g*). The examination of the aligned sequences revealed a unique register of *a* and *d* sequences that was apparent. In the N terminal helix, *a* and *d* positions consists of hydrophobic residues common to central interface of coiled-coil (e.g. leucine, isoleucine, methionine, and vainer). Polar or charged residues occupied the positions (b, c, and f positions) that were assumed to lie on the exterior face of the coiled-coil. The C-terminal heptad-repeat region showed a similar pattern which appears to end at C-terminal most *d* and *a* positions (K409 and D413 respectively). The analysis also shows that the hydrophilic residues at two *a* and d positions in the New world viruses (R392 and S399) are replaced by less polar amino acid residues in the Old World viruses (serine and alanine, respectively). The buried hydrophilic side chains may impart specificity to the process of coiled-coil folding at the expense of thermal stability (81, 111).

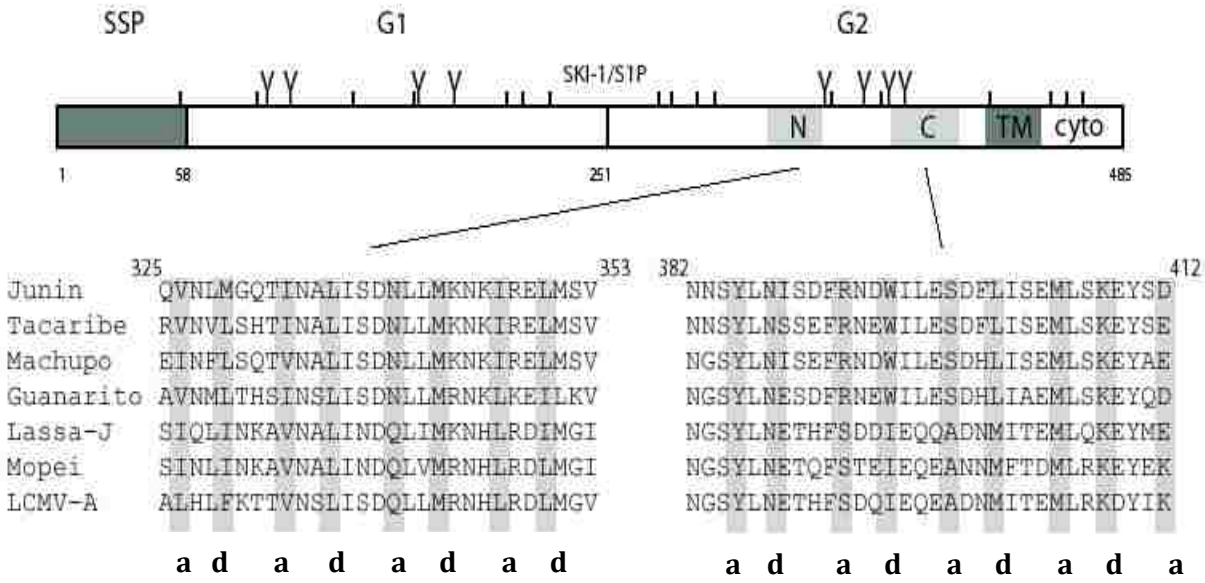

Figure 4. Heptad repeats of New World and Old World arenaviruses are aligned to demonstrate the high degree of conservation.

Top. **Schematic representation of the Junin virus GP-C.** Amino acids of the Junín virus envelope glycoprotein are numbered from the initiating methionine, and cysteine residues (|) and potential glycosylation sites (Y) are marked. The SSP and SKI-1/S1P cleavage sites, and the resulting SSP, G1 and G2 subunits are indicated. Within G2, the C-terminal transmembrane (TM) and cytoplamsic (cyto) domains are shown, as are the N- and C-terminal heptad-repeat regions (light gray shading).

Below. **N- and C-terminal heptad-repeats of arenaviruses**. The conservative and typically hydrophobic ***a*** and ***d*** positions are highlighted in light gray and indicated below.

Model of the proposed six-helix bundle

The six-helix structure involves a central coiled-coil, formed by a trimer of N-terminal heptad-repeat regions surrounded by three anti-parallel helices of the C-terminal heptad-repeats (Fig. 5A). The interhelical interactions are predominantly hydrophobic, with charged residues contributing to specificity (Fig. 5B). Formation of this thermodynamically favored six-helix bundle brings the viral and cellular membranes into apposition and is thought to drive membrane fusion.

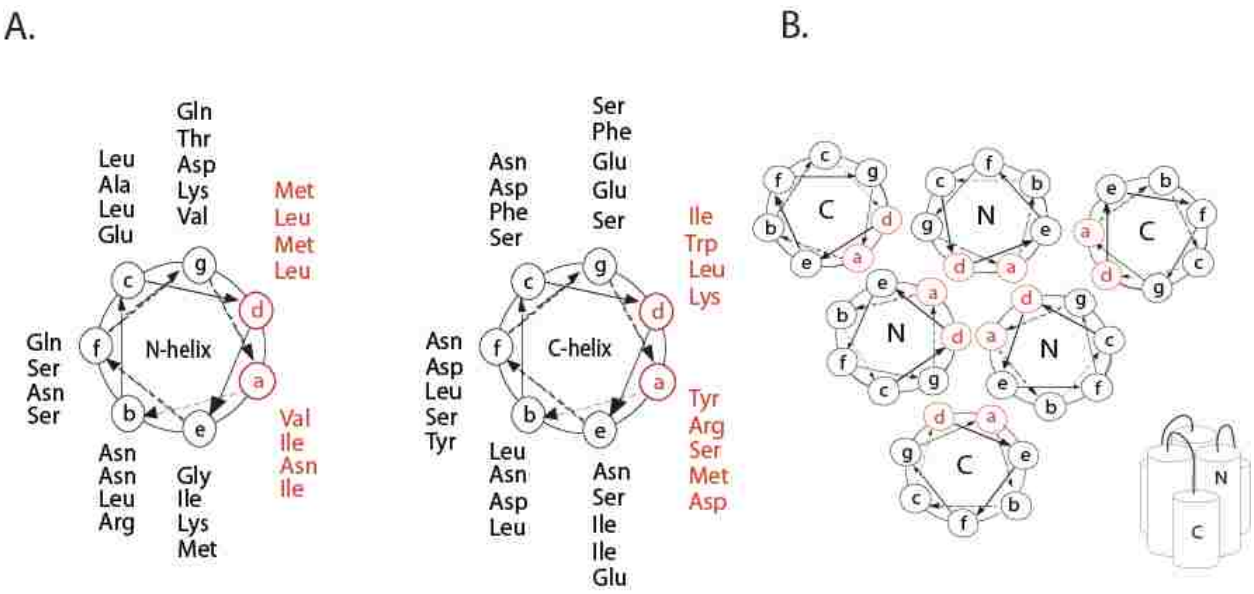

Figure 5. Helical wheel projections of proposed heptad-repeat periodicity.

A. Amino acids were placed in register to maximize hydrophobicity at *a* and *d* positions. These are highlighted in red.

B. A schematic of a six-helix bundle is at the lower right, and the details of the canonical interhelical packing arrangement are illustrated.

Expression of mutant GP-C envelope glycoproteins

To identify the role of proposed α-helical structures in promoting the pH dependent membrane fusion of arenaviruses, the heptad-repeating hydrophobic residues were subjected to scanning mutagenesis. Amino acids at the predicted *a* and *d* positions were individually changed to alanine, a small residue that is a good helix inducer yet contributes little to the hydrophobic forces that stabilize coiled-coil structures. Mutant GP-C`s were expressed in vero cells using the T7 promoter and a recombinant vaccinia virus encoding T7 polymerase, vTF7-3. Metabolically labeled glycoproteins were immunoprecipitated using the G1-specific MAb BF11 and separated using SDS-PAGE. The wild-type (wt) and SKI-1/S1P cleavage-defective (cd) glycoproteins are shown in Fig. 6 for comparison. All the mutant GP-C glycoproteins were expressed and cleaved by signal peptidase to generate the 5 kDa SSP (Fig. 6A). Majority of the mutant GP-C`s were proteolytically processed by SKI-1/S1P protease to generate mature G1 and G2 subunits (Fig. 6B). Mutants showed variation in the relative extent of SKI/S1-P cleavage, where some mutants (Y385A and L402A) had cleavage that was undetectable similar to the cdGP-C, while others exhibited reduced levels to levels greater than the wild type.

To quantitate the relative extents of SKI-1/S1P processing, the amount of radioactivity present in the mature G1 and G2 polypeptides and deglycosylated GP-C precursors (Fig. 6B) was determined using a Fuji 3000-G phosphorimager and Image Gauge software (Fuji). This analysis is shown in (Fig. 7). Mutants L336A, N340A, I388A, R392A, S399A, M405A and K408A were cleaved much as the wild-type glycoprotein (65-100% of wild-type). Several mutations in the N-terminal heptad-repeat region appeared to enhance proteolytic cleavage up to 2-fold (V326A, M329A, I333A, M343A and I347A).

Proteolytic maturation was essentially absent in the Y385A and L402A mutants, and significantly reduced in L350A and W395A (30 and 45%, respectively). In all these mutants, shedding of the G1 subunit in the cell culture supernatants correlated with the extent of proteolytic cleavage (data not shown).

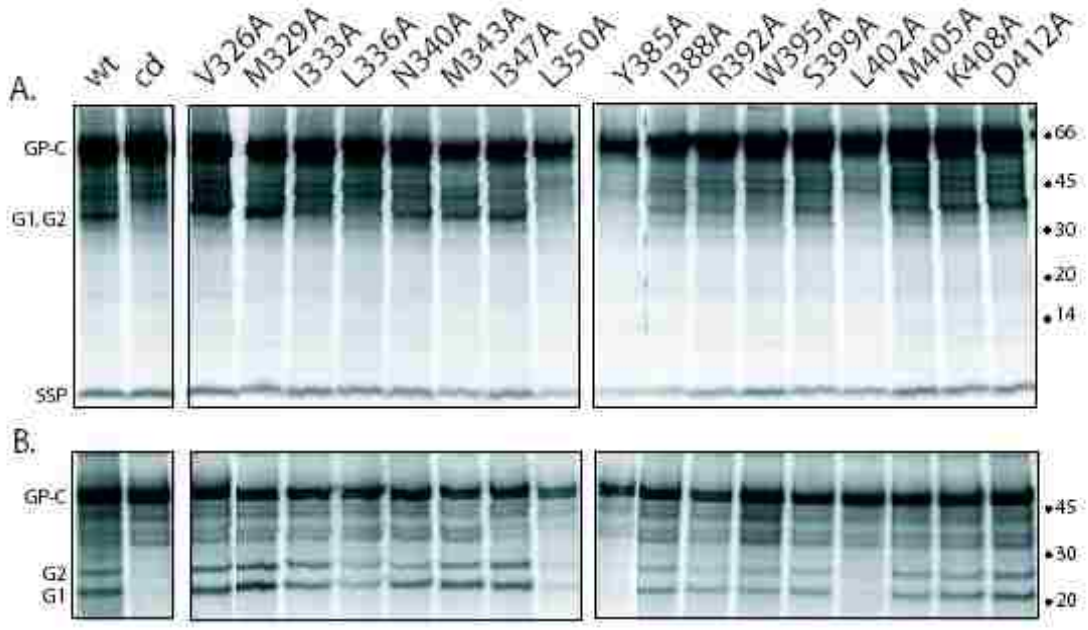

Figure 6. Expression of mutant GP-C proteins.

A. Phosphorimages of the immunoprecipated envelope glycoproteins separated on NuPAGE 4-12% Bis-tris gels. Molecular weights are indicated on the right.

B. Proteolytic cleavage by SKI-1/S1P is best resolved following deglycosylation using peptide: N-glycosidase F (PNGase F) in panel 2.

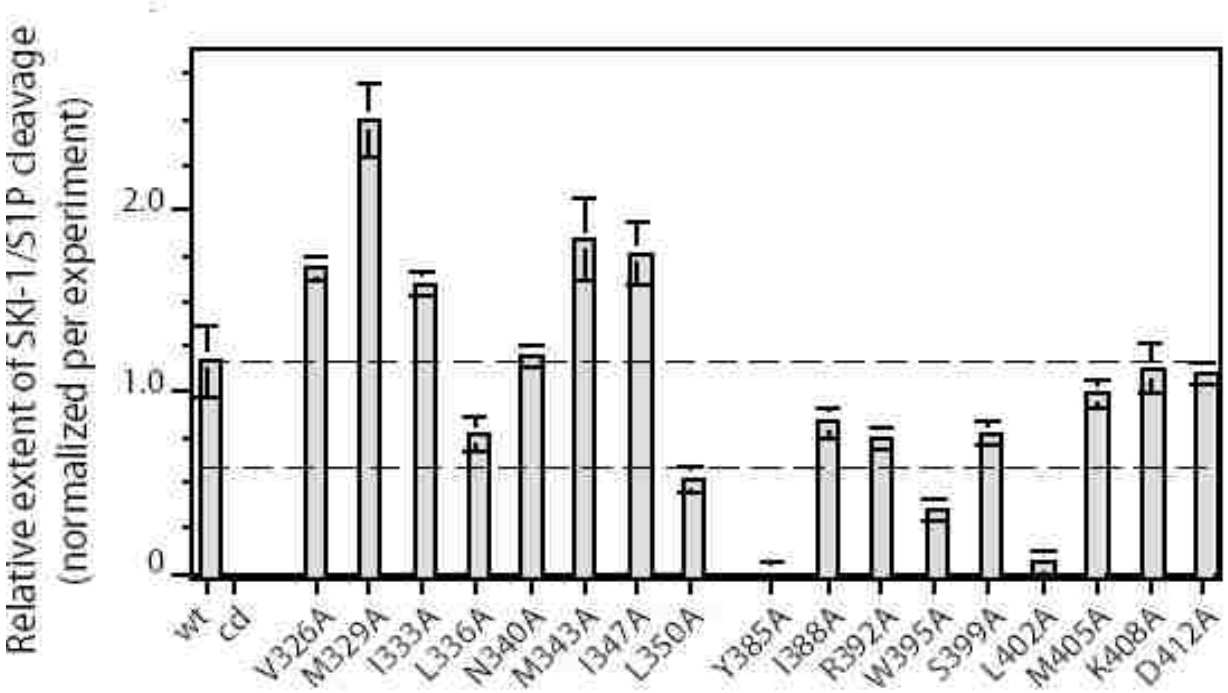

Figure 7. Quantitation of SKI-1/S1P cleavage and the formation of the mature G1 and G2 subunits.

Phosphorimages of the deglycosylated polypeptides were analyzed using Image Gauge software (Fuji) and the Profile and Background tools to quantitate the radioactivity (PSL units). The efficiency of SKI-1/S1P cleavage was defined as the ratio of PSL units in the sum of the G1+G2 peaks relative to the total number in both GP-C and G1+G2 peaks. Results were analyzed for two complete experiments. Because the absolute efficiency of cleavage varied between experiments, each experiment was normalized to determine the relative percentage of cleavage in each mutant. Error bars represent ± one standard deviation.

Mutations do not affect transport to the cell surface

Flow cytometry was used to determine cell surface expression of mutant envelope glycoproteins. Vero cells expressing wild type GP-C, cdGP-C, mock transfected and the alanines mutants were stained were immunostained using MAb BE08 and fixed with 2% formaldehyde. Two populations were discerned in cells transiently expressing GP-C: Cells that were expressing GP-C (≥30 fluorescence channel) and cells that escaped transfection (≤30fc). As the histograms indicate, proteolytic processing of GP-C was not essential for cell surface expression of GP-C as shown by the cdGP-C exhibiting cell surface expression similar to wild type GP-C. All mutants were expressed on the cell surface (Fig. 8**)** similar to the wild type GP-C, illustrating that the mutations at interhelical *a* and *d* positions did not affect transport to the cell surface. Our efforts to biochemically characterize the mutant GP-C`s on the cell surface was limited by the refractory nature of GP-C complex to covalent modification by biotinylation reagents. However, transport of these mutants through the Golgi to the cell surface indicates that the mutations did not affect the overall structural integrity in these mutants.

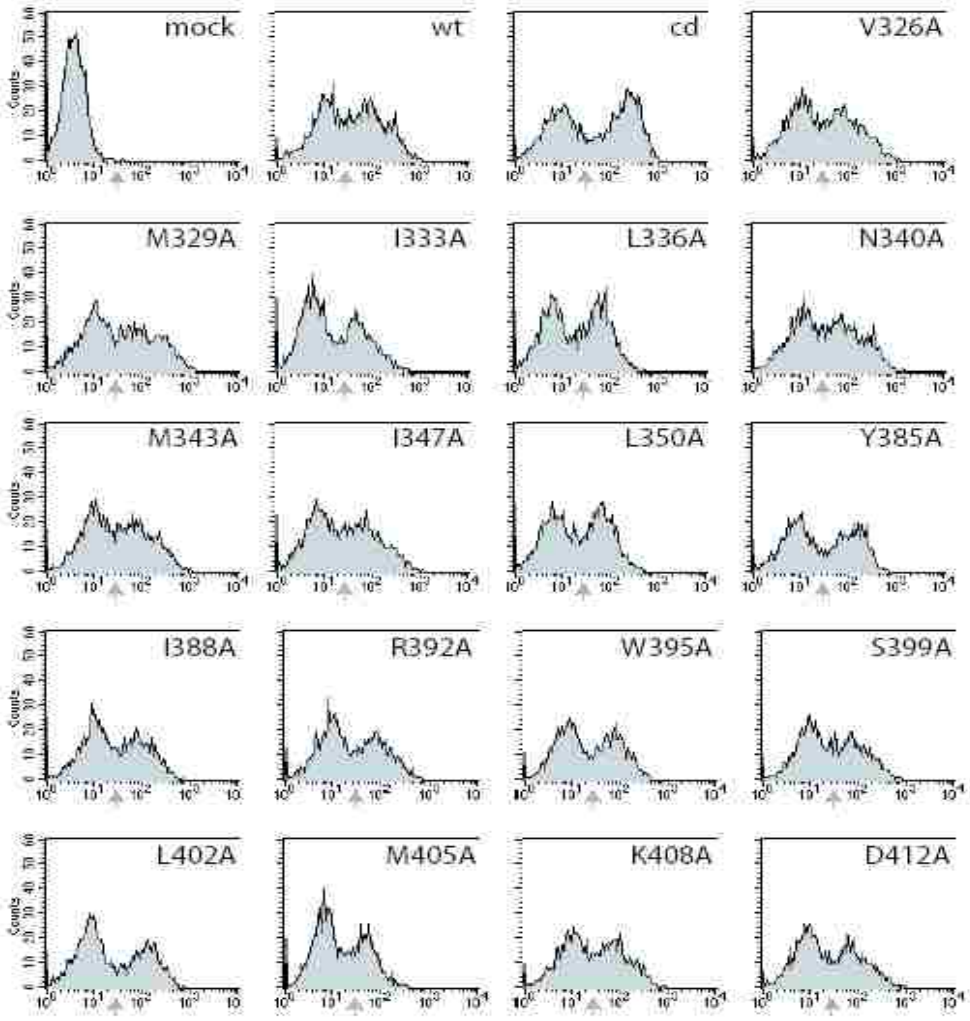

Figure 8. Flow cytometric analysis of cell-surface envelope glycoproteins.

Vero cells expressing the envelope glycoproteins were stained using the G1-specific neutralizing MAb BE08 and subsequently stained using propidium iodide to allow exclusion of dead cells in the population. Background staining of mock-transfected cells is shown in the first panel. The expressing cells within the transfected cultures were defined using a gate of ≥ 30 that included <0.1% of the mock-transfected population (arrow).

Mutations affect pH- dependent cell-cell fusion

The ability of the envelope glycoproteins to mediate pH-dependent cell-cell fusion was determined using the recombinant vaccinia virus-based β-galactosidase fusion-reporter assay (132, 186). Alanine substitutions at ***a*** and ***d*** positions had varying effects on cell-cell fusion (Fig. 9). Although several of the mutations did not affect cell-cell fusion, others resulted in the reduction from 50-95% of wild-type levels (I333A, L336A, I347A, L350A, Y385A, R392A, W395A and L402A. In all cases, cell-cell fusion required exposure of the culture to acidic (pH 5.0) medium.

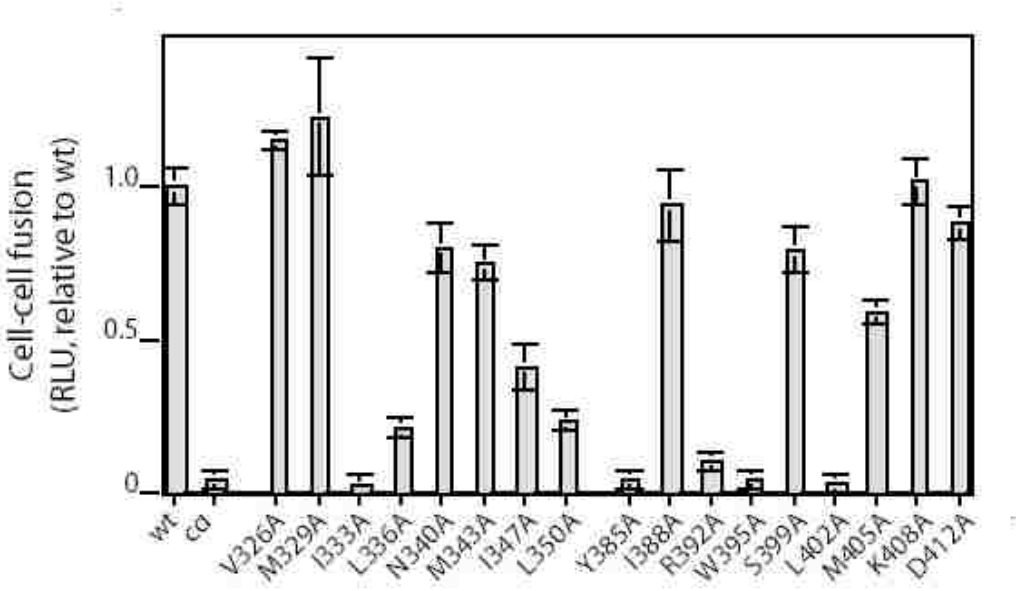

Figure 9. Fusogenic potential of wild-type and mutant envelope glycoproteins.

β-galactosidase activity induced upon cell-cell fusion was quantitated using the chemiluminescent substrate GalactoLite Plus (Tropix). Relative light units (RLU) were normalized to that of the wild-type GP-C control. Error bars represent ± one standard deviation among 6 replicate fusion cultures.

Relationship between cell-cell fusion and proteolytic cleavage

We have shown previously that proteolytic cleavage by SKI-1/S1P is essential for pH-dependent cell-cell fusion (186). In fact, the defects in cell-cell fusion by Y385A and L402A are likely due to the lack of proteolytic cleavage in these mutants. In several cases, however, mutants that displayed deficiencies in proteolytic cleavage showed cell-cell fusion activity similar to wild-type GP-C (*viz.*, I388A and S399A). By contrast, in other mutants, clear defects in membrane fusion arose despite wild-type levels of SKI-1/S1P cleavage (*viz.*, I333A and I347A).

These observations suggested that deficiencies in proteolytic cleavage alone could not account for the defects in cell-cell fusion. In order to more fully examine this point, we reconstructed the variable extents of proteolytic cleavage using mixtures of the wild-type and SKI-1/S1P cleavage-site mutant plasmids.

Although the total amount of envelope glycoprotein remained constant as the wild-type plasmid was diluted 1:3 and 1:9 with cd-JGPC (Fig. 10A**)**, the relative amounts of mature G1 and G2 decreased progressively, from 20% to 5% and 2%, respectively. Despite a 90% decrease in overall SKI-1/S1P cleavage, cell-cell fusion was unaffected (Fig. 10B). Within these limits, our measurements of cell-cell fusion appear not to be limited by the relative amount of proteolytically matured G1 and G2 glycoproteins, and we infer that mutants in which SKI-1/S1P cleavage is retained to at least 10% of the wild type levels can be considered informative in defining specific defects in membrane fusion.

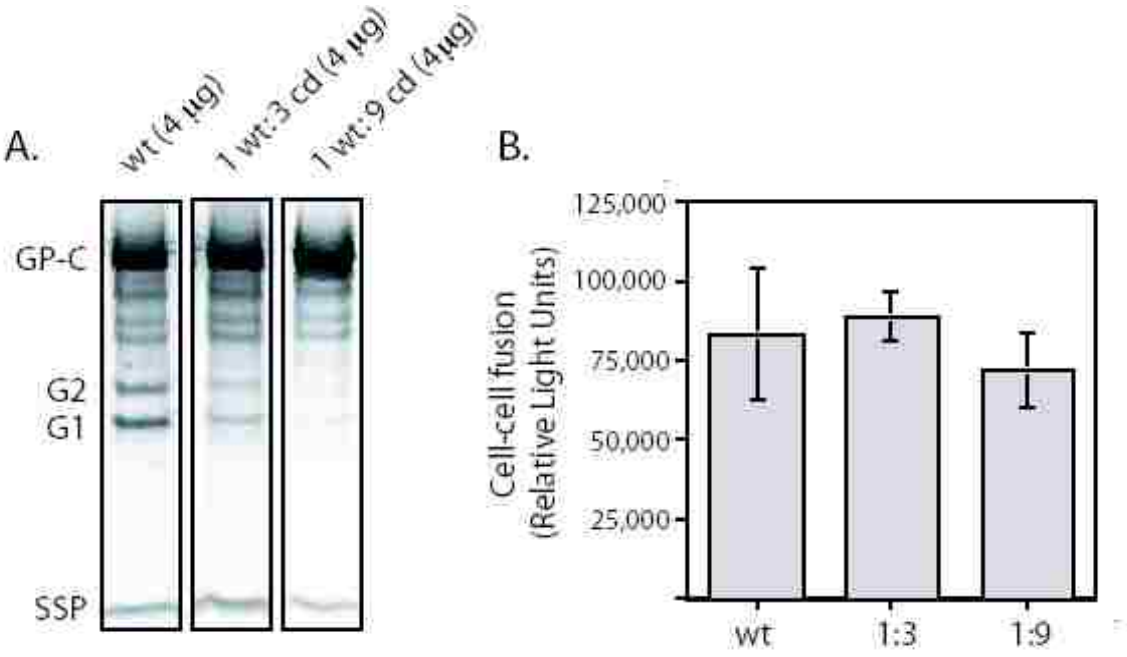

Figure 10. Reconstruction to determine the effect of variable SKI-1/S1P cleavage efficiency on envelope glycoprotein fusogenic potential.

A. Mixtures of metabolically labeled glycoproteins immunoprecipitated from the cell cultures transfected with DNA concentrations as mentioned on the top of each lane were separated on a NuPAGE 4-12% Bis-tris gels. Precursor GP-C and the matured G1 and G2 bands are indicated.

B**.** Bar graphs representing the fusion levels of GP-C in cell cultures transfected with wild-type and indicated mixtures of wild-type and cleavage-defective GPC.

4. Discussion

Taken together, these results identify several amino acid residues in the N- and C-terminal heptad-repeat regions in the G2 fusion subunit that are critical for the pH -dependent membrane fusion by GP-C. As shown in Fig. 10 B, the residues chosen for mutagenic analysis were modeled to lie at interhelical *a* and *d* positions, in view with the significance of these positions for the formation of coiled-coiled core. Alanine substitutions at these positions are often benign (112), and the pattern of fusion-deficient phenotypes with the mutants is consistent with the model, and the central role of α-helical coiled coil structure in promoting membrane fusion in Junín GP-C.

Many of the alanine mutants showed defects in the SKI-I/S1P proteolytic processing, possibly through structural changes that did not affect their trafficking to the cell surface. These mutations may imply the importance of these interhelical positions in folding of the native GP-C precursor during the biogenesis. In particular the results suggest that these defects in proteolytic maturation are not likely to account for the specific deficiencies in membrane effusion.

These studies provide the first genetic evidence to the model derived on the basis of amino acid analysis that membrane fusion in arenaviruses can be promoted by the formation of α-helical coiled-coil structure, as in other Class I viral fusion protein such as HIV and Influenza (64). Parallel evidence from our collaborator Dr. Min Lu (Weill Medical College of Cornell University) indicate that the peptides derived from N- and C-terminal heptad-repeat regions of Junin G2 refold to form six-membered trimeric structure with high level of helical content and thermal stability (unpublished). More specific details including limitations of N- and -C terminal α-helices and the mechanics

of interhelical interactions in the six-helix bundle, awaits structure determination at the atomic level.

Furthermore, this genetic evidence that supports the inclusion of GP-C as a Class I fusion protein opens up avenues towards the development of vaccines and small molecules that may block arenavirus infection. Peptides against C-terminal helical region of HIV gp41 that are shown to interfere with the membrane fusion step are in clinical use in the HIV treatment (87). Small molecule inhibitors and neutralizing antibodies that target the membrane proximal domain of gp41 ectodomain which is adjacently placed to the C-terminal heptad-repeat, are also shown to interfere with the membrane fusion in a similar manner (49, 61, 129, 163, 191). Structural and immunochemical studies of arenavirus GP-C in future no doubt will be useful in designing antiviral strategies that may help block arenavirus entry.

5. Materials and Methods

Alanine scanning mutagenesis

The amino acids at the predicted ***a*** and ***d*** positions of heptad-repeat regions of the Junin virus envelope glycoprotein were individually changed to alanine using QuikChange Mutagenesis (Stratagene). The GP-C gene of the pathogenic Junin virus isolate MC2 was used for these studies.

Expression of GP-C

The GP-C gene in a pcDNA 3.1 vector was expressed in Vero cells using the T7 promoter and a recombinant vaccinia virus encoding T7 polymerase vTF7-3 (63).

Analysis of GP-C biosynthesis and transport

Metabolically labeled glycoproteins were immunoprecipitated using the G1-specific MAb BF11 (153) and separated on NuPAGE 4-12% Bis-Tris gels. For analysis of cell surface expression, Vero cells expressing the envelope glycoproteins were stained using the G1-specific neutralizing MAb BE08 (70). Cells were fixed using 2% formaldehyde and analyzed using a FACSCalibur flow cytometer (BD Biosciences).

Analysis of pH-dependent cell-cell fusion

The ability of GP-C to mediate pH-dependent cell-cell fusion was determined using the recombinant vaccinia virus-based β-galactosidase fusion-reporter assay as described (186). In these studies, vero cells infected with vTF7-3 and expressing GP-C were co-cultured with vero cells infected with vCB21R-lacZ, a recombinant vaccinia virus expressing β-galactosidase under the control of the T7 promoter. After mixing of the GP-C expressing and target cells, the co-cultures were incubated for 5 hr prior to being subjected to a 30 min pulse of neutral or acidic (pH 5.0) medium. β-galactosidase expression, induced upon fusion of the effector and target cells, was detected after 5 hrs of continued cultivation at neutral pH, in cell lysates using the chemiluminescent substrate GalactoLite Plus (Tropix). Cell-cell fusion was quantified using a Tropix TR717 microplate luminometer.

CHAPTER THREE

ROLE OF THE STABLE SIGNAL PEPTIDE AND CYTOPLASMIC DOMAIN OF G2 IN REGULATING INTRACELLULAR TRANSPORT OF THE JUNÍN VIRUS ENVELOPE GLYCOPROTEIN COMPLEX

1. Abstract

Enveloped viruses utilize the membranous compartments of the host cell for the assembly and budding of new virion particles. In this report, we have investigated the biogenesis and trafficking of the envelope glycoprotein (GP-C) of the Junín arenavirus. The mature GP-C complex is unusual in that it retains a stable signal peptide (SSP) as an essential component in association with the typical receptor-binding (G1) and transmembrane fusion (G2) subunits. We demonstrate that, in the absence of SSP, the G1-G2 precursor is restricted to the endoplasmic reticulum (ER). This constraint is relieved by co-expression of SSP in *trans*, allowing transit of the assembled GP-C complex through the Golgi and to the cell surface, the site of arenavirus budding. Transport of a chimeric CD4 glycoprotein bearing the transmembrane and cytoplasmic domains of G2 is similarly regulated by SSP association. Truncations to the cytoplasmic domain of G2 abrogate SSP association yet now permit transport of the G1-G2 precursor to the cell surface. Thus, the cytoplasmic domain of G2 is an important determinant for both ER localization and its control through SSP binding. Alanine mutations to either of two dibasic amino acid motifs in the G2 cytoplasmic domain can also mobilize the G1-G2 precursor for transit through the Golgi. Taken together, our results suggest that SSP binding masks endogenous ER localization signals in the cytoplasmic domain of G2 to ensure that only the fully assembled, tripartite GP-C

complex is transported for virion assembly. This quality control process points to an important role of SSP in the structure and function of the arenavirus envelope glycoprotein.

* This chapter was taken from the paper published in Journal of Virology, selected for the "Spotlight" section in the same issue.

Agnihothram, S. S., J. York, and J. H. Nunberg. 2006. Role of the stable signal peptide and cytoplasmic domain of G2 in regulating intracellular transport of the Junin virus envelope glycoprotein complex. J Virol **80:**5189-98.

2.Introduction

Arenaviruses are endemic in rodent populations worldwide (152) and infection can be transmitted to humans to cause severe acute hemorrhagic fevers (121, 143). Recurring outbreaks are common in endemic regions, and therapeutic options to combat arenavirus infection are limited. Phylogenetic analyses divide the arenaviruses into the Old World species, such as Lassa fever and lymphocytic choriomeningitis viruses (LCMV), and the New World species, such as Junín and Machupo viruses. Up to 300,000 infections with Lassa fever virus occur annually in Africa (122), and outbreaks of New World viruses in the Americas are sporadic but routine (143). Recently, infections by LCMV in transplant recipients have been reported (28). In the absence of effective prophylaxis and treatment, the hemorrhagic fever arenaviruses remain an urgent public health concern.

The arenaviruses are enveloped viruses whose genome consists of two single-stranded RNA molecules, each of which encodes the ambisense expression of two of the four viral proteins (21, 34). The viral envelope glycoprotein (GP-C) is translated from a genomic-sense mRNA generated from the short (S) genomic RNA, whereas the nucleocapsid protein is translated from the antigenomic-sense mRNA. Similarly, the viral matrix protein (Z) and RNA-dependent RNA polymerase are encoded in an ambisense orientation by the long (L) RNA. During biogenesis, arenaviral particles assemble and bud at the plasma membrane (139, 164). Viral entry into target cells is initiated by GP-C binding to cell surface receptors followed by endocytosis of the virion into smooth vesicles (15). Although α-dystroglycan serves as a binding receptor for the Old World arenaviruses (24), the receptor utilized by the major New World group of arenaviruses is

unknown (161). GP-C-mediated membrane fusion is activated upon acidification of the maturing endosome (15, 27, 42, 43), to deposit the virion core into the cell cytoplasm and initiate replication.

The arenavirus envelope glycoprotein complex consists of three noncovalently associated subunits derived from the GP-C precursor: in addition to the typical receptor-binding (G1) and transmembrane (G2) fusion subunits, the complex contains a stable signal peptide (SSP) subunit (20, 50, 188) (Fig. 11). The 58 amino-acid SSP is generated by the cellular signal peptidase and is subsequently myristoylated (188). The mature G1 and G2 subunits are generated upon cleavage by the cellular SKI-1/S1P protease (10, 90, 98) in the early/mid Golgi compartment (19). This proteolytic maturation event is essential for membrane fusion activity. The arenavirus G2 is a member of Class I group of viral fusion proteins (64, 183) that orchestrate membrane fusion through the triggered formation of a stable six-helix bundle core ((47, 48, 79, 178) and references therein).

A tripartite envelope glycoprotein complex is unusual among viral envelope glycoproteins, and the role of the unique arenavirus SSP subunit has not been fully defined. In the GP-C complex, SSP exists as a transmembrane protein, likely in a Type II topology with an extended luminal C-terminus (51, 62). The N-terminus is modified by myristoylation, which is important for efficient membrane fusion activity (188). Recombinant GP-C constructs in which SSP is replaced by a conventional signal peptide do not undergo significant proteolytic maturation by the SKI-1/S1P protease (50, 188). In the Old World Lassa fever arenavirus, this defect can be rescued by co-expression of SSP in *trans* (50).

In light of these observations, we hypothesized that SSP might be essential for the transport of the G1-G2 precursor to Golgi compartment, where the proteolytic cleavage o fthe precursor by SKI/S1P protease generates the mature glycoprotein complex. In the present report, we examine the biogenesis of the GP-C complex of the Junín virus, a member of the New World Tacaribe complex of arenaviruses that is responsible for recurring outbreaks of hemorrhagic fever in the pampas grasslands of Argentina. We show that SSP association is required for transport of the G1-G2 precursor from the endoplasmic reticulum (ER), and thereby for proteolytic maturation in the Golgi. In the absence of SSP, the G1-G2 precursor is constrained to the ER by dibasic amino acid sequences in the cytoplasmic domain of G2. Association with SSP overcomes this block to permit transit of the fully assembled complex through the Golgi and to the cell surface. Moreover, our studies suggest that, in addition to modulating trafficking of GP-C, SSP association may also be important for the membrane fusion activity of the GP-C complex. The unique roles for SSP in the arenavirus life cycle may suggest novel strategies towards the prevention and treatment of arenaviral disease.

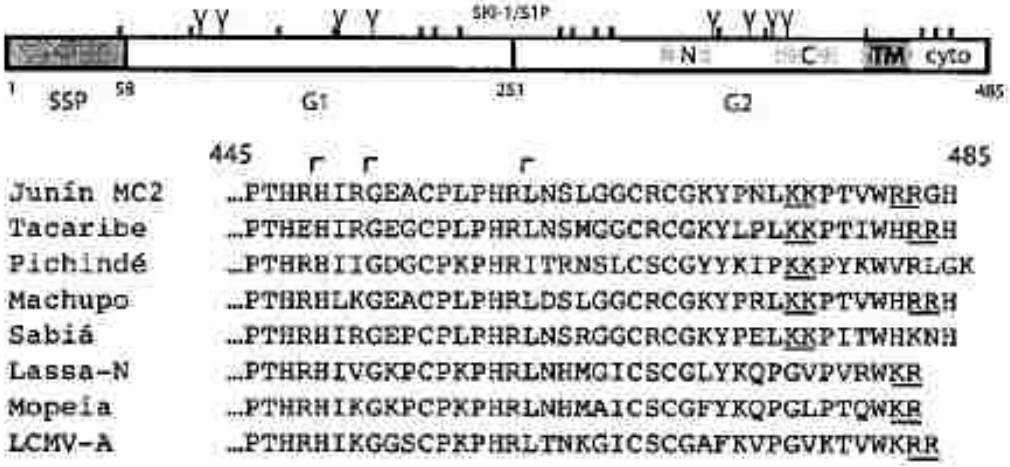

Figure 11. Schematic representation of the Junín virus GP-C glycoprotein and G2 cytoplasmic domain sequences. Amino acids of the Junín virus envelope glycoprotein are numbered from the initiating methionine, and cysteine residues (|) and potential glycosylation sites (Y) are marked. The SSP and SKI-1/S1P cleavage sites, and the resulting SSP, G1 and G2 subunits are indicated. Within G2, the C-terminal transmembrane (TM) and cytoplasmic (cyto) domains are shown, as are the N- and C-terminal heptad-repeat regions (light gray shading). A comparison of G2 cytoplasmic domain sequences among arenavirus species is detailed below. Sequences include the New World isolates Junín (D10072), Tacaribe (M20304), Machupo (AY129248), and Guanarito (AAN05423), and Old World isolates Lassa–Josiah (M15076), Mopeia (M33879), and LCMV-Armstrong (M20869). The sites used to generate truncations in the Junín virus cytoplasmic tail are indicated by angle brackets and dibasic amino acid sequences are underlined.

3. Results

SSP association is required for proteolytic maturation.

The arenavirus SSP is distinct from conventional signal peptides in that it is retained as an essential subunit of the mature GP-C envelope glycoprotein complex and mediates functions beyond translocation of the nascent polypeptide to the ER (50, 52, 188). We previously showed that a recombinant Junín virus GP-C glycoprotein in which SSP was replaced by the conventional signal peptide of human CD4 (CD4sp-GPC) was unable to undergo efficient maturation by the SKI-1/S1P protease (188), extending similar observations with GP-C of the Old World Lassa fever virus (50). In this Old World virus, the deficiency in proteolytic cleavage in the absence of SSP was reversed by co-expression of SSP in *trans* (50).

To investigate the role of SSP in the proteolytic maturation of the Junín virus GP-C, we determined whether co-expression of SSP in *trans* could likewise rescue cleavage. In these studies, the Junín virus CD4sp-GPC construct was co-transfected with the SSP-term plasmid encoding the 58 amino-acid SSP peptide. Optimal expression in vero cells was dependent on T7 RNA polymerase provided by the recombinant vaccinia virus vTF7-3 (63). Cells were metabolically labeled and GP-C glycoproteins were immunoprecipitated using the G1-directed MAb BE08 (153). Baseline studies were performed using the native GP-C glycoprotein, that included its endogenous SSP. Expression of the native glycoprotein resulted in the isolation of a 60 kDa G1-G2 precursor glycoprotein and a heterodisperse smear of G1 and G2 subunits (30-35 kDa; Fig. 12A, top panel). These mature subunits are best-resolved following deglycosylation by PNGase F to yield 22 and 27 kDa polypeptides, respectively (Fig. 12A, bottom panel). The G1 and G2 subunits

were absent upon expression of an SKI-1/S1P cleavage-defective glycoprotein (cd-GPC (188)). A GP-C precursor glycoprotein bearing SSP is often detected as a minor species, suggesting incomplete signal peptidase cleavage in transfected cells (52, 62, 188). As previously reported (50, 52, 62, 188), SSP was co-precipitated as part of the wild-type and cleavage-defective GP-C complex (Fig. 2A, top panel).

Expression of the CD4sp-GPC glycoprotein in the absence of SSP generated the 60 kDa G1-G2 precursor (Fig. 12A, top panel, -SSP, marked in red) and considerably lesser amounts of the cleaved glycoproteins (bottom panel). By contrast, expression of SSP in *trans* (+SSP, marked in red) enabled efficient cleavage of the G1-G2 precursor glycoprotein to produce mature G1 and G2 subunits (bottom panel). The relative efficiency of proteolytic maturation of CD4sp-GPC in *trans* was similar to that of the native GP-C glycoprotein. Furthermore, SSP was co-precipitated with the CD4sp-GPC complex (top panel). Thus, co-expression of SSP appears to rescue wild-type assembly and proteolytic processing in the New World Junín virus CD4sp-GPC complex.

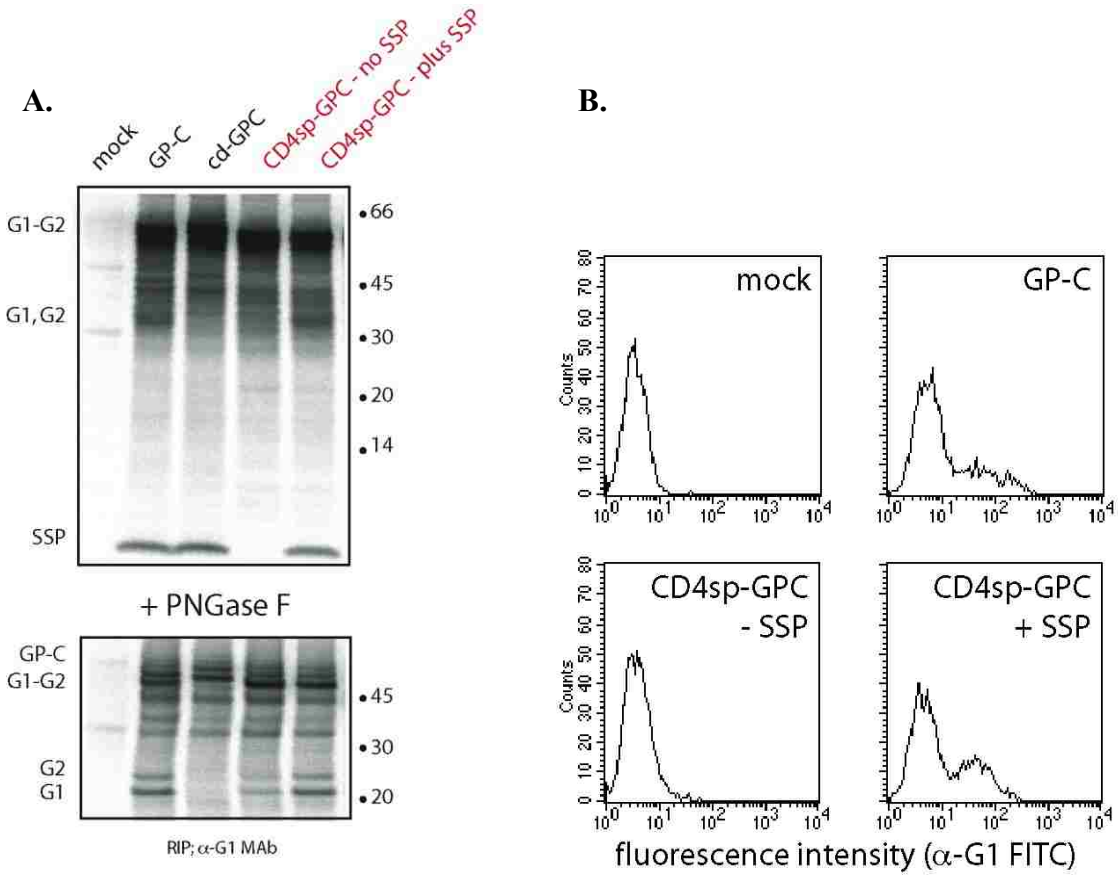

Figure 12. Co-expression of SSP in *trans* rescues SKI-1/S1P cleavage and cell-surface expression of the G1-G2 precursor.

(A) Metabolically labeled glycoproteins were immunoprecipitated using the G1-specific MAb BE08 and separated on NuPAGE^{TM} 4-12% Bis-Tris gels. The wild-type (GP-C) and SKI-1/S1P cleavage-defective (cd-GPC) glycoproteins are shown for comparison with the CD4sp-GPC construct encoding the conventional signal peptide of human CD4. CD4sp-GPC was expressed alone (-SSP) or with SSP (+SSP). In the bottom panel, the glycoproteins have been treated with PNGase F to resolve G1 and G2 polypeptides. The deglycosylated GP-C polypeptides reveal both the G1-G2 precursor and, in SSP-containing constructs, the pre-GP-C precursor (188); additional species that migrate more

slowly than the G1-G2 precursor and with the pre-GP-C precursor are likely products of incomplete deglycosylation. cd-GPC contains a C-terminal S-peptide affinity tag and migrates slightly slower than the other G1-G2 precursors. Known GP-C species are labeled at left; minor unidentified bands are also present. The [^{14}C]-labeled protein markers (Amersham Biosciences) are indicated (in kilodaltons). (B) Cell-surface expression of GP-C in vero cells was determined by flow cytometry using the G1-specific MAb BE08 (153). The cell population was subsequently stained using propidium iodide (1 μg/ml) to exclude dead cells. Cells were fixed using 2% formaldehyde and analyzed using a FACSCalibur flow cytometer (BD Biosciences). Background staining of mock-transfected cells is shown to identify non-expressing cells in the transfected cell populations.

SSP rescues cell-cell fusion activity in *trans*

To determine whether the *trans*-complemented complex was also able to mediate pH-dependent membrane fusion, we co-cultured cells expressing GP-C glycoproteins with vero target cells infected with the fusion reporter vaccinia virus vCB21R-LacZ, expressing the β-galactosidase gene under control of the T7 promoter (132). In this assay, activation of GP-C-mediated membrane fusion by acidic pH (5.0) results in syncytium formation between the effector and reporter cells, and expression of β-galactosidase; the enzymatic activity is then monitored using a chemiluminescent substrate (183). As shown in Fig. 13, pH-dependent cell-cell fusion is readily detected using the native GP-C glycoprotein and absent in the cleavage-defective cd-GPC mutant. Cells expressing the CD4sp-GPC glycoprotein in the absence of SSP were unable to mediate cell-cell fusion (Fig. 13, CD4sp; first of the bracketed pair of bars). By contrast, co-expression of SSP reconstituted pH-dependent cell-cell fusion activity in the *trans*-complemented CD4sp-GPC complex (second of bracketed pair) to levels greater than those seen with the native GP-C glycoprotein. Thus expression of SSP in *trans* can fully restore membrane fusion activity to the Junín virus G1-G2 precursor glycoprotein.

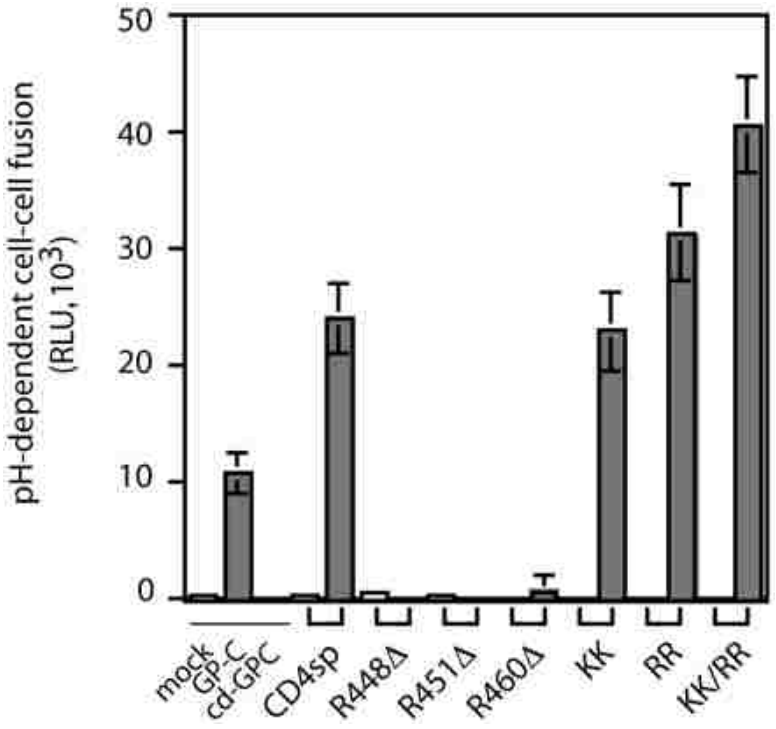

Figure 13. pH-dependent cell-cell fusion activity.

pH-dependent fusion was detected using the recombinant vaccinia virus-based β-galactosidase-reporter assay (132) as previously described (183, 188). β-galactosidase activity was quantitated using the chemiluminescent substrate GalactoLite Plus (Tropix). Relative light unit (RLU) measurements from cultures treated at pH 5.0 are shown after subtraction of background levels from neutral-pH cultures (average background = 1500 RLU). Control conditions are shown in the underlined bars at left (mock, wild-type GP-C and cd-GPC). Note that CD4sp-GPC constructs are bracketed in pairs (below the axis) representing minus (open bars) and plus (gray bars) SSP, respectively. Some bars are not discernible on the scale of the graph. All conclusions were replicated using X-gal staining of parallel co-cultures.

SSP association is required for exit from the ER.

To investigate the role of SSP in the biogenesis of GP-C, we examined the intracellular localization of the complex by confocal microscopy. In these experiments, vero cells expressing the wild-type and CD4sp-GPC glycoproteins were fixed, permeabilized, and immunochemically stained using the anti-G1 MAb BF11 (153) and an Alexa Fluor 488-conjugated secondary antibody. Non-permeabilized cells were similarly stained to detect GP-C accumulation on the cell surface. As shown in Fig. 14, the native GP-C glycoprotein accumulated in the ER and Golgi-like perinuclear structures (GP-C, permeabilized) and on the cell surface (GP-C, surface). Localization to the Golgi apparatus was confirmed using a rabbit polyclonal antibody directed against an integral Golgi membrane protein, giantin (106) and a secondary Alexa Fluor 568-conjugated antibody. Co-localization of GP-C with the Golgi marker is visualized by a yellow color in the merged images. Expression of CD4sp-GPC in the presence of SSP resulted in a pattern of localization and transport to the cell surface similar to that of native GP-C (Fig. 14, CD4sp and right panel/+SSP). These findings highlight the reconstitution of the GP-C complex upon *trans*-complementation with SSP.

In the absence of SSP, however, the G1-G2 precursor of CD4sp-GPC exhibited a diffuse reticulate pattern of intracellular expression consistent with retention in the ER (Fig. 14, CD4sp and left panel/–SSP). Notably absent was any concentration of GP-C staining to a morphologically defined Golgi apparatus or specific co-localization with the anti-giantin MAb (merged image). The orange color in the merged image likely reflects the spatial coincidence of green and red fluorescence rather than specific co-localization to a definable Golgi structure. Also absent was any staining of CD4sp-GPC on the cell

surface (surface). The lack of transport to the cell-surface is not due to the absence of proteolytic cleavage *per se*, because the cleavage-site-defective cd-GPC mutant is transported to the cell surface as the wild-type glycoprotein (not shown, (10, 90)). Nor did we detect punctate staining in the ER that might suggest misfolding of the G1-G2 precursor in the absence of SSP. The difference in trafficking of the G1-G2 precursor to the Golgi in the presence or absence of SSP likely accounts for the effect of *trans*-complementation on proteolytic cleavage (Fig. 12A), consistent with the activation of SKI-1/S1P protease in the cis-medial Golgi compartment (39, 53).

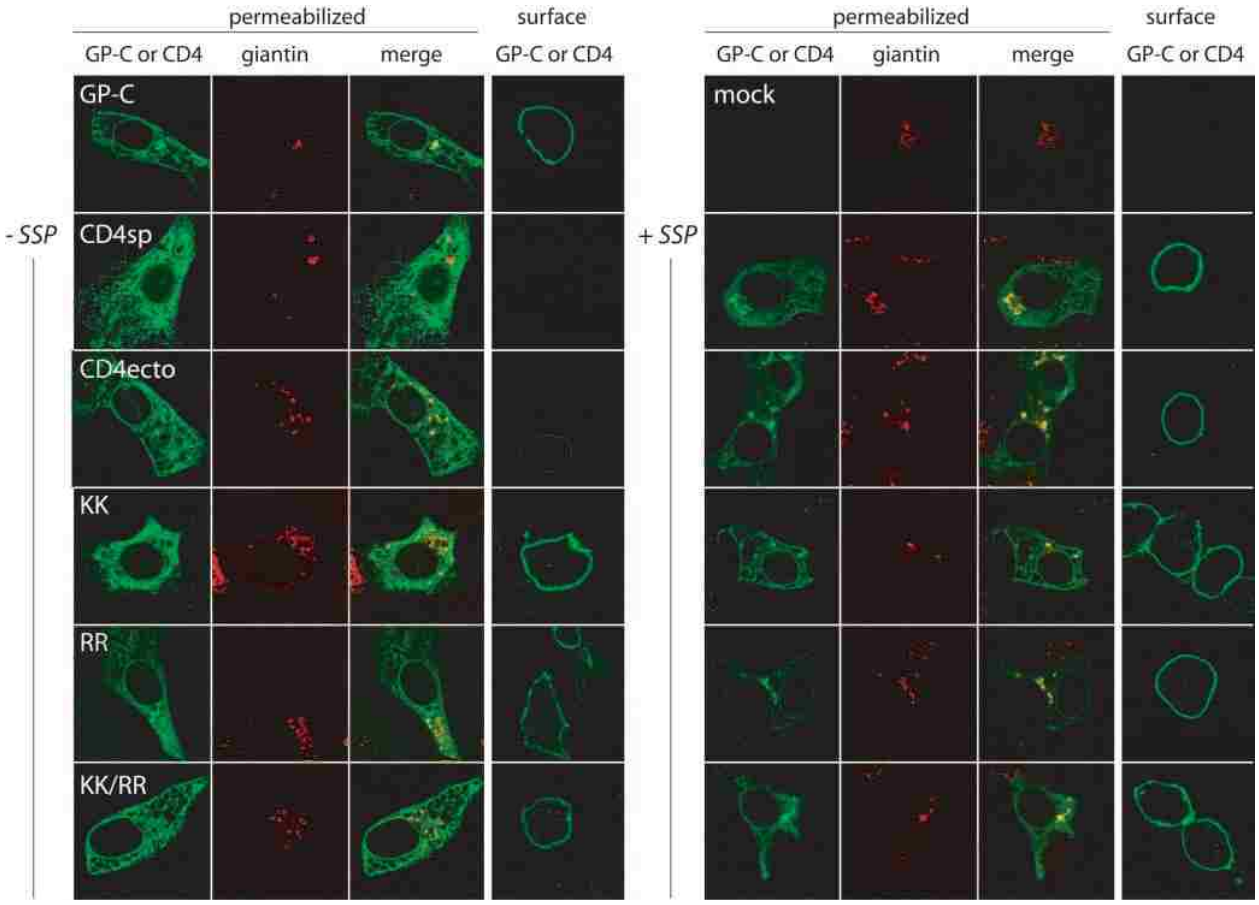

Figure 14. Intracellular and cell-surface visualization of glycoproteins.

Confocal images were obtained as described in Materials and Methods. Permeabilized cells were stained in green using either the MAb BF11 (GP-C) or, for CD4ecto, SIM.2 (CD4). Golgi were identified using a rabbit polyclonal antiserum and stained in red. Merged images (merge) were created using Lasersharp software. Non-permeabilized cells (surface) were stained in green using either MAb BF11 or SIM.2. The expressed glycoproteins are indicated in white letters superimposed on the left-most image. The top row depicts cells expressing native GP-C or mock-transfected cells (all infected with the recombinant vaccinia virus vTF7-3). In subsequent rows, the glycoproteins were expressed either in the absence (left panel/-SSP) or presence (right panel/+SSP) of SSP.

In some images, the Golgi apparatus is vesiculated and dispersed, perhaps due to infection of the cells by vaccinia virus.

Next, we examined the role of SSP in transport of the GP-C complex to the cell surface by using flow cytometry and the G1-specific MAb BE08. In cell cultures transiently expressing the wild-type GP-C glycoprotein, a clear population of GP-C expressing cells was evident (Fig. 12B, top right). A comparison of cells expressing CD4sp-GPC in the presence or absence of SSP revealed that the GP-C glycoproteins were present on the cell surface only upon co-expression of SSP (bottom panels). Cell surface accumulation of the *trans*-complemented CD4sp-GPC glycoprotein was comparable to that of the native GP-C glycoprotein. Taken together, these results demonstrate that SSP is essential for GP-C transport to the Golgi and the cell surface. In the absence of SSP, the G1-G2 precursor is localized to the ER.

Transit of a CD4 chimera bearing G2 sequences.

To further investigate the role of the G2 subunit in ER localization, and the role of SSP in regulating transit to the cell surface, we determined whether control by SSP and the G2 subunit might be transferable to a heterologous cell-surface protein. Because the ectodomain of human CD4 forms a soluble and secreted protein (40, 160), we fused the CD4 signal peptide and ectodomain to the transmembrane and cytoplasmic regions of G2. In the CD4ecto construct, the C-terminus of soluble CD4 (TPV_{372} (40)) was spliced at the G2 ectodomain sequence TPL_{420}, three residues upstream of D_{424} that nominally defines the junction with the transmembrane domain.

Cells expressing the CD4ecto chimera, or native CD4, were metabolically labeled and cell lysates were immunoprecipitated using the anti-CD4 ectodomain MAb SIM.2. The CD4ecto chimera was expressed as a 55 kDa glycoprotein that co-migrated with native

CD4 (Fig. 15A, left panel). Upon co-expression, SSP was found to co-precipitate with CD4ecto (Fig. 15A; left panel). This association was specific to G2 sequences in the CD4ecto glycoprotein; SSP did not bind to native CD4 (when co-expressed, not shown). Thus, the transmembrane and cytoplasmic domains of G2 are sufficient for SSP binding.

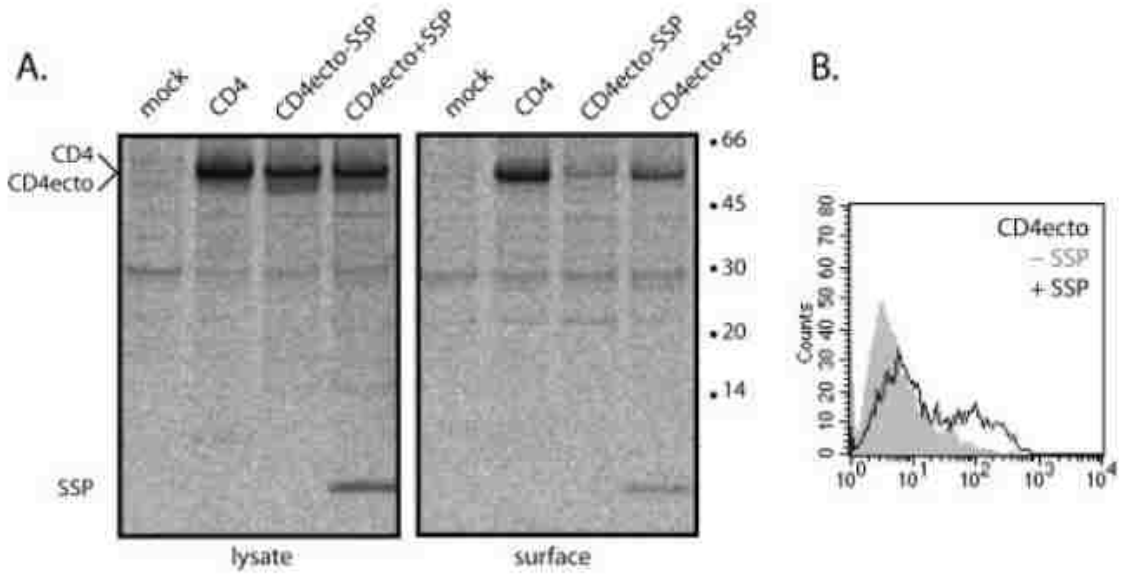

Figure 15. The chimeric CD4 glycoprotein bearing the transmembrane and cytoplasmic domains of G2 requires SSP for transport to the cell surface.

(A) The chimeric CD4ecto construct was expressed alone (-SSP) or with SSP (+SSP) and metabolically labeled. Intact cells were incubated with the anti-CD4 MAb SIM.2 (120, 135) and the cell-surface glycoproteins were subsequently isolated from cleared cell lysates using Protein A-Sepharose (surface). Intracellular CD4ecto glycoprotein was immunoprecipitated from the post-Protein A-Sepharose supernatant using additional SIM.2 MAb (lysate). Mock- and human CD4-transfected cells served as controls. (B) Flow cytometry using SIM.2 MAb was otherwise performed as described in Fig. 12. The filled gray histogram (-SSP) and open (+SSP) histograms are overlaid.

Importantly, transport of the CD4ecto chimera through the Golgi apparatus and to the cell surface was dependent on co-expression of SSP. As shown by immunochemical staining using SIM.2 MAb and confocal microscopy (Fig. 14, CD4ecto, permeabilized), the chimeric glycoprotein was largely constrained to the ER in the absence of SSP, and failed to co-localize with the Golgi apparatus (left panel/-SSP). In addition, only trace amounts of the CD4ecto glycoprotein were detected in the absence of SSP on the cell surface, either through confocal microscopy (Fig. 14, surface) or flow cytometry (Fig. 15B, -SSP). Thus, fusion to the G2 transmembrane and cytoplasmic domains prevented transport of the CD4 ectodomain from the ER.

By contrast, co-expression with SSP resulted in significant localization of CD4ecto in the Golgi (Fig. 14, right panel/+SSP) and expression on the cell surface (surface). Mobilization of the chimeric glycoprotein by SSP was confirmed by flow cytometry (Fig. 15B, +SSP). Furthermore, immunoprecipitation studies of CD4ecto expression on the cell surface (Fig. 15A; right panel) identified the surface moiety as the complex of CD4ecto and SSP. Together, these findings demonstrated that the essential elements of ER localization, and its control by SSP binding, can be recapitulated in a chimeric CD4ecto glycoprotein bearing the transmembrane and cytoplasmic domains of G2.

Analysis of C-terminal truncations in the G2 cytoplasmic domain.

Among transmembrane proteins that are retained in the ER, specific localization signals are often encoded within the cytoplasmic domain ((54, 97, 171) and references therein). In order to define the determinants in G2 that are required for ER localization, we constructed a series of C-terminal truncations in the cytoplasmic domain of G2. Three

arginine residues, spaced 4, 7, and 17 amino acids from the nominal transmembrane domain, were used as endpoints in the truncations (Fig. 11). These positively charged termini were chosen to facilitate anchoring of the truncated CD4sp-GPC glycoprotein in the membrane. The arginine codons were fused to those encoding an S-peptide affinity tag (88) to facilitate analysis of the G2 moiety (188). Metabolically labeled glycoprotein was isolated using the Spep affinity tag and S-protein agarose (Novagen). The truncated CD4sp-GPC glycoproteins (R448Δ, R451Δ, and R460Δ, respectively) were well expressed in Vero cells yet failed to co-precipitate significant amounts of SSP (Fig. 16A, top panel). Nonetheless, all three truncated glycoproteins were subjected to SKI-1/S1P cleavage, in the presence or absence of SSP, to produce truncated and affinity-tagged G2 moieties (Fig. 16A, bottom panel). The relative migrations of the truncated G2 polypeptides correspond to their expected molecular weights, but cause them to overlap with the intact G1 polypeptide. The association between G1 and the truncated G2 subunits was separately confirmed by co-immunoprecipitation using a MAb directed to G1 (not shown). By contrast, similar truncations in G2 of the Old World LCM virus were reported to prevent SKI-1/S1P cleavage (35).

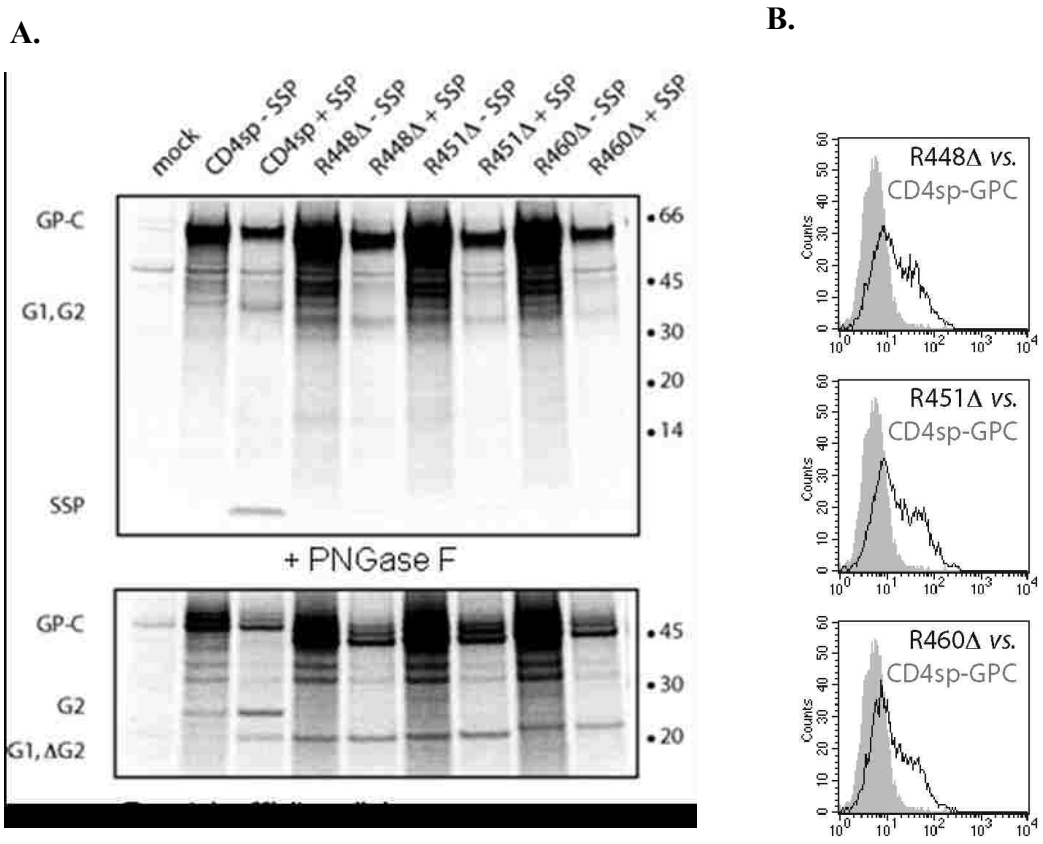

Figure 16. Truncations to the cytoplasmic domain of G2 ablate SSP binding yet enable transport to the cell surface.

(A) The wild-type and truncated CD4sp-GPC glycoproteins (R448Δ, R451Δ, and R460Δ) were expressed alone (-SSP) or with SSP (+SSP). Metabolically labeled glycoproteins were precipitated using the C-terminal Spep affinity tag and S-protein agarose (Novagen) and analyzed as described in Fig. 12. The G1 and G2 glycoproteins are best resolved following deglycosylation with PNGase F (bottom). Note that the truncated G2 moieties (ΔG2) migrate near the wild-type G1 polypeptide; co-association between G1 and ΔG2 was formally demonstrated by immunoprecipitation using anti-G1 MAb BF11, which co-precipitated ΔG2 (not shown). Although co-precipitation of SSP was markedly reduced

with the truncated glycoproteins, trace amounts could be discerned upon darkening of the image (not shown). This low level of SSP association is judged to be insignificant, as the properties of the truncated glycoproteins are independent of SSP co-expression. (B) Cell-surface expression of the truncated glycoproteins was determined by flow cytometry as described in Fig. 12. Note that expression of the wild-type CD4sp-GPC glycoprotein (gray histogram in all) is compared with that of the truncations (open histograms), all in the absence of SSP.

Flow cytometry was used to determine whether the truncated Junín virus glycoproteins were also transported to the cell surface without SSP. As shown in Fig. 16B, all three truncation mutants were expressed on the cell surface in the absence of SSP, at levels comparable to the *trans*-complemented CD4sp-GPC glycoprotein (see Fig. 12B). Truncations in the context of CD4ecto likewise enabled transport from the ER (not shown). In the LCMV virus (35), the truncated GP-C was also expressed on the cell surface. Taken together, these results suggest that amino acid sequences within the cytoplasmic domain of G2 are important in constraining the G1-G2 precursor to the ER. The cytoplasmic region is also important for SSP association.

We have demonstrated that GP-C glycoproteins bearing truncations in the cytoplasmic domain of G2 can be proteolytically processed and transported to the cell surface in the absence of SSP. Surprisingly, however, none of the truncated complexes was able to mediate pH-dependent cell-cell fusion (Fig. 13). It is possible that this failure may be due to insufficient cleavage or transport of the truncated glycoproteins. Alternatively, the failure might reflect a requirement for either SSP or the cytoplasmic domain of G2 for membrane fusion activity.

Dibasic amino acid sequences participate in ER localization.

Sequence analysis of the G2 cytoplasmic domain revealed conserved motifs that may be involved in protein trafficking and ER localization. In particular, dibasic amino acids sequences such as the canonical KKXX and RXR motifs are widely utilized in the retrieval of transmembrane proteins to the ER (see (54, 97, 171) and references therein). The cytoplasmic domain of Junín virus G2 contains two related dibasic sequences: $KKPT_{479}$ and a C-terminal $RRGH_{485}$. Variants of these sequences appear in other arenavirus G2 proteins (Fig. 11). To assess the potential role of these sequences in ER localization, we mutated the two basic amino acids at each site to alanines, both individually (KK and RR glycoproteins) and as the double mutant (KK/RR).

Immunoprecipitation studies of metabolically labeled whole cell lysates revealed that all of the mutant CD4sp-GPC glycoproteins were able to associate with SSP (Fig. 17A, top panel). Neither of the dibasic sequences was essential for SSP binding. *Trans*-complementation with SSP enabled wild-type levels of cell-surface expression (Fig. 17B, +SSP) and efficient pH-dependent cell-cell fusion (Fig. 13), arguing against significant adverse effects of the mutations on overall protein folding.

In the absence of SSP, importantly, both the single and double mutants were now capable of transport to the cell surface. This phenotype was evident upon confocal microscopic analysis of non-permeabilized cells (Fig. 14, surface), although specific localization in the Golgi was difficult to discern (green and merged images). Flow cytometric studies of cell-surface expression indicated that both the single and double mutations provided modest, albeit significant, relief of ER retention (Fig. 17B, -SSP). Evidence for enhanced

SKI-1/S1P cleavage of the mutant glycoproteins was, however, difficult to discern in whole cell lysates, above the residual level of cleavage in the wild-type glycoprotein (Fig. 17A, bottom panel). It is possible that the cleaved species in the wild-type G1-G2 glycoprotein reflect transient residence in the Golgi, prior to retrieval to the ER. In the Old World Lassa fever virus glycoprotein, where cleaved products are not observed in the absence of SSP (50), retrieval of the G1-G2 precursor may be more rapid. Nonetheless, mobilization of the mutant glycoproteins to the cell surface was consistently observed and distinct from the strict intracellular retention seen with the wild-type glycoprotein. Both KK and RR mutations appeared to be comparably efficacious, and no synergy was observed in the double KK/RR mutant. However, none of the mutant glycoproteins was able to mediate cell-cell fusion in the absence of SSP (Fig. 13). This defect is not attributable to the amino acid substitutions *per se*, as wild-type levels of fusion were restored upon *trans*-complementation with SSP.

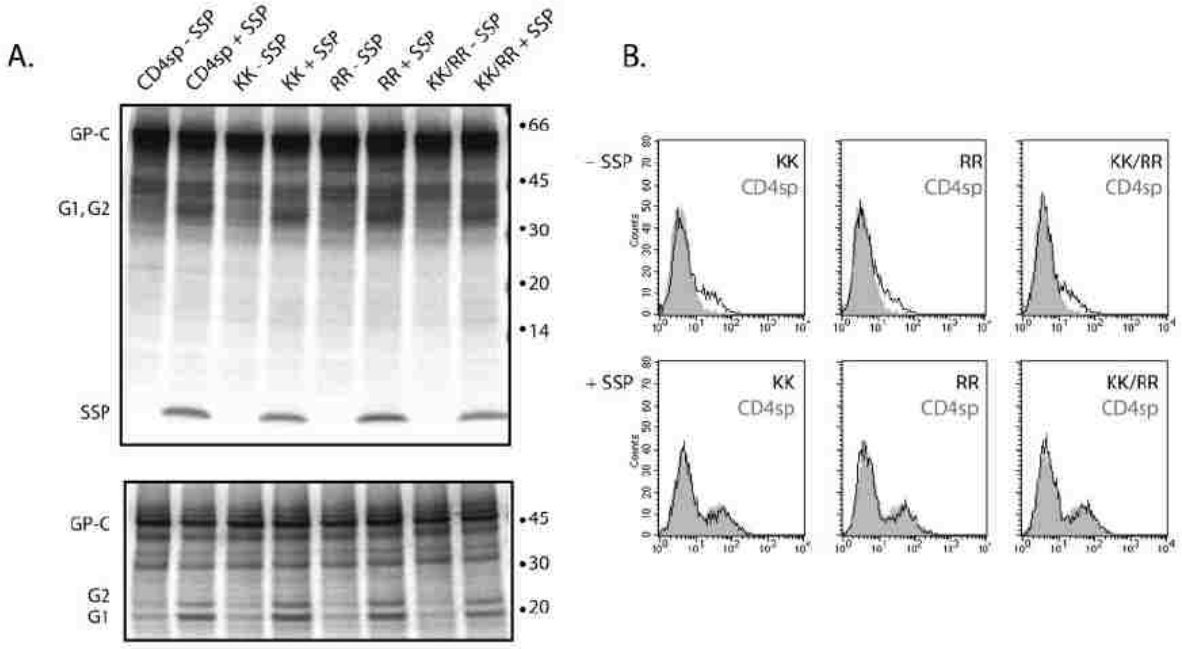

Figure 17. Alanine mutations to dibasic amino acid motifs enable transport from the ER.

(A) CD4sp-GPC constructs containing KK, RR, and double KK/RR mutations were expressed alone (-SSP) or with SSP (+SSP). Metabolically labeled glycoproteins were immunoprecipitated and analyzed as described in Fig. 12. (B) Flow cytometry was performed as described in Fig. 12. Note that the top panels compare expression of the CD4sp-GPC glycoprotein (gray histogram in all) with that of the mutants (open histograms) in the absence of SSP. Expression with SSP is shown in the bottom panels.

To confirm that the mutations are sufficient for significant mobilization of the G1-G2 precursor in the absence of SSP, we examined the glycoprotein by immunoprecipitation from the cell surface (Fig. 18). These experiments confirmed significant expression of the dibasic-sequence mutants on the cell surface and demonstrated a preponderance of the proteolytically processed G1-G2 complex, reflecting access to the SKI-1/S1P protease in the Golgi. The efficiency of cleavage in the mutant glycoproteins was relatively unaffected by the presence or absence of SSP (60% cleaved *vs*. 40% cleaved, respectively).

Taken together, these studies identify the two dibasic amino acid sequences ($KKPT_{479}$ and $RRGH_{485}$) as important determinants of ER localization in the absence of SSP. Alanine mutations at either or both of these sites result in partial relief from ER retention and enable transport to the cell surface in the absence of SSP. On the other hand, these mutations do not completely obviate the requirement for SSP association in transport of the G1-G2 precursor (Fig. 18). Quantitative analysis of the glycoproteins indicated that whereas the mutations were able to increase cell-surface expression at least 10-fold, co-expression of SSP resulted in an additional 10-fold increase in all mutants, to the levels of the wild-type glycoprotein. These findings are consistent with our results from confocal microscopy and flow cytometry studies (Figs. 14 and 17). Thus, constraints on the trafficking of the G1-G2 precursor include the dibasic sequence motifs in the cytoplasmic domain of G2, but also involve additional structural elements provided upon full assembly with SSP.

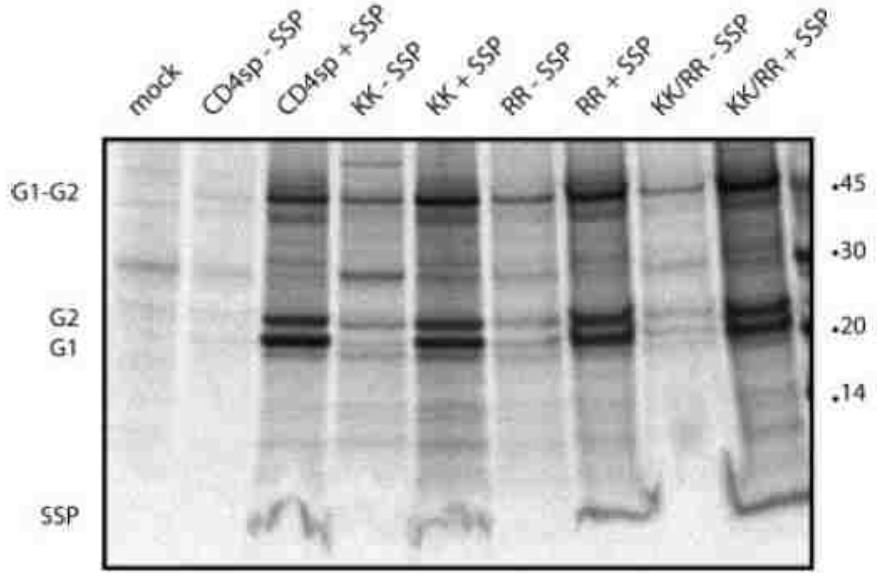

Figure 18. Cell-surface expression of dibasic amino acid motif CD4sp-GPC mutants.

Intact cells expressing the constructs in Figure 17 were incubated with the G1-specific MAb BE08 and the cell-surface GP-C glycoproteins were isolated from cleared cell lysates using Protein A-Sepharose, and deglycosylated. The relative amounts of G1+G2 and G1-G2 precursor in each lane were quantitated from the phosphorimage using Image Gauge software (Fuji), and the efficiency of cleavage was determined as the sum of G1 + G2 relative to total of all forms. Distortion of the SSP band is due to detergents used in PNGase F treatment.

4. Discussion

The regulation of trafficking through intracellular membranous compartments is central to the biogenesis of membrane glycoproteins (45, 54). Quality control mechanisms for protein folding and assembly are proposed to operate through checkpoints on exit from the ER and through bidirectional transport to and from the Golgi apparatus. Viruses make use of these cellular pathways in the biosynthesis, assembly, and release of new virion particles (45). In our studies, we have characterized the biogenesis of the arenavirus envelope glycoprotein and the requirement for tripartite assembly to enable transport of the GP-C complex from the ER. Without the association of SSP, the wild-type G1-G2 precursor remains localized to the ER. We show that localization is mediated by the cytoplasmic domain of G2, and that the control of trafficking by SSP association is transferable to a chimeric CD4 molecule bearing the G2 transmembrane and cytoplasmic domains. Conversely, regulation of intracellular transport of the GP-C complex does not require G1 or the ectodomain of G2.

Our studies demonstrate that ER localization is mediated in part through dibasic amino acid sequences in the cytoplasmic domain of G2. Alanine mutations to either of two dibasic motifs provide partial relief from ER localization and enable expression of the proteolytically cleaved G1-G2 complex on the cell surface. Upon exit from the ER and transit through the Golgi, the mutant G1-G2 precursor is now fully susceptible to proteolytic maturation by SKI-1/S1P protease. Thus, absent ER localization signals, the arenavirus GP-C precursor can undergo proteolytic maturation much as the precursor glycoproteins of other Class I viral fusion proteins.

Dibasic amino acid sequences are known to mediate ER localization through retrograde transport (retrieval) from the Golgi ((54, 97, 171) and references therein). The specific dibasic sequences we have identified as important for ER localization in the Junín virus G2 glycoprotein do not match precisely either of the canonical ER retrieval motifs: the C-terminal KKXX or internal RXR sequences. Although the internal KK sequence studied here is conserved among the New World arenaviruses, the C-terminal RRXX sequence shows considerable variation (Fig. 11). Among the Old World viruses, only the C-terminal motif is identifiable. However, variants to the canonical motifs are also common in other ER-localized transmembrane proteins (124, 155, 171) and the efficiency of retention by these sequences is often highly context-dependent (67, 158, 189). Many details regarding the mechanisms and molecular determinants involved in ER-Golgi trafficking remain unresolved.

It is noteworthy that a viral envelope glycoprotein destined for the cell surface should encode an ER localization signal. For cellular transmembrane proteins that traverse the Golgi and beyond, dibasic ER localization motifs are commonly found to control the assembly and trafficking of heteromultimeric membrane protein complexes ((41, 83, 101, 115, 190) and reviewed by (54, 124)). These endogenous signals prevent transport of the individual subunits, and are overcome upon assembly of the multimeric complex. This quality control mechanism ensures that only the fully and properly assembled complex is transported from the ER. In the biogenesis of the Junín virus GP-C complex, we propose an analogous role for SSP association – namely, to mask endogenous ER localization signals in the cytoplasmic domain of G2 and thus enable transport of only the fully assembled tripartite complex.

This strategy for assembly-dependent control of viral envelope glycoprotein trafficking is likely not unique to the arenaviruses. The bunyavirus G_C glycoprotein also contains a non-canonical basic amino acid cluster that may be involved in ER localization (74). In these viruses, transport of G_C from the ER requires association with a second envelope glycoprotein G_N (77, 93), which in turn retains the G_C-G_N complex in the Golgi (69, 74, 157), the site of virus budding. Together, these observations highlight the use of cellular ER-Golgi trafficking mechanisms during the viral life cycle to control the assembly and transport of multimeric envelope glycoprotein complexes.

Despite mutations that enable transport of the G1-G2 complex in the absence of SSP, wild-type levels of trafficking were not restored by point mutations to the dibasic amino-acid sequences or by truncations in the cytoplasmic domain (not shown). It is possible that additional constraints on GP-C transport lie within the transmembrane domain of G2. Moreover, it is likely that the association with SSP remains essential for the integrity of the GP-C complex. The SSP subunit has uniquely evolved within the arenaviruses, for purposes other than simply to relieve ER retention of an envelope glycoprotein precursor. It is telling then that despite the accumulation of cleaved G1-G2 complex on the cell surface, none of the glycoproteins lacking SSP is able to mediate membrane fusion (Fig. 3). Notably, GP-C glycoproteins bearing mutations at the dibasic amino-acid motifs are unable to promote fusion in the absence of SSP, yet are restored to full activity by co-expression of SSP. This defect in fusion is likely not due to the lower levels of cell-surface glycoprotein in the absence of SSP, as robust fusion is observed with comparably low levels of cleaved wild-type glycoprotein (Figure 6 of reference (183)). Rather, we

suggest that SSP may be directly involved in modulating pH-dependent membrane fusion by the GP-C complex.

In addition, the G1-G2 complex lacking SSP is not myristoylated. GP-C complexes in which myristoylation is blocked by a G2A mutation are less able to mediate cell-cell fusion than the wild-type glycoprotein (188), perhaps due to alterations in trafficking to specific membrane microdomains (150, 169). The G2A glycoprotein, however, retains 30% of the wild-type fusion activity, significantly more than the present G1-G2 complexes in the absence of SSP. This comparison suggests defects beyond the lack of acylation in G1-G2 complexes lacking SSP. Separately, myristoylation may also be important during virion assembly in facilitating the co-localization of GP-C with the myristoylated Z matrix protein (142).

Further studies will no doubt delineate the additional roles of the unique SSP subunit in the arenavirus life cycle. Unique solutions embodied in the assembly, trafficking, and membrane fusion activity of the arenavirus GP-C complex may suggest novel approaches for intervention towards the prevention and treatment of arenavirus hemorrhagic fevers.

5. Materials and Methods

Molecular reagents, recombinant vaccinia viruses, and monoclonal antibodies

The GP-C coding region from the pathogenic Junín virus strain MC2 (71) was provided by Victor Romanowski (Universidad National de La Plata, Argentina) and introduced into the mammalian expression vector pcDNA 3.1+ as described (188). For *trans*-complementation studies (50), the CD4sp-GPC construct in which SSP was replaced by the conventional signal peptide of CD4 (188) was co-expressed with an SSP construct in

which a stop codon was introduced following the C-terminal SSP amino acid T58 (SSP-term). A chimeric glycoprotein (CD4ecto) bearing the CD4 signal peptide and ectodomain fused to the transmembrane and cytoplasmic domains of G2 was constructed using the human CD4 cDNA (113) obtained through the National Institutes of Health (NIH) AIDS Research and Reference Reagent Program. Mutations were introduced by QuikChange mutagenesis (Stratagene), and polymerase chain reaction was used to generate truncations and chimeric plasmids. For the cytoplasmic-domain truncation series and in a control cleavage-defective GP-C plasmid (cd-GPC; (188)), a C-terminal 15 amino-acid S-peptide (Spep) affinity tag (88) was introduced to facilitate biochemical analysis (188). All constructs were verified by DNA sequencing and three independent clones were typically tested to assure consistent phenotypes.

Optimal expression of the Junín virus GP-C gene and its derivatives in Vero 76 cells was achieved using the bacteriophage T7 promoter of the pcDNA3.1 vector and infection by a recombinant vaccinia virus expressing the T7 polymerase (vTF7-3; (63)). The vaccinia virus vCB21R-lacZ expressing the β-galactosidase gene under the control of the T7 promoter was used in our analysis of cell-cell fusion (132). These recombinant vaccinia virus reagents were provided by T. Fuerst and B. Moss, and C. Broder, P. Kennedy and E. Berger, respectively, through the NIH AIDS Research and Reference Reagent Program.

Mouse monoclonal antibodies (MAbs) QC03-BF11 (BF11) and GB03-BE08 (BE08) (153), directed against the G1 subunit of GP-C, were kindly provided by Drs. Tom Ksiasek and Tony Sanchez (Special Pathogens Branch, CDC, Atlanta). The anti-CD4

ectodomain hybridoma producing MAb SIM.2 (120, 135) was obtained through the NIH AIDS Research and Reference Reagent Program.

Expression of GP-C and its derivatives.

The glycoproteins were expressed and characterized as previously described (183, 188). Briefly, Vero 76 cells were infected with the recombinant vaccinia virus vTF7-3 (63) at a multiplicity of two in Dulbecco's Minimal Essential Medium (DMEM) containing 2% fetal bovine serum (FBS) and 10 μM cytosine arabinoside (araC) (78). After 30 min, the cells were washed and transfected with the GP-C expression plasmid using Lipofectamine 2000 reagent (Invitrogen). Metabolic labeling using 32-50 μCi/ml of [^{35}S]-ProMix (Amersham Pharmacia Biotech) was initiated 6 hr post-transfection in methionine- and cysteine-free medium containing 10% dialyzed FBS and 10 μM araC, and was continued for 12-16 hr. Cultures were then washed in physiological buffered saline (PBS) and lysed using cold Tris-saline buffer (50 mM Tris-HCl and 150 mM NaCl at pH 7.5) containing 1% Triton X-100 nonionic detergent and protease inhibitors (1 μg/ml each of aprotinin, leupeptin, and pepstatin). The expressed glycoproteins were isolated from cleared lysates by immunoprecipitation using either the G1-directed MAbs or the CD4-directed MAb SIM.2, and Protein A-Sepharose (Sigma). In some experiments, glycoproteins containing the C-terminal Spep affinity tag were isolated using S-protein agarose (Novagen). Isolated glycoproteins were deglycosylated using peptide: N-glycosidase F (PNGase F, New England Biolabs). Proteins were analyzed by SDS-polyacrylamide gel electrophoresis using NuPAGE 4-12% Bis-Tris gels (Invitrogen) and the recommended sample buffer containing lithium dodecyl sulfate and reducing agent. Molecular size markers included [^{14}C]-methylated Rainbow proteins

(Amersham Pharmacia Biotech). Radiolabeled proteins were imaged using a Fuji FLA-3000G imager and analyzed using ImageGauge software (Fuji).

For immunoprecipitation of cell-surface glycoproteins, monolayers of metabolically labeled cells were incubated with MAb BE08 or SIM.2 in ice cold PBS containing 2% FBS and 0.1% NaN_3 for 2 hr. Following extensive washing, cells were resuspended by scraping in PBS and lysed as described above. Immune complexes were isolated from cleared lysates using Protein A-Sepharose.

Flow cytometry.

Vero 76 cells expressing GP-C or its derivatives were labeled using the G1-specific MAb BE08 (153) and a secondary fluorescein isothiocyanate (FITC)-conjugated goat anti-mouse antibody (Jackson ImmunoResearch). CD4 was detected using a fluorescein isothiocyanate-conjugated mouse anti-CD4 MAb (BD Biosciences). Cells were subsequently stained using propidium iodide (1 μg/ml) and then fixed in 2% formaldehyde (183). Populations were analyzed using a FACSCalibur flow cytometer and CellQuest software (BD Biosciences).

GP-C-mediated cell-cell fusion.

The β-galactosidase fusion reporter assay (132) was used to characterize the ability of the envelope glycoproteins to mediate pH-dependent cell-cell fusion (183, 188). Briefly, Vero cells infected with vTF7-3 and expressing the envelope glycoprotein were co-cultured with reporter cells infected with vCB21R-lacZ, a recombinant vaccinia virus expressing β-galactosidase under the control of the T7 promoter. The reporter cells were obtained by incubating Vero 76 cells with vCB21R-lacZ at a multiplicity of two and

allowing the infection to proceed overnight in the presence of 100 μg/ml rifampicin (78). The GP-C-expressing cells and reporter cells were co-cultured in medium containing both araC and rifampicin for 5 hr and then subjected to a 30 min pulse of neutral or acidic (pH 5.0) medium. β-galactosidase expression is induced upon fusion of the effector and reporter cells and was detected, after 5 hrs of continued cultivation at neutral pH, in cell lysates (Tropix) using the chemiluminescent substrate GalactoLite Plus (Tropix). Cell-cell fusion was quantified using a Tropix TR717 microplate luminometer.

Confocal Microscopy.

Cells expressing GP-C glycoproteins were harvested by trypsinization 6 hrs after transfection and reseeded to 8-well chambered coverglasses (Lab Tek II) in medium containing 10 μM araC. After 18 hrs, cultures were washed in PBS and fixed with 4% formaldehyde for 10 min at room temperature. Following washing and quenching with 50 mM Tris pH 7.4 in PBS, cultures were either permeabilized in PBS containing 0.1% Triton X-100 and blocked in the same buffer containing 5% FBS (for intracellular staining) or simply blocked in the absence of detergent (for cell-surface staining). GP-C glycoproteins were detected using the G1-directed MAb BF11 and an Alexa Fluor 488-conjugated anti-mouse antibody (Molecular Probes) in the appropriate blocking buffer. The Golgi marker giantin was detected using a rabbit polyclonal antiserum (Covance Research Products) and an Alexa Fluor 568-conjugated anti-rabbit antibody (Molecular Probes). Chambers were covered with Slow Fade Gold (Molecular Probes) and visualized using an inverted Nikon TE-300 microscope. Fluorescence was examined using a BioRad Radiance 2000 confocal laser scanning microscope and images were merged using Lasersharp software (BioRad).

CHAPTER FOUR

BITOPIC MEMBRANE TOPOLOGY OF THE STABLE SIGNAL PEPTIDE IN THE TRIPARTITE JUNÍN VIRUS GP-C ENVELOPE GLYCOPROTEIN COMPLEX

1. Abstract

The stable signal peptide (SSP) of the GP-C envelope glycoprotein of the Junín arenavirus plays a critical role in trafficking of the GP-C complex to the cell surface and in its membrane-fusion activity. SSP therefore may function on both sides of the lipid membrane. In this study, we have investigated the membrane topology of SSP by confocal microscopy of cells treated with the detergent digitonin to selectively permeabilize the plasma membrane. By using an affinity tag to mark the termini of SSP in the properly assembled GP-C complex, we find that both the N and C termini reside in the cytosol. Thus, SSP adopts a bitopic topology in which the C terminus is translocated from the lumen of the endoplasmic reticulum to the cytoplasm. This model is supported by i) the presence of two conserved hydrophobic regions in SSP (hφ1 and hφ2) and ii) our previous demonstration that lysine-33 in the ectodomain loop is essential for pH-dependent membrane fusion. Moreover, we demonstrate that introduction of a charged side chain or single amino-acid deletion in the membrane-spanning hφ2 region significantly diminishes SSP association in the GP-C complex and abolishes membrane-fusion activity. Taken together, our results suggest that bitopic membrane insertion of SSP is centrally important in the assembly and function of the tripartite GP-C complex.

* This chaper is taken from the paper cited below published in Journal of Virology.

Agnihothram, S. S., J. York, M. Trahey and J. H. Nunberg. 2007. Bitopic membrane toplogy o fthe stable signal peptide in the tripartite Junin virus glycoprotein complex. J Virol **81:**4331-37.

2. Introduction

Arenaviruses species are found worldwide, each with their respective rodent host (33, 152). Infection in humans occurs through contact with rodents and can cause severe acute hemorrhagic fevers (121, 143). In Africa, up to 300,000 infections by the Lassa fever virus occur annually (122), and outbreaks of Junín, Machupo, and Guanarito viruses arise sporadically in South America (143). Transplant-associated infections by lymphocytic choriomeningitis (LCM) virus have recently been reported in the United States (28). Without effective treatment or immunization, the hemorrhagic fever arenaviruses remain an urgent public health and biodefense concern.

The arenaviruses are enveloped viruses whose genome consists of two single-stranded RNA molecules that encode ambisense expression of four viral proteins (21, 34). The envelope glycoprotein (GP-C) mediates entry of the virus into the host cell and is the primary target for virus-neutralizing antibodies (56, 153). In contrast to other viral envelope glycoproteins, the arenavirus GP-C retains its cleaved, stable signal peptide (SSP) as an essential element of the mature complex, in addition to the conventional receptor-binding (G1) and transmembrane fusion (G2) subunits (52, 62, 188). In the nascent GP-C protein, the signal sequence acts to direct polypeptide synthesis to the endoplasmic reticulum (ER), where it is cleaved from the G1-G2 precursor by the cellular signal peptidase (SPase) in the ER lumen (20, 52, 185). The mature G1 and G2 subunits are generated through cleavage of the G1-G2 precursor glycoprotein by the cellular SKI-1/S1P protease (10, 90, 98) in the early Golgi compartment (23, 39, 53). The tripartite GP-C complex is ultimately transported to the cell surface for virion assembly and budding (139, 164).

During virion entry, the G1 subunit interacts with cell-surface receptors (8, 43) and the virion is endocytosed into smooth vesicles (15). GP-C-mediated fusion of the viral and cellular membranes is activated upon acidification of the maturing endosome to initiate viral replication (15, 27, 42, 43). Membrane fusion is promoted by a series of structural rearrangements in the ectodomain of the G2 subunit, to form a highly stable six-helix bundle typical of the so-called Class I viral fusion proteins (64, 183).

SSP is distinguished from conventional signal peptides by its length (58 amino-acid) (52) and by myristate addition at its N-terminus (188). On co-expression of a stand-alone SSP peptide with a recombinant G1-G2 precursor containing a conventional signal sequence, the components are able to associate in *trans* to reconstitute a functional GP-C complex (1, 50, 188). Recent studies in our laboratory have demonstrated that SSP is specifically required for GP-C transport from the ER and to the cell surface (1), as well as for the pH-dependent membrane-fusion activity of the mature GP-C complex (187). SSP association overcomes endogenous ER localization signals in the cytoplasmic domain of G2 so as to permit transit of the complex through the Golgi, and proteolytic maturation of the G1-G2 precursor (1). By contrast, a positively charged side chain in the central region of SSP (K33) is likely exposed on the extracellular face of the membrane to modulated the pH at which membrane fusion is activated (187). Thus, SSP appears to interact with both the cytoplasmic tail and ectodomain of the G2 transmembrane fusion protein. To investigate the structure and function of this unique subunit in GP-C, we sought to define the topology of SSP in the membrane.

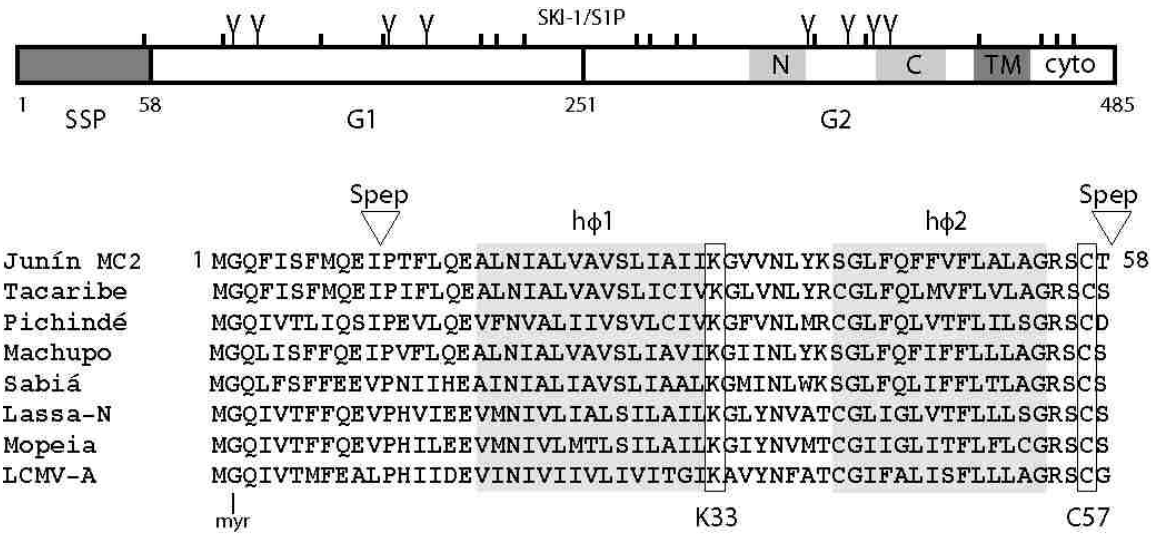

Figure 19. Schematic representation of the Junín virus GP-C glycoprotein and SSP sequences.

Amino acids of the Junín virus envelope glycoprotein are numbered from the initiating methionine, and cysteine residues (|) and potential glycosylation sites (Y) are marked. The SSP and SKI-1/S1P cleavage sites, and the resulting SSP, G1 and G2 subunits are indicated. Within G2, the C-terminal transmembrane (TM) and cytoplasmic (cyto) domains are shown, as are the N- and C-terminal heptad-repeat regions (light gray shading). A comparison of SSP sequences among arenavirus species is detailed below. Sequences include the New World isolates Junín (D10072), Tacaribe (M20304), Pichindé (U77601), Machupo (AY129248), and Sabiá (YP_089665) and Old World isolates Lassa–Nigeria (X52400), Mopeia (M33879), and LCMV-Armstrong (M20869). The two hydrophobic regions (hφ1 and hφ2) are highlighted in gray, and critical K33 (187) and C57 (185) residues are highlighted in grey. The N- and C-terminal sites for insertion of the 15 amino acid S-peptide (Spep) are indicated as inverted triangles.

Sequence analysis of the SSP among New World and Old World arenaviruses (Fig. 19) suggests two hydrophobic regions (hφ1 or hφ2) (51, 62) that may potentially be inserted in the lipid bilayer. The N terminus of SSP is myristoylated in the cytosol, whereas the C terminus is generated by SPase cleavage in the lumen of the ER (20, 52, 185). Although the C-terminal region of SSP in the GP-C precursor obeys well-documented rules for recognition by SPase (175), the sequence requirements for SSP function in the mature complex are quite different. Specifically, the invariably conserved cysteine residue at position -2 from the SPase cleavage site (C57) is dispensable for SPase cleavage, but is absolutely essential for *trans*-complementation by the SSP peptide (185). The requirement at C57 does not arise through disulfide-bond formation, as the SSP subunit is noncovalently associated in the mature GP-C complex (185, 188). This observation has led us to hypothesize that the penultimate C-terminal C57 side chain may lie in the reducing environment of the cytoplasm. Here, we demonstrate that SSP of the New World Junín arenavirus GP-C displays bitopic membrane topology with both the N and C termini residing in the cytosol. This model will guide further investigations of the requirements for SSP association in the tripartite GP-C complex and the interactions that modulate pH-dependent membrane fusion.

3. Results

We have used digitonin to selectively permeabilize cells expressing Junín virus GP-C in order to examine the intracellular disposition of the N and C termini of SSP. Low concentrations of digitonin permeabilize the plasma membrane (due to its higher cholesterol content) while leaving intracellular membranes intact (92). Protein epitopes that lie in the cytosol are thus accessible in digitonin-permeabilized cells, whereas

luminal targets are protected. To validate this methodology, we confirmed the luminal localization of the G1 subunit in wild-type GP-C using a monoclonal antibody directed to G1 (MAb BE08) (153). As illustrated in Fig. 20A (top panel), the G1 subunit was found on the surface of intact cells using MAb BE08 and an Alexa Fluor 488-conjugated (green) secondary $F(ab')_2$ antibody. On complete solubilization of the cell membranes with 0.1% Triton X-100 detergent, G1 was also detected intracellularly in the ER and Golgi compartments (Fig. 20A and (1)). On the other hand, in cells treated with 5 μg/ml digitonin, the G1 subunit was only detected at the plasma membrane and not intracellularly. This pattern is in accordance with the localization of G1 on the outside of the cell, and its protection from staining in the lumen of the internal membranes.

As a positive control for permeabilization of the plasma membrane, digitonin-treated cells were also stained using an antibody directed to the cytoplasmic domain of giantin, an integral Golgi protein (105). The cytosolic epitope was visualized with a rabbit polyclonal antibody (PRB-114C; Covance Research Products) and an Alexa Fluor 568-conjugated secondary antibody (Fig. 20A). This red staining confirms disruption of the plasma membrane. The green (anti-G1) and red fluorescence signals in digitonin-treated cells were spatially distinct and non-overlapping, in keeping with their respective cell-surface and cytosolic locations. Taken together, these studies confirm the utility of digitonin treatment to distinguish between cytosolic and luminal domains of transmembrane proteins.

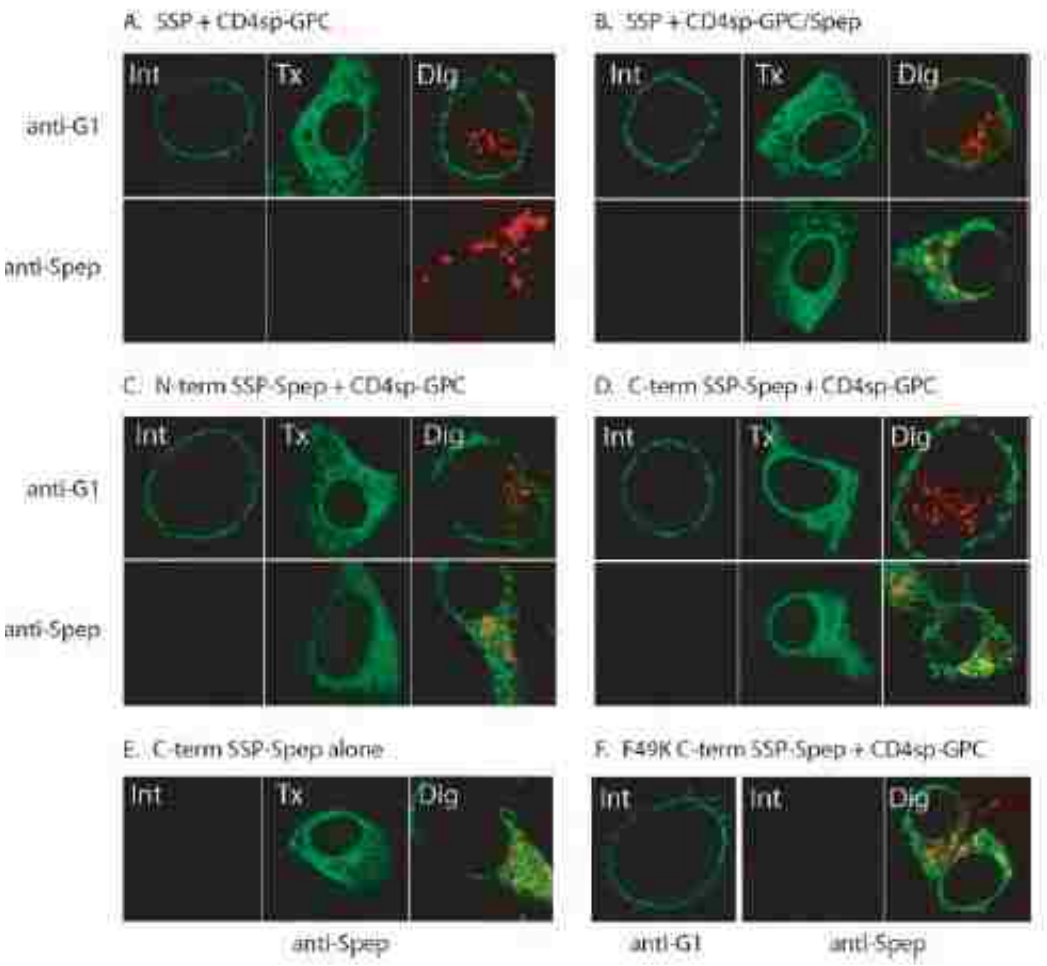

Figure 20. Confocal microscopy of digitonin-permeabilized cells.

Vero cells on 2-well chambered coverglasses (Lab Tek II) were infected with the recombinant vaccinia virus vTF7-3 expressing T7 polymerase (63), transfected to express the indicated GP-C proteins, and grown for 6 hrs in growth medium containing 10 μM araC (1). Intact cells (Int) were incubated in the cold with anti-G1 MAb BE08 (anti-G1) or anti-Spep MAb MA1-198 (anti-Spep) and an Alexa Fluor 488-conjugated (green) anti-mouse immunoglobulin secondary $F(ab')_2$ fragment (Molecular Probes) prior to fixation with 2% formaldehyde. For staining of cells treated with 0.1% Triton X-100 (Tx), cultures were fixed prior to permeabilization. Selective permeabilization with 5 μg/ml

digitonin (Dig) was done in the cold using live cells, prior to incubation with primary and secondary antibodies and fixation. Intact and digitonin-treated cells were also incubated with a rabbit polyclonal antibody directed against the cytoplasmic domain of giantin (PRB-114C, Covance Research Products) and an Alexa Fluor 568-conjugated (red) secondary antibody (Molecular Probes) in parallel with the respective anti-G1 or anti-Spep antibodies, to detect permeabilization of the plasma membrane. Chambers were covered with Slow Fade Gold (Molecular Probes) and visualized using an inverted Nikon TE-300 microscope. Fluorescence was examined using a BioRad Radiance 2000 confocal laser scanning microscope and images were merged using Lasersharp software (BioRad). Note that the left-most image in panel F was captured at greater laser power than others to enhance visibility; the intensity of cell-surface anti-G1 staining in the F49K mutant was approximately 25% of wild-type levels. The images omitted in the layout of panel F were all unremarkable.

N- and C-terminally Spep-tagged SSPs reveal bitopic membrane topology.

A 15 amino acid S-peptide affinity tag (Spep (88)) was introduced into the recombinant SSP peptide to examine the localization of the N and C termini of SSP. We have previously shown that Spep could be appended to the C-terminus of SSP without affecting the ability of the SSP subunit to *trans*-complement a G1-G2 precursor bearing the conventional signal peptide of CD4 (CD4sp-GPC) (185). This C-terminally tagged SSP construct containing a T58R mutation (to prevent SPase cleavage (185)) is termed C-term SSP-Spep. The Spep tag can also be appended at the cytosolic C-terminus of G2 in CD4sp-GPC without detriment (183, 188). Both tagged molecules, C-term SSP-Spep and CD4sp-GPC/Spep, can promote pH-dependent membrane fusion when *trans*-complemented by their respective untagged partners (185, 188).

Here, we engineered Spep into the N-terminal region of SSP (Fig. 1), between residues I11 and P12 (N-term SSP-Spep). This tagged SSP associated with CD4sp-GPC in *trans* comparably to C-term SSP-Spep (Fig. 21A). N-term SSP-Spep also supported SKI-1/S1P maturation of the G1-G2 precursor in the Golgi (bottom panel) and transport of the GP-C complex to the cell surface (Fig. 21B). Interestingly, the GP-C complex containing N-term SSP-Spep was unable to mediate pH-dependent cell-cell fusion (not shown). Nonetheless, both N- and C-terminally tagged SSPs allow for assembly of the tripartite GP-C complex and its transit to the cell surface, and therefore provide biologically relevant structures for the determination of SSP membrane topology.

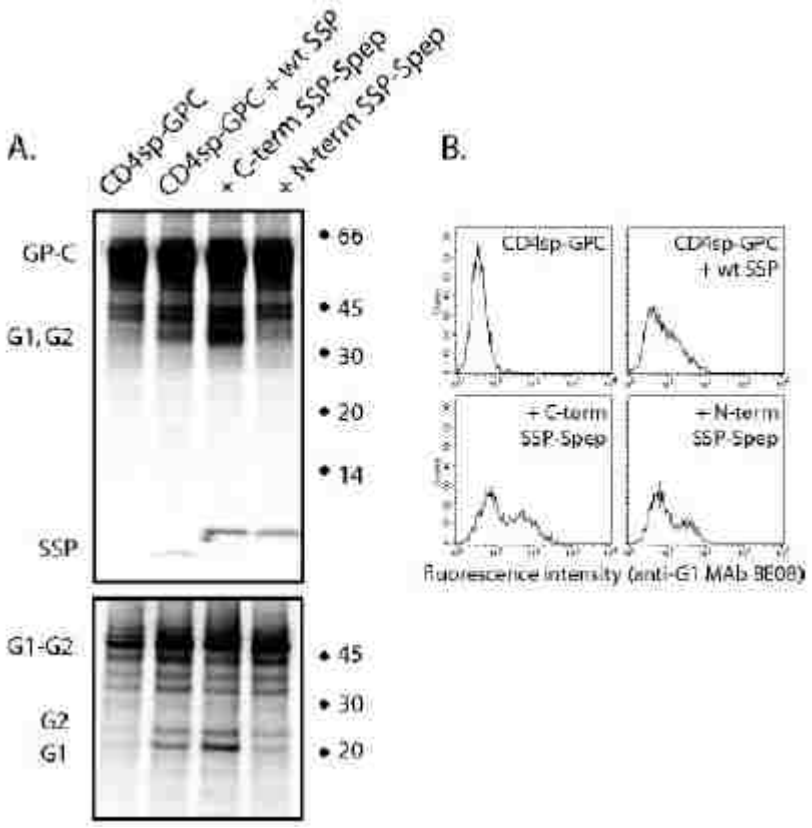

Figure 21. Expression of GP-C complex containing terminally-tagged SSP.

(A) Vero cells were transfected to express CD4sp-GPC alone or in *trans* with wild-type SSP, C-term SSP-Spep or N-term SSP-Spep (187). In all cases, transcription was directed by the T7 polymerase of vTF7-3 (63, 188). Metabolically labeled glycoproteins were immunoprecipitated using a G1-specific MAb BF11 (153) and separated on NuPAGE (Invitrogen) 4-12% Bis-Tris gels under denaturing and reducing conditions (top panel). The G1 glycoprotein migrates heterogeneously with the discrete G2 subunit, and together is labeled G1, G2. In the bottom panel, the glycoproteins were first treated with PNGase F to resolve both the G1 and G2 polypeptides (188). [14C]-labeled protein markers (Amersham Biosciences) are indicated (in kilodaltons). (B) Cell-surface expression of the GP-C complex was determined by flow cytometry using MAb BE08 (1, 187). The cell

population was subsequently stained using propidium iodide (1 μg/ml) to exclude dead cells. Formaldehyde-fixed cells were analyzed using a FACSCalibur flow cytometer (BD Biosciences).

GP-C complexes containing either the N-term or C-term SSP-Spep subunit were readily detected on the surface of intact cells with the G1-directed MAb BE08 (Figs. 20B and C respectively), reflecting their wild-type assembly and transport. In contrast, a MAb raised against the S-peptide (MA1-198; ABR) was unable to detect Spep on the surface of cells expressing the *trans*-complemented complexes, as indicated by the lack of green fluorescence in the lower panels. The cytoplasmic tag at the C-terminus of G2 in CD4sp-GPC/Spep was likewise not detected on the cell surface upon *trans*-complementation (Fig. 20B). With complete solubilization of the cell membranes using 0.1% Triton X-100, both G1 and Spep were visualized intracellularly by their respective MAbs. Importantly, the Spep tag was detected inside cells selectively permeabilized with 5 μg/ml digitonin. These cells expressing *trans*-complemented N-term SSP-Spep or C-term SSP-Spep (Fig. 20B and C) showed intracellular staining of Spep comparable to that of *trans*-complemented CD4sp-GPC/Spep (Fig. 20D), indicating cytosolic localization of the Spep tags. Colocalization of some of the Spep tag (in green) with the Golgi marker giantin (red) is indicated by the orange/yellow color.

Collectively, these results suggest that SSP assumes a bitopic topology in the membrane with both the N and C termini in the cytosol (Fig. 22). In this model, hφ1 and hφ2 span the membrane in opposite orientations. The intervening central region of SSP forms a short ectodomain loop that includes the K33 residue critical for pH-dependent membrane fusion (187).

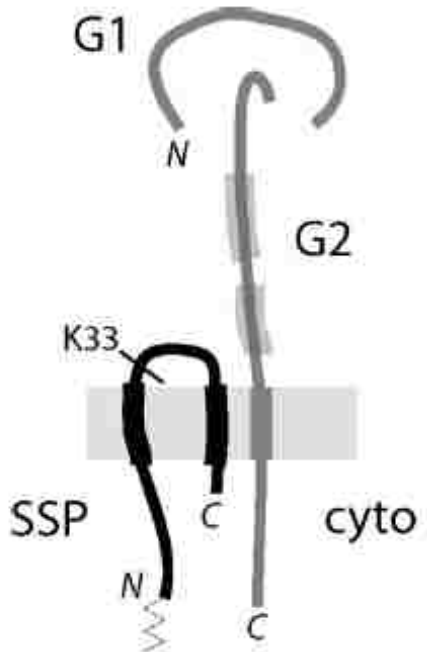

Figure 22. Model for bitopic topology of SSP in the GP-C complex.

In this drawing, insertion of the hφ1 and hφ2 regions of SSP in the membrane results in both N and C termini of SSP residing in the cytosol. The intervening ectodomain of SSP includes the K33 side chain that is critical for pH-dependent membrane fusion (187), perhaps through interaction with the membrane-proximal or heptad-repeat (thicker lines) regions of the G2 ectodomain. The drawing is not to scale.

Bitopic topology of SSP is independent of G1-G2 expression.

Our model for membrane insertion of SSP requires that the C terminus of SSP be translocated across the membrane following SPase cleavage. To determine whether this translocation is dependent on SSP interaction with the G1-G2 precursor, we examined the intracellular localization of the C terminus of C-term SSP-Spep upon expression without CD4sp-GPC. As shown in Fig. 20E, the pattern of Spep staining in digitonin-permeabilized cells was indistinguishable in the presence and absence of the G1-G2 precursor. The SSP amino-acid sequence alone is sufficient for translocation of the C terminus of SSP into the cytosol. Because our methods do not specifically detect Spep in the lumen, we cannot exclude the possibility that the SSP C terminus is distributed on both sides of the membrane. If so, small effects of the G1-G2 precursor on this balance may be difficult to visualize.

The orientation of membrane-spanning protein segments is thought to be determined co-translationally during passage of the nascent protein through the channel of the translocon machinery (137, 181). In membrane proteins with type II topology, the N terminus generated by SPase cleavage is likely translocated to the cytosol prior to insertion of the transmembrane domain into the lipid bilayer. Similarly, the C termini of the signal sequences of the hepatitis C virus envelope glycoproteins are reoriented into the cytosol upon SPase cleavage (35). In some polytopic proteins, transmembrane segments can be reoriented post-translationally (110, 136). This dynamic flexibility in membrane insertion allows certain proteins to assume two distinct membrane topologies (110, 123, 130, 136). We surmise that the short cytoplasmic C terminus of SSP is translocated to the cytosol prior to SSP insertion in the membrane.

Genetic analysis of the hφ2 amino-acid sequence.

We utilized site-directed mutagenesis to further investigate the role of hφ2 as a membrane-spanning region and identify sequence determinants of SSP association in the GP-C complex. Previous studies have shown that charged residues flanking hφ2 (K40 and R55) are dispensable for SSP function (187). In this study, we individually replaced positions F44, Q45, F46, F47 and F49 at the center of hφ2 with alanine in order to examine the effect of sequence alterations. In all five mutants, SSP associated with the GP-C complex (Fig. 23A left) and supported wild-type levels of pH-dependent membrane fusion (Fig. 23B). We subsequently replaced these residues in blocks of three (44FQF46 and 47FVF49) with alanines and again did not observe a defect in SSP function (Fig. 23B). Only when all six residues in SSP were changed to alanine (44-49A) did the mutant show a deficiency in SSP association and abrogation of GP-C-mediated cell-fusion activity. We conclude that the side chain requirements in hφ2 for SSP association in the GP-C complex and membrane fusion are minimal, consistent with hφ2 insertion in the lipid bilayer.

Introducing a charged residue within the region hφ2 of SSP would however be expected to be disruptive. In fact, F46K and F49K mutants of SSP were markedly reduced in their ability to associate with GP-C (Fig. 23A right). Nonetheless, the lysine side chain did not prevent insertion of hφ2 into the membrane, as judged by the retention of bitopic topology in digitonin-permeabilized cells expressing a C-terminally tagged F49K mutant of SSP (Fig. 20F, anti-Spep MAb). Positively charged residues have been reported to be accommodated in other naturally occurring and model transmembrane helices (126, 179).

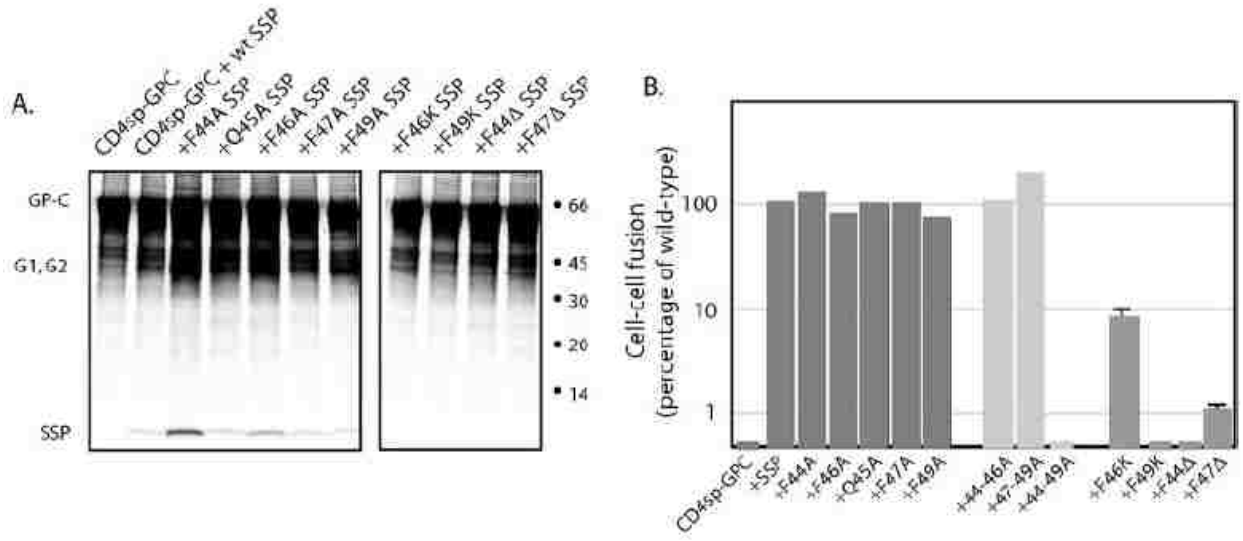

Figure 23. Genetic analysis of the hφ2 region of SSP.

(A) SSP mutants without Spep tags were expressed in *trans* with CD4sp-GPC, and the radiolabeled GP-C complex was immunoprecipitated using the anti-G1 MAb BF11 as described in the legend of Figure 21. Stable association of SSP in the GP-C complex is demonstrated by co-precipitation of the SSP subunit. Right and left panels were imaged at comparable settings; excessive darkening of the right panel reveals low levels of SSP (see text). (B) pH-dependent cell-cell fusion by the *trans*-complemented GP-C complex was initiated by a pulse of medium at pH 5.0 and detected using the recombinant vaccinia virus-based β-galactosidase-reporter assay (132) as previously described (187, 188). β-galactosidase expression induced upon syncytium formation was quantitated using the chemiluminescent substrate GalactoLite Plus (Tropix), and the percentage of pH-dependent fusion relative to the wild-type GP-C complex is indicated. Error bars (± 1 standard deviation) are drawn where discernible on the scale of the graph.

Interestingly, SSP association in GP-C was not completely abrogated by the F46K and F49K mutations and could be detected in overly darkened images of Fig. 23A (not shown). Notably, the level of F49K SSP association was sufficient to enable limited transport of the assembled GP-C complex to the cell surface (Fig. 20F, anti-G1 MAb). Residual cell-surface expression was approximately 25% of wild-type levels and was also observed in complexes containing 44-49A SSP (not shown). By comparison, no G1-G2 glycoprotein is detected on the surface of intact cells in the absence of SSP (1). Despite transit of the complex to the cell surface, the F46K and F49K mutants were largely unable to support membrane-fusion activity (Fig. 23B). F46K SSP allowed fusion at 10% of wild-type levels whereas the complex containing F49K SSP was entirely defective. The elimination of membrane-fusion activity by the F49K mutation is likely not due to the low level of GP-C on the cell surface, as cell-cell fusion by wild-type complex is retained at far lower levels of expression ((183) and unpublished). Although the mutation at F49K is compatible with a bitopic topology of SSP and with limited assembly and transport of the GP-C complex, we infer that the placement of the mutant SSP in the membrane is sufficiently perturbed to abolish membrane-fusion activity.

Further evidence that hφ2 spans the membrane was obtained by examining the effects of single amino-acid deletions. These changes would shorten the putative transmembrane domain and may preclude proper positioning in the membrane. Additionally, the deletions will affect the register of any transmembrane helical regions. Single amino-acid deletions at F44 or F47 (F44Δ and F47Δ) markedly reduced SSP association with GP-C (Fig. 23A left) and ablated its membrane-fusion activity (Fig. 23B). Taken together, these results are consistent with hφ2 region spanning the membrane to bring the C terminus of

SSP to the cytosol, and suggest an important role for this region in the assembly and function of the GP-C complex.

4. Discussion

SSP topology in the Old World arenaviruses.

Previous attempts to determine the membrane topology of the SSP of the Old World LCM and Lassa fever viruses have yielded different and mutually conflicting results (51, 62). Our model for a bitopic topology in the New World Junín arenavirus SSP differs from both previous suggestions. These differences may reflect the phylogenetic division between New World and Old World arenaviruses (33), or the use of different recombinant SSP constructs. In our studies of the Junín virus SSP, we have confirmed the functional integrity of the Spep-tagged N- and C-term SSP peptides in assembly and transport, and thus the biological relevance of their membrane disposition. However, our studies do not assess whether termini of SSP also reside in the ER lumen. Because membrane insertion can be dynamic, it remains possible that the hydrophobic regions in SSP can display mixed orientations, some of which give rise to the luminal C-terminus proposed for the Old World viruses (51, 62). If so, none of these alternative topologies was found on the surface of cells expressing the GP-C complex of Junín virus.

Role of bitopic topology in the stable association of SSP.

Although the C-terminus of SSP is able to translocate to the cytosol in the absence of the G1-G2 precursor, it is plausible that interactions in the GP-C complex may stabilize the bitopic form of SSP under natural conditions. The cytoplasmic domain of G2 is itself required for SSP association (1). Here we demonstrate that SSP mutations that likely

perturb the placement of hφ2 in the membrane (F46K, F49K, F44Δ and F47Δ) greatly reduce SSP association in the GP-C complex. Stable association of SSP in GP-C is also dependent on the penultimate C-terminal residue in SSP, C57 (185). Although C57 does not participate in disulfide-bond formation in the mature GP-C complex, the requirement for the thiol side chain at this cytosolic position is absolute. The C57S mutant of SSP, for instance, is unable to associate with G1-G2 precursor (185). In the absence of precedents from other viral envelope glycoproteins, the structure and function of SSP remain to be fully defined. It is possible that the critical C57 residue interacts noncovalently with the cytoplasmic domain of G2 to stabilize the bitopic form of SSP and thus position the ectodomain loop for its role in pH-dependent membrane fusion. The unique organization of the arenavirus GP-C complex may also present novel opportunities for antiviral intervention (14).

5. Materials and Methods

Confocal microscopy

Vero cells on 2-well chambered coverglasses (Lab Tek II) were infected with the recombinant vaccinia virus vTF7-3 expressing T7 polymerase (63), transfected to express the indicated GP-C proteins, and grown for 6 hrs in growth medium containing 10 μM araC (1). Intact cells were incubated in the cold with anti-G1 MAb BE08 or anti-Spep MAb MA1-198 and an Alexa Fluor 488-conjugated (green) anti-mouse immunoglobulin secondary F $(ab')_2$ fragment (Molecular Probes) prior to fixation with 2% formaldehyde. For staining of cells treated with 0.1% Triton X-100 cultures were fixed prior to permeabilization. Selective permeabilization with 5 μg/ml digitonin was done in the cold

using live cells, prior to incubation with primary and secondary antibodies and fixation. Intact and digitonin-treated cells were also incubated with a rabbit polyclonal antibody directed against the cytoplasmic domain of giantin (PRB-114C, Covance Research Products) and an Alexa Fluor 568-conjugated (red) secondary antibody (Molecular Probes) in parallel with the respective anti-G1 or anti-Spep antibodies, to detect permeabilization of the plasma membrane. Chambers were covered with Slow Fade Gold (Molecular Probes) and visualized using an inverted Nikon TE-300 microscope. Fluorescence was examined using a BioRad Radiance 2000 confocal laser scanning microscope and images were merged using Lasersharp software (BioRad)

Expression of GP-C complex containing terminally-tagged SSP

Vero cells were transfected to express CD4sp-GPC alone or in *trans* with wild-type SSP, C-term SSP-Spep or N-term SSP-Spep (187). In all cases, transcription was directed by the T7 polymerase of vTF7-3 (63, 188). Metabolically labeled glycoproteins were immunoprecipitated using a G1-specific MAb BF11 (153) and separated on NuPAGE (Invitrogen) 4-12% Bis-Tris gels under denaturing and reducing conditions. To resolve both the G1 and G2 polypeptides, the glycoproteins were treated with PNGase F as described elsewhere (188).

Flow cytometry

Cell-surface expression of the GP-C complex was determined by flow cytometry using MAb BE08 as described (1, 187). The cell population was subsequently stained using propidium iodide (1 μg/ml) to exclude dead cells. Formaldehyde-fixed cells were analyzed using a FACSCalibur flow cytometer (BD Biosciences).

Cell-cell fusion assay

pH-dependent cell-cell fusion by the *trans*-complemented GP-C complex was initiated by a pulse of medium at pH 5.0 and detected using the recombinant vaccinia virus-based β-galactosidase-reporter assay (132) as previously described (187, 188). β-galactosidase expression induced upon syncytium formation was quantitated using the chemiluminescent substrate GalactoLite Plus (Tropix), and the percentage of pH-dependent fusion relative to the wild-type GP-C complex is represented.

CHAPTER FIVE

ROLE OF GP-C COMPLEX IN ARENAVIRUS ASSEMBLY AND MORPHOGENESIS

1. Abstract

The arenavirus envelope glycoprotein complex retains a myristoylated stable signal peptide (SSP) that has been shown to play a crucial role in intracellular trafficking (1) and pH-dependent membrane fusion (187) of the envelope glycoprotein complex. Immunogold electron microscopy was utilized to investigate the organization of GP-C on the plasma membrane. GP-C was found to cluster into membrane microdomains of 120 nm sizes independent of other viral proteins. Evidence from biochemical studies pointed out that these GP-C containing microdomains may represent detergent-soluble regions on the plasma membrane. Surprisingly, clustering of GP-C was not affected by SSP mysristoylation as the G2A mutant exhibited a phenotype similar to the wild type GP-C. Co-expression of the matrix protein Z did not alter clustering of wild type GP-C, since the pattern of GP-C organization into 120 nm microdomains remained the same in the presence of the Z protein. Z was distributed randomly with respect to GP-C, and regions of the plasma membrane containing Z protein did not colocalize with GP-C containing microdomains. Taken together, these results provide support to a model that clustering of proteins or lipids on the plasma membrane might bring Z and GP-C together to form arenavirus budding sites.

2. Introduction

An important step in the life cycle of enveloped viruses is the assembly of viral structural proteins at the cellular compartment where virion budding occurs. Among the structural proteins, the membrane-associated matrix protein typically promotes virion assembly and budding. During this process, specific interactions between envelope glycoprotein and the matrix protein at the site of virion assembly allow for incorporation of the envelope glycoprotein in the budding virions (65). Signals for membrane targeting of matrix and envelope proteins could be specified by the amino acid sequence or could arise as a result of post translational modification such as acylation. Some viruses like Mouse hepatitis virus (MHV) and Hepatitis B virus bud intracellularly from membranes of Golgi and ER respectively (65), whereas others including Human immunodeficiency virus type-1 (HIV-1), Influenza virus (IV) and Human respiratory syncitial virus (HRSV) bud from the plasma membrane (65). Viruses that bud from the plasma membrane often employ membrane microdomains, that are specifically enriched in protein and lipid content, as a platform for virus assembly. Membrane microdomains are postulated to have dynamic and lateral mobility that facilitates clustering of proteins and lipids and is implicated in a variety of cellular processes including signal transduction, protein trafficking and assembly of viruses (17, 30, 159). Lipid rafts are a group of membrane microdomains that have been highly studied till date. These sphingolipid and cholesterol rich microdomains range from 100-150 nm in size and are operationally defined by their insolubility in low concentrations of non-ionic detergents such as TX-100 (6, 30, 159). Rafts function as platforms for protein-protein interaction and macromolecular assembly in the cell (30, 149). Several enveloped viruses including HIV-1, Influenza, Ebola,

Marburg, Measles, and Newcastle disease virus utilize lipid rafts as a platform for virus assembly and budding (3, 9, 44, 91, 100, 118, 131, 133, 154, 166, 174), where the matrix and envelope proteins interact with each other and thereby promote virus budding (29). Membrane association of matrix protein in such cases can be mediated by myristoylation co-operating with a cluster of basic amino acid residues as in Gag protein of retroviruses (76), or a stretch of α-helical hydrophobic residues as in M1 protein of IV (156). Similarly, membrane association of envelope glycoproteins may be regulated by palmitoylation as in the case of HIV gp41 (11) and coronavirus S protein (173). In several cases, fatty acid modifications has been found to target cellular and viral proteins to membrane microdomains including lipid rafts (149, 150).

Arenavirus particles bud from the plasma membrane (128) and the 11KDa RING zinc-finger protein Z is the matrix protein that self assembles at the plasma membrane to direct the budding of enveloped VLPs (139, 164). Myristoylation of Z is critical for both membrane association and formation of VLPs (142). Although Z is sufficient to form VLPs, incorporation of GP-C is essential for the formation of infectious virions. GP-C is also myristoylated at its N terminus (188) , and is transported to the cell surface in the absence of other viral proteins (10, 90). Mechanisms underlying arenavirus assembly have not been characterized and the membrane organization of arenavirus structural proteins is less clear. In particular, there is no information regarding the pattern of GP-C distribution on the plasma membrane and the genetic determinants in GP-C that contribute to its membrane trafficking. Electron cryomicroscopic studies of arenavirus virions show a close apposition of GP-C and Z on the internal side of the virion (100), and co-immunoprecipation studies have demonstrated a biochemical association between

Z and GP-C (25). These data along with the observations that both Z and GP-C are myristoylated (142, 188) led us to hypothesize that they both may be targeted to detergent resistant membrane microdomains (DRMs) on the plasma membrane, where the unusual cytoplasmic face of GP-C including myristoylated SSP may mediate specific protein-protein interactions with Z to facilitate arenavirus morphogenesis. Thus membrane microdomains containing GP-C and Z could serve as precursor sites for arenavirus budding.

Brown and Lyles have developed a clustering analysis technique for investigating the membrane organization of proteins using data obtained from Immunogold labeling (18, 167). In collaboration with Dr. Doug Lyle`s group at Wake Forest University School of Medicine, we employed Immunogold electron microscopy and clustering analysis to evaluate organization of GP-C in the regions of the plasma membrane. G2A mutant was included in the study to investigate the contribution of myristoylation in membrane trafficking of GP-C. We show that GP-C clusters into membrane microdomains of approximately 120 nm size on the plasma membrane in vero cells expressing GP-C under the control of vTF7-3 . Biochemical studies described in this report point out that these microdomains may represent detergent soluble membranes on the plasma membrane, indicating that they do not resemble lipid rafts. These data hint a possibility that GP-C containing microdomains could serve as precursors for virus budding sites, or they could merge together to form virus budding sites. Surprisingly, myristoylation did not affect clustering of GP-C into membrane microdomains as the G2A mutant partitioned into microdomains of approximately 120 nm in size, similar to the wild-type GP-C. We also show that co-expression of Z does not alter the pattern of GP-C distribution as GP-C was

found to cluster into microdomains of 120 nm size either in the presence or absence of Z. These results indicate that membrane trafficking of GP-C is not influenced by Z, but may be directed either by other viral proteins or determinants in GP-C including the transmembrane or ectodomain of G2. Moreover, Z showed random distribution on the plasma membrane in correlation with GP-C and the regions of the membrane that contained Z protein were found not to co-localize with GP-C containing microdomains. Taken together, these observations provide support to a model where clustering of proteins or lipids on the plasma membrane may bring Z and GP-C together to form arenavirus budding sites. This chapter also describes the development of a reverse-genetic system to study the role of GP-C in arenavirus morphogenesis and infectivity.

3. Results

Recombinant GP-C associates with the DRMs

The mechanism by which GP-C is incorporated into the budding virions has not been studied. The observation that both GP-C is myristoylated (188) raises a possibility that GP-C may be targeted to DRMs or lipid rafts on the plasma membrane, where interaction with the matrix protein Z might promote its incorporation into budding virions. To investigate this hypothesis, we sought out to determine association of GP-C with DRMs, which are insoluble in cold 1% TX-100 because of their high sphingolipid and cholesterol content (16, 159) and can be isolated by floatation in Optiprep gradients (103, 104). These experiments were done in collaboration with Dr. Mark Grimes, at the Division of Biological Sciences, University of Montana.

In these experiments, BHK-21 cells expressing Junin GP-C under the control of a nuclear promoter (125) were lysed in cold 1% TX-100 and the DRMs were prepared and subjected to floatation in Optiprep density gradient as described in materials and methods. Gradient fractions were collected and analyzed for GP-C distribution by western blotting using an antibody to ectodomain of G2 subunit. The G2 Ab identified two predominant molecular species of GP-C (Fig. 24A, top panel): a heterodisperse smear of the G1-G2 precursor glycoprotein (~66-kDa), and a G2 glycoprotein (~45-kDa), in the detergent resistant membranes that floated at a density of 1.2 g/ml. Both of these molecular species are different from the previously reported G1-G2 precursor (60-kDa) and the proteolytically mature G2 (35-kDa) (1). Staining for caveolin, a classical lipid raft marker (168) (Fig. 24A, bottom panel) indicated that majority of GP-C containing rafts were distinct from the caveolin containing rafts as shown below (Fig. 24B)

A.

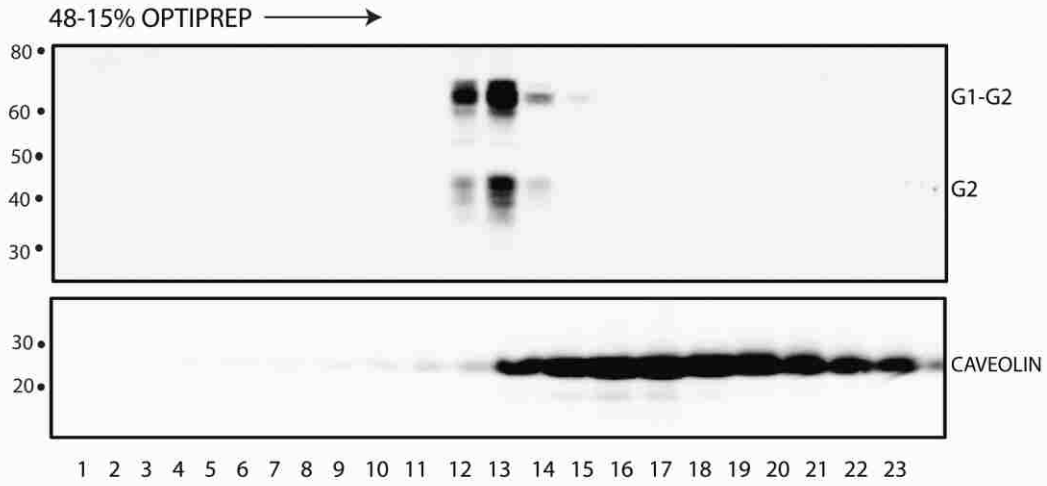
48-15% OPTIPREP
80
60
50
40
30
G1-G2
G2
30
20
CAVEOLIN
1 2 3 4 5 6 7 8 9 10 11 12 13 14 15 16 17 18 19 20 21 22 23

B.

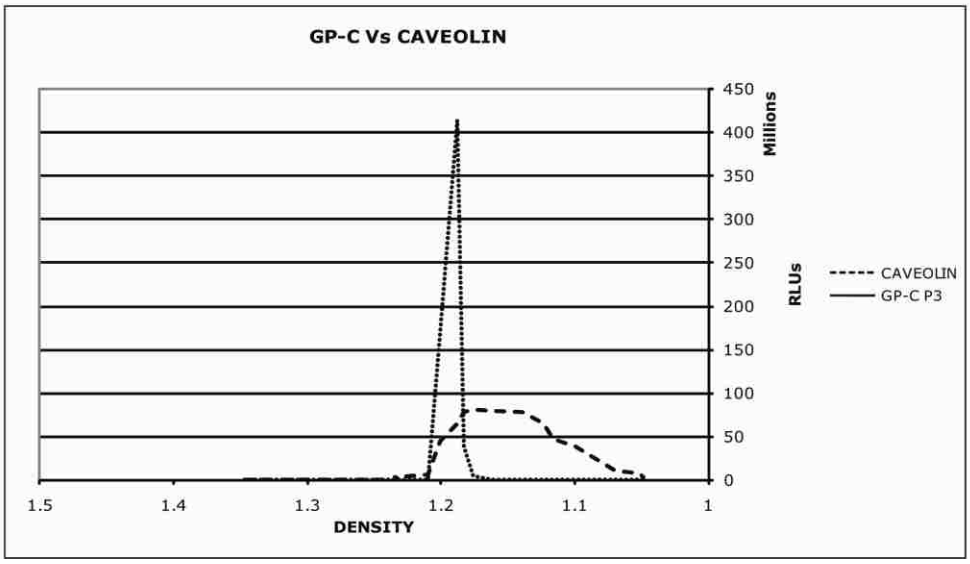
GP-C Vs CAVEOLIN
450
400
350
300
250
200
150
100
50
0
Millions
RLUs
CAVEOLIN
GP-C P3
1.5
1.4
1.3
1.2
1.1
1
DENSITY

Figure 24. GP-C associates with detergent-resistant raft microdomains that are different from caveolin containing rafts.

(A) Detergent-resistant membranes prepared from BHK 21 cells expressing GP-C were floated in an Optiprep density gradient as described in materials and methods. Gradient fractions were collected and the density of the fractions was determined by refractometer. Precipitated proteins from the gradient fractions were resolved on a 10% Bis-Tris gel and transferred to nitrocellulose membrane, which was probed with an antibody for G2. The antibody identified a heterodisperse smear of G1-G2 precursor (~66-kDa) and a G2 subunit (~45-kDa), at a density of 1.2 g/ml. The bottom panel shows caveolin staining in the gradient fractions. (B) Western blot images were analyzed using Image-gauge software (Fuji) using the profile and background tools to quantify the chemiluminiscence from GP-C and caveolin staining. The intensity of GP-C (string of beads) and caveolin (dotted lines) were plotted against the density of the fractions analyzed

Myristoylation of GP-C does not alter the association of recombinantly expressed GP-C to DRMs

To identify the role of myristoylation in raft association of GP-C, BHK-21 cells expressing the myristoylation defecient mutant of GP-C (G2A), were lysed in cold 1% TX-100, and DRMs were analyzed for GP-C distribution. Surprisingly, myristoylation did not influence the association of GP-C to detergent-resistant membranes. Western blotting showed the presence of a heterodisperse smear of the G1-G2 precursor (~66-kDa) and the G2 glycoprotein (~45-kDa) in the DRMs that float at a density of 1.2 g/ml, a pattern similar to the wild type GP-C (Fig. 25A, top panel) The G2A protein containing rafts were also different from caveolin containing rafts, as shown in the bottom panel. Taken together, these results point out that the myristoylation in SSP does not influence the membrane trafficking of recombinantly expressed GP-C.

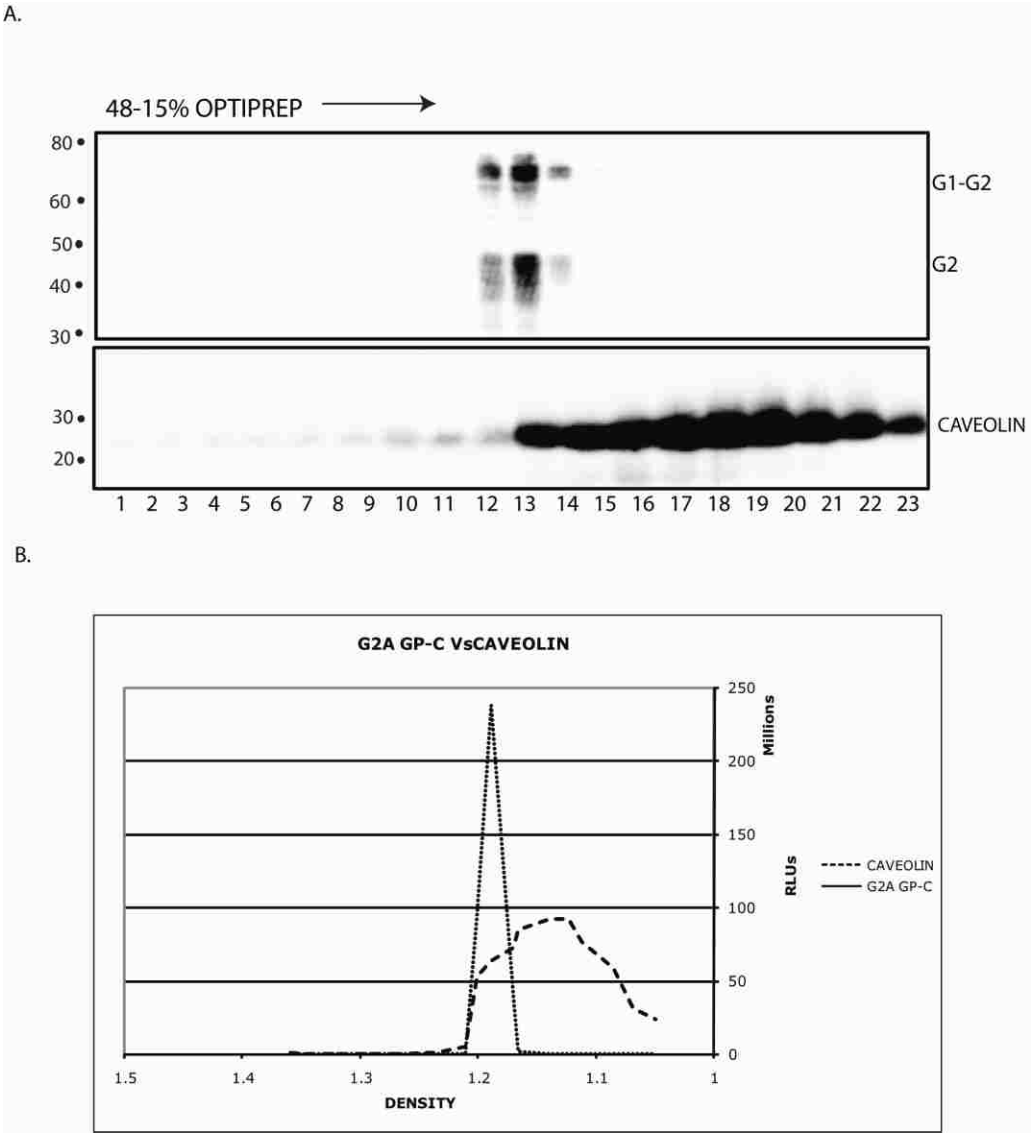

Figure 25. SSP myristoylation does not affect GP-C association to non-caveolae rafts.

(A) Western blot of the density gradient fractions containing DRMs from cells expressing G2A was analyzed as described in Panel A of Fig. 24. The bottom panel shows caveolin staining in the fractions analyzed for G2A expression. (B) The intensity of G2A and caveolin in the fractions were plotted against the density of the fractions as described in Panel B of Fig. 24.

GP-C from Candid virus infected cells completely partitions to detergent soluble fraction

To validate the observations from the recombinantly expressed GP-C, we determined the membrane trafficking pattern of GP-C from Junin virus infected cells. For these studies, DRMs prepared from vero cells infected with the Candid-1 strain of Junin virus (see materials and methods) were subjected to floatation in an Optiprep density gradient and the collected fractions were examined for GP-C distribution using the G2Ab. To our surprise, GP-C was found to be completely excluded from DRMs (Fig. 26, top panel) and all the GP-C including the G1-G2 precursor (~60-kDa) and the proteolytically mature G2 subunit (~35-kDa) was found to partition to the detergent soluble fraction (Fig. 26, two lanes indicated at the right). The molecular mass of the GP-C species described here was consistent with those previously identified by radio-immunoprecipation assay using an antibody against G1 subunit from metabolically labeled candid virions (186).

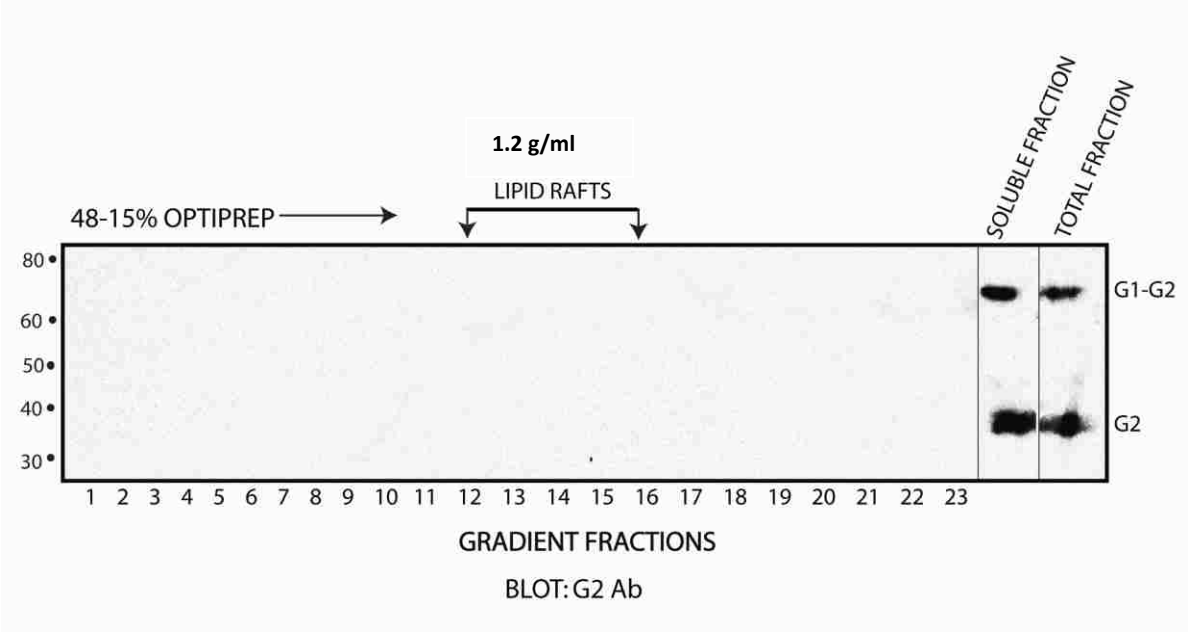

Figure 26. GP-C from Candid infected cells shows no association with detergent-resistant membrane rafts and completely partitions to detergent soluble fractions.

Detergent resistant membranes from vero cells infected with Candid-1 strain of Junin virus were analyzed for GP-C expression as described in Fig. 24, Panel A. Ten percent of total cell lysate (total fraction) and detergent soluble fraction of the lysate (soluble fraction) were also analyzed for GP-C expression. Gradient fractions from 12-16 with a density of 1.2 g/ml, where GP-C was found associated in experiments described in Fig. 25 and 26, are marked as lipid rafts.

The following observations were noteworthy from the results described above. None of the GP-C expressed from the Junin virus were associated with DRMs unlike the observation from the cells expressing recombinant GP-C. The detergent soluble GP-C species that were identified in the Junin virus infected cells migrated at a different molecular weight relative to the GP-C species that were found associated with DRMs. The heterodisperse smear of G1-G2 precursor glycoprotein from DRMs resolved at 66-kDa whereas the precursor species in the Junín virus infected cells resolved at 60-kDa. The G2 subunit in the DRMs was found to resolve at 45-kDa whereas the mass of G2 subunit from the candid virus infected cells was found to be 35-kDa. These findings clearly pointed out that GP-C expressed from Junin virus are not found associated with lipid rafts.

Co-expression of Z does not modulate membrane trafficking of GP-C

We hypothesized that the association of GP-C with other viral proteins may be a prerequisite to rescue GP-C from the detergent-resistant precursor compartment and redirect it to the detergent soluble microdomains where they may be processed to molecular species of GP-C that are relevant for incorporation into budding virions. According to this model, majority of GP-C expressed independently of other viral proteins associates with DRMs, which may be a compartment that harbors the higher molecular weight species of the precursor and G2 subunit. Expression of GP-C in the presence of other viral proteins modifies this trafficking pattern due to its association with other viral proteins and majority of the of the expressed GP-C is targeted to the detergent soluble compartment containing the right molecular weight species of GP-C to be incorporated into the budding virions.

Membrane trafficking of envelope glycoprotein has been shown to be influenced by the matrix protein in several enveloped viruses, where the raft association of envelope glycoprotein is promoted by co-expression of matrix protein (3, 70). To test the hypothesis that Z might alter the membrane trafficking of GP-C, DRMs from BHK-21 cells co-expressing GP-C and Z-Spep (Z protein with an appended S-peptide tag at the C-terminus to facilitate biochemical analysis) were subjected to density gradient floatation and the fractions were analyzed for GP-C and Z distribution.

Expression of Z resulted in identification of Z monomers and dimers that associated with the detergent-resistant membrane fractions floating at a density of 1.2 g/ml (Fig. 27, bottom panel). Interestingly, these fractions also contained the molecular species of GP-C that resembled the ones described in DRMs of GP-C and G2A expressing cells (Fig. 27, top panel). These results indicated that co-expression of the matrix protein Z does not affect the association of GP-C with DRMs.

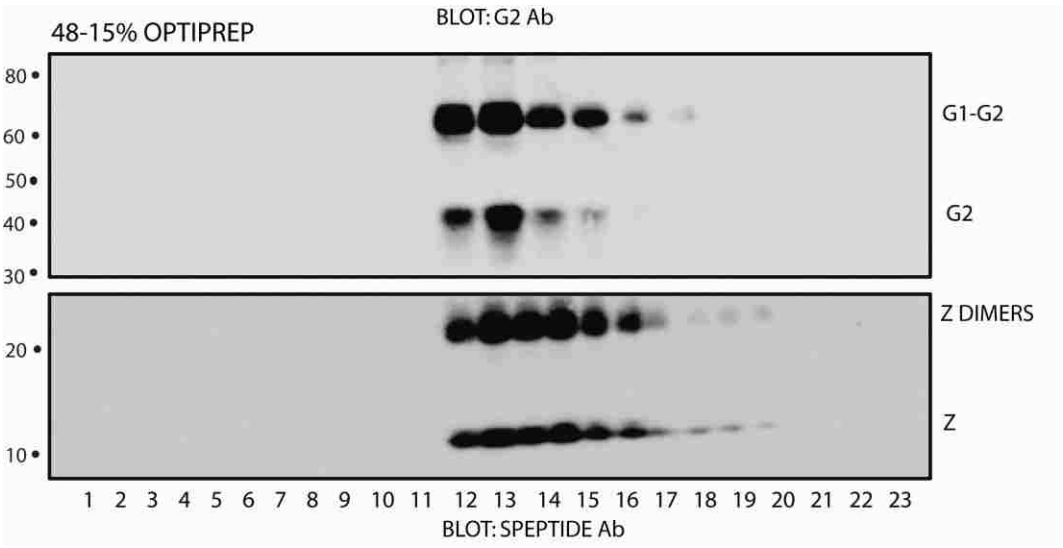

Figure 27. Co-expression of the matrix protein Z does not affect GP-C association to detergent-resistant membrane rafts.

Detergent resistant membrane fractions from cells co-expressing GP-C and Z were prepared and analyzed for distribution of GP-C (using G2 Ab) and Z distribution (anti S-peptide Ab). Z dimers (~22-kDa) are indicated.

GP-C associated with DRMs may represent proteolytic products of protein degradation in the early secretory pathway.

To examine the nature of higher molecular weight species of GP-C found in DRMs, a fraction (5%) of total cell lysates from cells expressing GP-C, G2A in the presence or absence of Z were subjected to deglycosylation by PNGase-F. Equal amounts of detergent soluble fractions from each sample mentioned above and from the candid-1 infected cells were also treated with PNGase F under similar conditions to compare the GP-C species from both the compartments. Deglycosylated proteins were resolved by SDS PAGE and identified by western blot using a G2 antibody. An aliquot of the soluble fraction from cells expressing GP-C and Z was also analyzed for Z expression using an anti S-peptide antibody. The fraction of total cell lysate in all the samples contained two distinct species of GP-C that were not present in soluble fractions. The higher molecular weight form of G1-G2 precursor (alt G1-G2, ~55k-Da) and the G2 subunit (alt G2, ~35-kDa) were found exclusively in the DRMs and absent in the detergent-soluble fraction (Fig. 28, Panel A lanes 1, 4, 7, 10). The detergent-soluble fractions in all the samples showed only the presence of lower molecular weight G1-G2 precursor (~50-kDa) and the G2 subunit (~28kDa), (Fig. 28, Panel A lanes 2, 5, 8, 11), which exactly matched with the observations from candid infected cell lysates (Fig. 28, Panel B lane 2). The glycoprotein from the detergent-soluble fraction is shown in lane 1 to illustrate the drop in molecular weights after deglycosylation of the GP-C species. Z was found to be distributed similarly in both detergent-soluble and total lysate fractions (Fig. 28, Panel E) These findings indicated that the soluble fraction in cells expressing recombinant GP-C harbors the molecular species of GP-C relevant to what is found in Junin virus infected

cells. Z reduced the expression of GP-C (Fig. 28, Panel A: compare lanes 1&2 with lanes 4&5), an observation that could be reasoned by the previous reports that arenavirus Z is an inhibitor of protein translation in eukaryotes (82).

To further explore the origin and localization of the DRM forms of GP-C, we used GP-C mutants that had well characterized phenotypes of proteolytic processing and intracellular trafficking form previous studies (1). The SKI/S1-P cleavage defective mutant (cd GP-C) that does not generate proteolytically mature G2 subunit of 35-kDa (1) and the CD4sp GPC, which is localized to the ER in the absence of SSP and does not show SKI-S1P cleavage (1) were analyzed similarly as described above. To our surprise, the alt G1-G2 and alt G2 species were identified to be present in the DRM fractions of both the GP-C mutants (Fig. 28, Panel C and D, lane1) where as the detergent-soluble fractions showed only the G1-G2 precursor as identified before (1). These experiments indicated that the higher molecular weight forms of GP-C found in DRMs are not proteolytic products of SKI/S1-P but may represent the species found associated with vesicles of the degradative pathway in between the ER and Golgi compartments. These GP-C species might represent one of the post translational modifications (e.g., ubiquitination or sumoylation) for these proteins to be sorted any specific cellular compartment, which is detergent resistant. This notion is highly supported by the fact that the in the absence of SSP much of CD4spGPC is retained in the ER (1), and quantitation of GP-C species in the DRMs shows that 97% of the expressed GP-C is found associated with DRMs, where as 3% is the G1-G2 precursor found in the detergent-soluble fraction. Thus, GP-C found in the detergent soluble compartment may represent the molecular species with right conformation which is trafficked through the Golgi and is found on the cell surface.

These results also demonstrate that the molecular species of GP-C associated with the DRMs in cells expressing recombinant GP-C are possibly products related to protein over expression and the GP-C species relevant to incorporation into budding virions partitions to detergent soluble fractions, as found in Junin virus infected cells. Taken together, these data conclude that Junin virus does not employ lipid rafts for assembly, but may utilize other microdomains on the plasma membrane where GP-C is found to cluster, as described by the Immunogold electron microscopy studies in the following section.

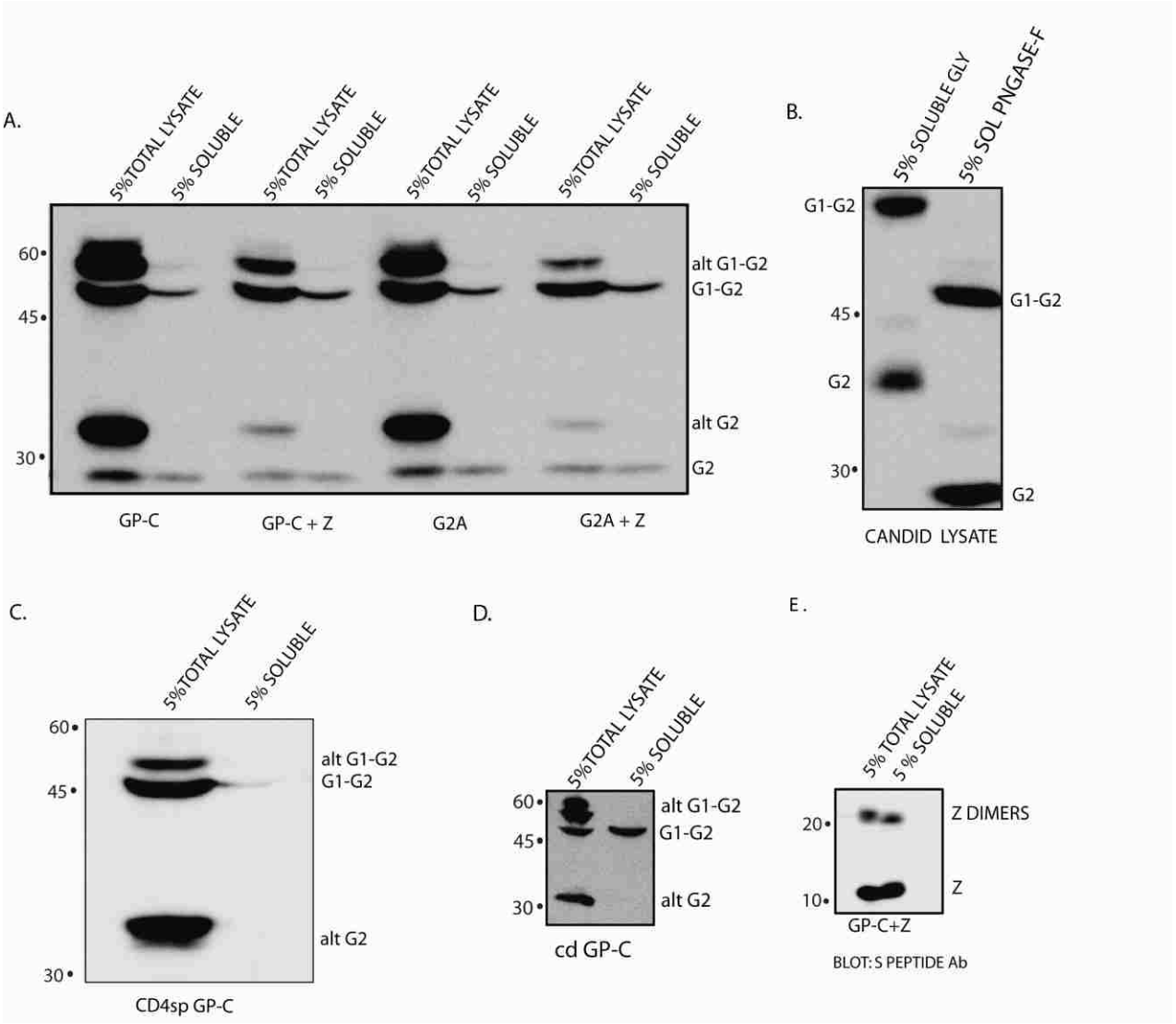
A.
5%TOTAL LYSATE
5% SOLUBLE
60•
45•
30•
alt G1-G2
G1-G2
alt G2
G2
GP-C
GP-C + Z
G2A
G2A + Z
B.
5% SOLUBLE GLY
5% SOL PNGASE-F
G1-G2
45•
G2
30•
G1-G2
G2
CANDID LYSATE
C.
5%TOTAL LYSATE
5% SOLUBLE
60•
45•
30•
alt G1-G2
G1-G2
alt G2
CD4sp GP-C
D.
5%TOTAL LYSATE
5% SOLUBLE
60•
45•
30•
alt G1-G2
G1-G2
alt G2
cd GP-C
E.
5% TOTAL LYSATE
5 % SOLUBLE
20•
10•
Z DIMERS
Z
GP-C+Z
BLOT: S PEPTIDE Ab

Figure 28. Identification of higher molecular weight species of GP-C.

(A) Cells expressing GP-C glycoproteins alone or with Z were lysed in 1% TX-100 and 5% of the total cell lysate and 5% of detergent-soluble fraction were treated with Peptide N glycosidase F (PNGase-F) to resolve the glycoprotein species. The glycoproteins were resolved on 10% Bis-Tris gels and were transferred to nitrocellulose membrane. The membrane was then probed with an antibody to G2 subunit and the bands were visualized using chemilumiscence. Note that in all the GP-C glycoproteins, the higher molecular weight species of G1-G2 (alt G1-G2, 55kDa) and G2 (altG2, 35kDa) were present in the total cell lysate and not in the detergent soluble fraction, indicating that they are localized exclusively to DRMs. The detergent soluble fraction contained proteolytically mature G2 (28-kDa) the G1-G2 precursor (50-kDa) consistent with our previously reported results (1). Co-expression of Z reduces glycoprotein expression in both GP-C and G2A expressing cells (lanes 4, 10). (B) Vero cells infected with Candid-1 strain of Junin virus were lysed in 1% TX-100 and 5% of detergent soluble fraction (treated or not treated with PNGase-F were loaded on a 10% Bis-Tris Gel and the glycoproteins were identified by western blots as described in Panel A. Note that the detergent-soluble fraction contains only the G1-G2 precursor and proteolytically mature G2, similar to be found in detergent soluble fractions of cells expressing GP-C as shown in Panel A. (C and D) Cells expressing CD4sp GPC (1) and cd GP-C (1) respectively, were treated as described in Panel A glycoprotein species were identified by western blot using an antibody to G2 subunit. (E) The fractions described in lanes 4 and 5 in panel A were probed for Z expression using an antibody to s-peptide tag.

GP-C is organized into membrane microdomains on the plasma membrane

To identify the organization of GP-C on the plasma membrane, we utilized clustering analysis approach developed by Brown and Lyles (18, 167). Vero cells expressing GP-C under the control of a recombinant vaccinia virus expressing T7 polymerase (1) were fixed, permeabilized with 5μg/ml digitonin (2) and labeled using a BEO8 mouse monoclonal antibody to G1 subunit (153) and a anti-mouse IgG conjugated to 12 nm colloidal gold particles. To avoid high density of GP-C labeling in the lumen of internal cellular membranes, we chose to permeabilize GP-C expressing cells with digitonin, instead of a non-ionic detergent such as TX-100. High intensity of GP-C labeling in the cytosol after TX-100 permeabilization might pose a practical problem to analyze the distribution of GP-C on the plasma membrane. Lower concentrations of digitonin selectively permeabilize the plasma membrane due to its high cholesterol content while the internal membranes stay intact (92). Epitopes that lie in the cytosol are accessible after digitonin treatment where as the luminal epitopes stay protected. We have previously shown that cells expressing GP-C stain for G1 only on the plasma membrane and not in the cytosol when permeabilized with 5μg/ml digitonin (2), and we used this method for immunogold electron microscopy studies

Cells labeled for GP-C were prepared for electron microscopy as described in materials and methods, with particular emphasis to obtain high contrast of labeling using gold particles. Mock transfected samples showed complete absence of labeling (data not shown) indicating high specificity of labeling by anti-G1 and the secondary gold antibodies. Immunogold labeling identified GP-C particles only in the regions surrounding plasma membrane, and not in the cytosol (Fig. 29, Panel B) consistent with

the luminal localization of G1 as described previously (2). For clustering analysis, gold particles that were localized in 30 nm trace of either side of the plasma membrane were selected with the consideration that they were membrane associated.

The clustering analysis approach developed by Brown and Lyles (18) analyses the pair wise distance between gold particles on a large number of micrographs. Twenty five micrographs of randomly selected plasma membrane from individual cells were collected for analysis. Image pro software was used to measure the distance between each gold particle that was located at a 30 nm distance from the curvilinear trace of the plasma membrane. A representative image of the analysis is shown in (Fig. 29, Panel A). The distance measurements between the gold particles were converted into pair wise distances between all the gold particles analyzed in the micrograph. The distances were sorted in 20nm increments and the pair wise distances were then plotted on to a histogram. The density of labeling plotted on the Y axis was obtained by normalizing the number of pair wise distances to the number of gold particles that were analyzed at each increment. The distance between the particles on the membrane was plotted on to the X axis. The rationale for this analysis is that if GP-C is organized into microdomains, gold particles separated by shorter distances (e.g., 120 nm) will be found more frequently relative to the average density of gold particles on the membrane. As Fig. 29, Panel A indicates, there are two possible outcomes upon the analysis of large number of micrographs. Clustering of GP-C into membrane microdomains (curve 1) will be indicated by high density of short distances of separation compared to larger distances of separation. Random distribution of GP-C will be signified by the presence of same density at all distances (curve 2). The average density (0.126) of GP-C in the plasma membrane was obtained by

dividing the total number of gold particles by total number of distances analyzed in 50 micrographs. The results of this analysis showed that the density of gold particles with in smaller distances of separation was considerably higher than the average density, where as the density in the larger distances of separation was similar to the average density. The data indicates that GP-C is organized into membrane microdomains, whose diameter is approximated by an X axis intercept where the slope of the plot changes. The diameter of these microdomains was found to be 120 nm. As described in the clustering analysis (18), the percentage of GP-C in the microdomains and the density of labeling inside and outside the microdomains influence the slope and the Y intercepts of the graph. These results suggest that GP-C is organized into membrane microdomains, which may form precursor of virus budding sites.

A.

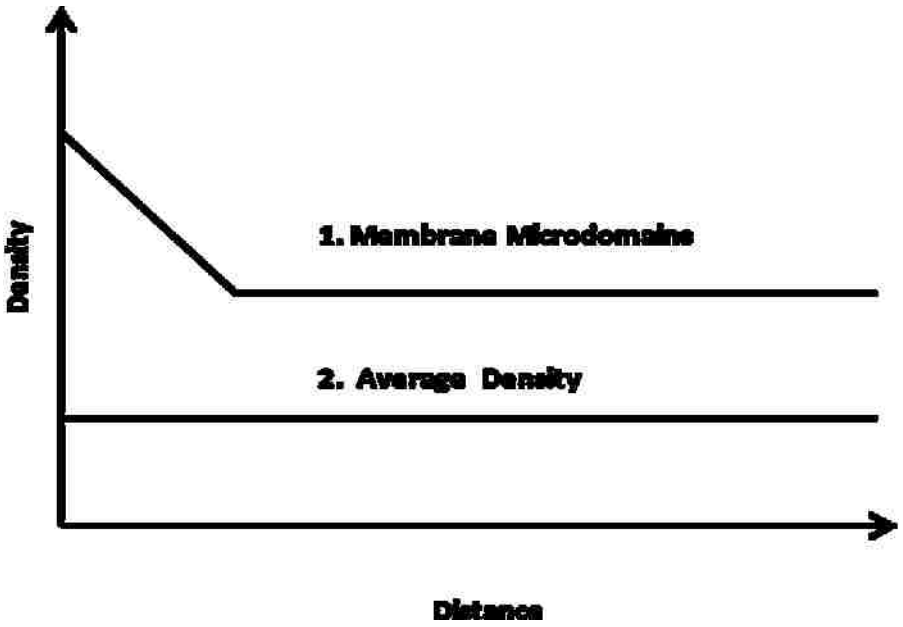
Density
1. Membrane Microdomains
2. Average Density
Distance

B.

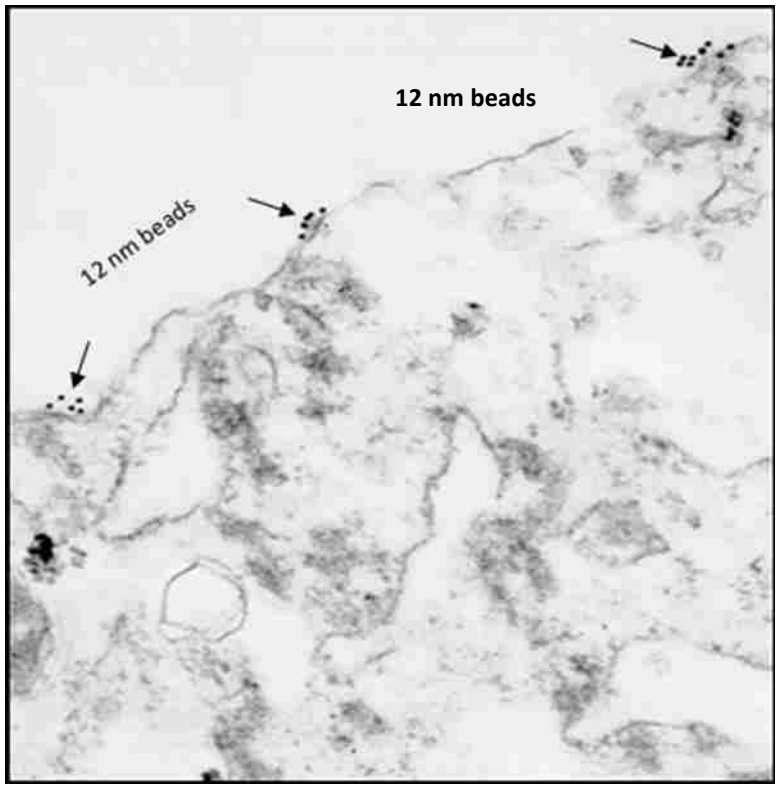
12 nm beads
12 nm beads

C.

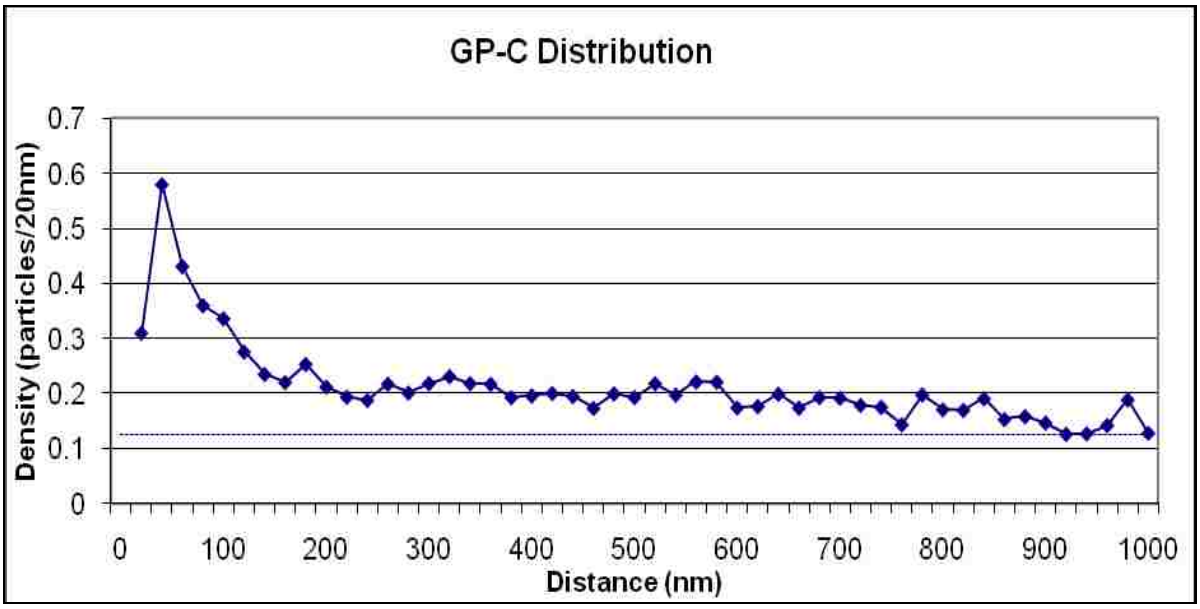

Figure 30. GP-C partitions into membrane microdomains independent of other viral proteins.

Vero cells were expressing GP-C under the control of T7 promoter (1) were fixed, permeabilized and labeled with BEO8 Ab to G1 subunit and a 12 nm colloidal gold antimouse IgG. Cells were prepared for electron microscopy as described in materials and methods, and 25 micrographs of plasma membrane from individual cells were collected. (A) Theoretical histogram of pair wise distances depicting the possible outcomes 1) high density of short distances of separation indicating organization into membrane microdomains 2) proteins distributed with the average density describing random distribution. (B) Representative electron micrograph of GP-C labeling on the plasma membrane. The 12 nm gold beads labeling GP-C are indicated with the arrowheads. (C) Histogram of the GP-C distribution on the plasma membrane in vero cells expressing GP-C. Clustering analysis is done as follows. The distance between each

gold particle in the micrograph was measured for 25 micrographs and the pair wise distances between all the particles in 25 micrographs were calculated from the measurements obtained. The density was calculated as the number of particles in 20 nm increments normalized to the number of particles that could have been analyzed within each increment. The normalized density of particles per 20nm was plotted on Y axis against the distance between the particles on the X axis in the histogram. The size of the microdomains (indicated by the arrow) is estimated as the X intercept where the graph changes the slope. The horizontal broken line in blue indicates the average density of GP-C particles on the plasma membrane, which is 0.126 particles per 20 nm. This value was obtained by dividing the total number of gold particles in 25 micrographs by the total length of the membranes analyzed in 25 micrographs.

Myristoylation in SSP does not affect GP-C clustering into membrane microdomains

Fatty acid modifications have been shown to be essential for membrane organization in many viral and cellular proteins (131, 180). Arenavirus assembly may be mediated by myristoylation dependent co-trafficking of Z and GP-C to membrane microdomains on the plasma membrane where specific interaction between Z and GP-C may orchestrate virus budding. A support to this hypothesis comes from previous report from our lab indicating that G2A mutant of GP-C exhibits 30% of cell-cell fusion levels relative to wild-type GP-C, although cell surface expression levels were comparable to wild type GP-C (188). We hypothesized that this reduction in cell-cell fusion levels may due to its inability to concentrate in membrane microdomains, as has been reported for the non-raft mutant of influenza HA (169). We reasoned that SSP myristoylation might allow for clustering of GP-C into membrane microdomains, which may be a prerequisite for efficient membrane fusion activity of GP-C. To investigate this hypothesis, we sought out to determine the pattern of G2A distribution in vero cells using immunogold microscopy and clustering analysis as described above. Consistent with the previous results of the surface expression (188), the amount of G2A labeling on the plasma membrane was similar to the wild type GP-C. Surprisingly, G2A was found to partition into microdomains as shown by the clustered gold beads (Fig. 31, Panel A) in a pattern that was exactly similar to wild type GP-C. Clustering analysis further indicated the presence of high density of gold particles separated by shorter distances relative to the average density (0.09), illustrating that G2A is partitioned into membrane microdomains on the plasma membrane. Thus, SSP myristoylation does not affect the membrane organization

of GP-C, a result that was in contradiction to our hypothesis. Membrane distribution of GP-C may be dictated by genetic determinants in SSP or other regions of G2 including the transmembrane, ecto or cytoplasmic domains of G2. Several other reasons may therefore underlie the defect observed in cell-cell fusion of G2A mutant, including a defect in efficient formation of six-helix bundle structure or inefficient insertion of fusion peptide in the target membrane due to defects in conformational state of G2A mutant.

A.

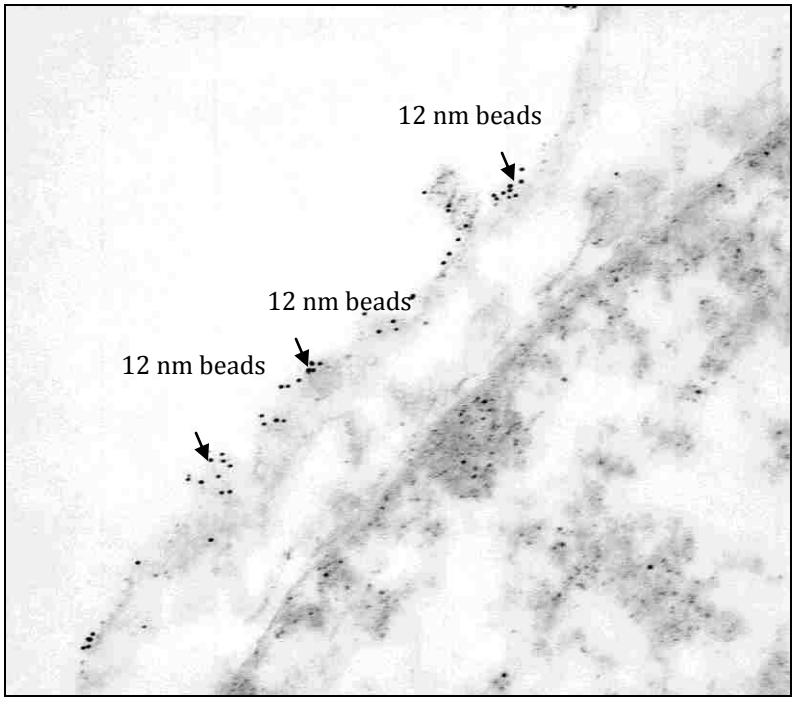

B.

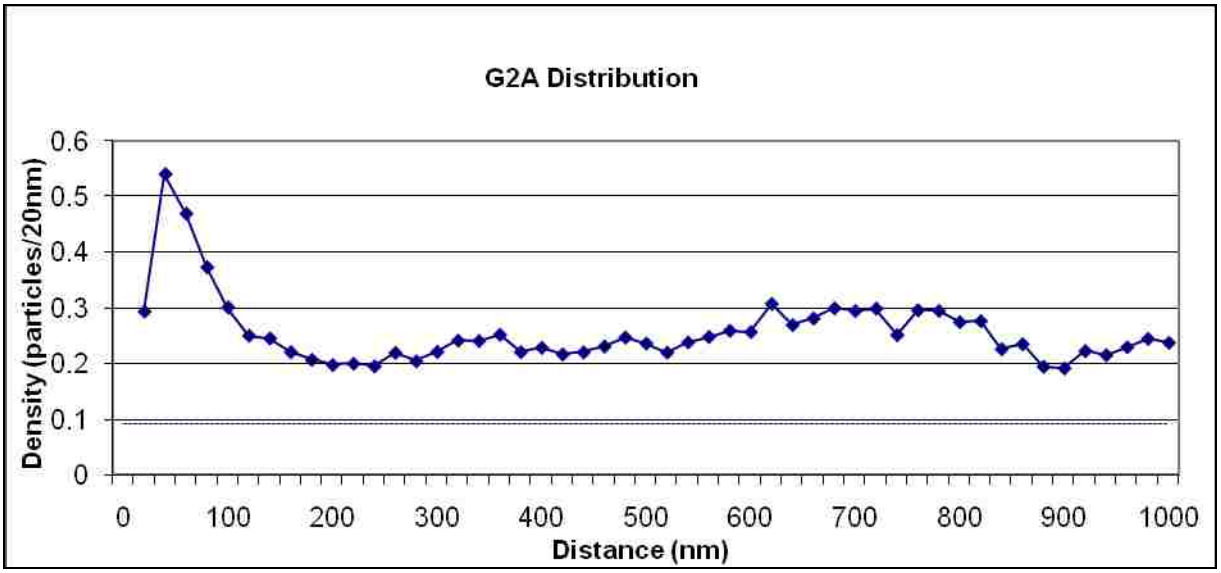

* — Average density

Figure 31. SSP myristoylation does not affect clustering of GP-C into membrane microdomains.

Vero cells expressing G2A under the control of T7 promoter were fixed, permeabilized and labeled as indicated in Fig. 30. Cells were prepared for electron microscopy as described in materials and methods and the quantification of gold particle distribution was done exactly similar to the one described in Fig. 30. (A) Representative electron micrograph of GP-C labeling on the plasma membrane. The 12 nm gold beads labeling GP-C are indicated with the arrowheads. (B) Histogram of G2A distribution on plasma membrane in vero cells. The average density of G2A particles is 0.09 particles/ 20 nm which is represented by the dotted blue line.

The matrix protein Z does not co-localize with GP-C containing microdomains and does not alter clustering of GP-C

Although the matrix protein Z forms VLPs on its own, generation of infectious arenavirus particles requires the envelope glycoprotein GP-C due to its roles in receptor recognition, binding and cell entry. Mechanisms underlying the interaction between Z and GP-C in the context of virus assembly have been less clear for NW arenaviruses, while reports from biochemical and immunofluorescence studies in OW LFV and LCMV have demonstrated colocalization and biochemical interaction between Z and GP-C. Furthermore, cryoelectron microscopy studies of LCMV virion have demonstrated a close apposition of Z on the internal face of the virion. Based on these observations, we hypothesized that Z and GP-C may localize to same microdomains on the plasma membrane to mediate arenavirus assembly and budding. To examine this hypothesis we used Zspep, the Z protein appended to the S-peptide tag on its C-terminus to enable immunolabeling for microscopy studies. This construct forms virus like particles on its own, and can be detected in purified VLPs (unpublished data). Vero cells expressing Z and GP-C were fixed, permeabilized with digitonin and Z was stained using a biotinylated-S-protein that recognizes an epitope in the S-peptide appended to Z. A 6 nm gold bead coupled strepatavidin was utilized to recognize the biotinylated-S-protein. GP-C staining and preparation of cells for electron microscopy was done as described above. Consistent with our results of immunofluorescence microscopy (data not shown), Z was found to be associated with the plasma membrane as indicated by the 6nm gold bead labeling. Twenty-five micrographs of randomly chosen plasma membrane of individual cells showing Z and GP-C labeling were chosen for clustering analysis, and a

representative micrograph showing Z and GP-C labeling is shown in Fig. 32, Panel A. To our surprise, Z was found to be distributed randomly on the plasma membrane in correlation with GP-C particles, as shown by the green arrow heads pointing upwards indicating 6 nm gold beads. GP-C was found to cluster into microdomains of 120 nm size, and clustering analysis indicated a high density of particles separated by shorter distances relative to the average density, indicating that GP-C is organized into membrane microdomains (Fig. 32, Panel C). Furthermore, microdomains containing GP-C did not contain Z particles suggesting an absence of co localization between Z and GP-C. Clustering analysis to determine whether Z and GP-C co-localize with each other on the plasma membrane, was done as follows. Distances were measured from every 6 nm gold particle to each 12 nm gold particle with in 30 nm curvilinear trace of the plasma membrane to a distance of 1000 nm. Pair wise distances were then sorted into 20 nm increments and were normalized to the number of gold particles analyzed in each increment. Similar to analysis described in Fig. 30, the data was plotted and the results are shown in Fig. 32, Panel B. The density of Z labeling was similar at short distances versus long distances from gold particles labeling GP-C. The average density of Z labeling relative to GP-C labeling was found to be 0.182. These results confirmed that GP-C and Z does not co-localize in the same membrane microdomains on the plasma membrane.

A.

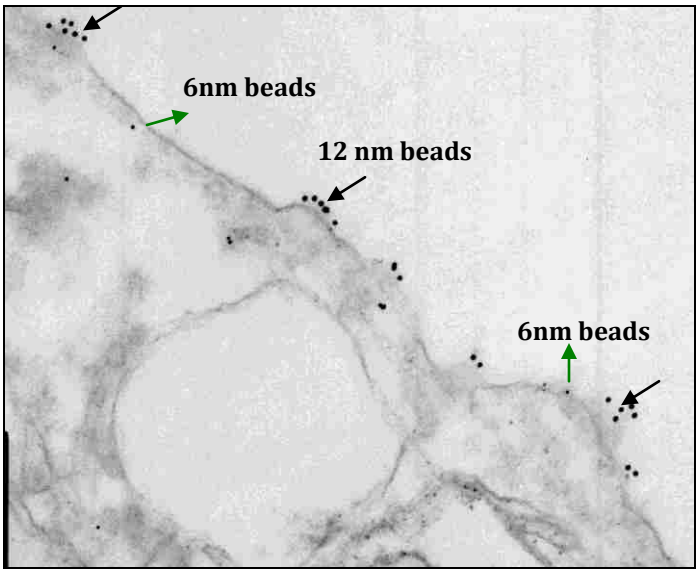
6nm beads
12 nm beads
6nm beads

B.

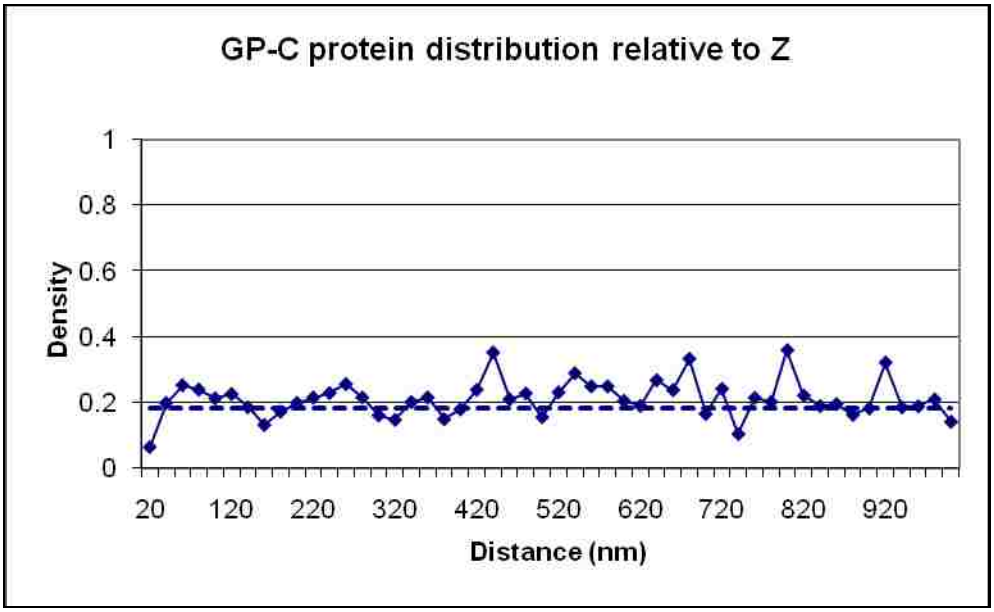
GP-C protein distribution relative to Z
Density
1
0.8
0.6
0.4
0.2
0
20
120
220
320
420
520
620
720
820
920
Distance (nm)
Average density

C.

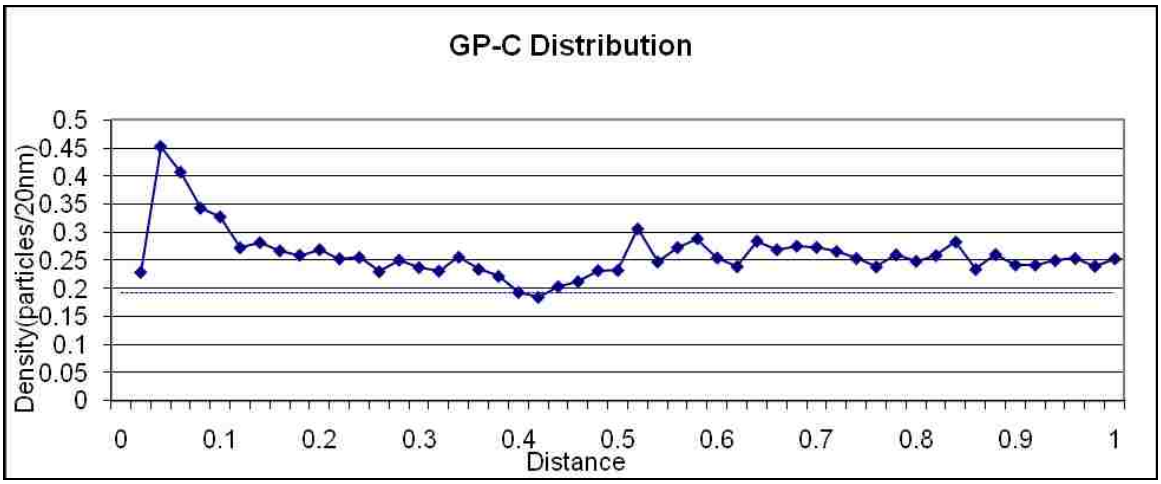

Figure 32. Z protein does not co localize with GP-C containing microdomains.

Vero cells expressing Z-Spep and GP-C under the control of T7 promoter were fixed permeabilized and double labeled with BE08 Ab and biotinylated-S-protein and then with 12 nm anti-mouse IgG and 6 nm gold coupled streptavidin. Cells were prepared for electron microscopy as described in materials and methods. Twenty five electron micrographs of plasma membrane showing Z and GP-C labeling from individual cells were selected for analysis and a representative image is shown (A). The 12 nm particles labeling GP-C are indicated with black arrow heads and the 6 nm particles labeling Z are indicated by grey arrowheads pointing upwards. Note that GP-C is still found clustered despite Z expression indicating that coexpression of Z does not modulate the clustering pattern of GP-C. (B) Histogram showing distribution of Z and GP-C. Distances between each Z particle to every GP-C particle with in 30 nm curvilinear trace of the plasma membrane was measured up to a distance of 1000 nm. The density was calculated as the number of gold particles in 20 nm increments normalized over the number of gold

particles that could have been analyzed at each increment. The normalized density of the particles per 20 nm was plotted on the Y axis against the distance from the G protein on the X axis, giving rise to the histogram. The average density of Z protein relative to the GP-C protein was 0.182. The histogram indicates that there was no change in density of Z protein labeling at short distances versus long distances from GP-C labeling gold particles, which indicates an absence of co-localization between Z and GP-C particles. (C) Histogram of GP-C distribution on the plasma membrane in cells co-expressing Z and GP-C. The average density is 0.126, which is indicated by the dotted blue line.

Reverse-genetic system to dissect the determinants in GP-C essential for arenavirus morphogenesis and infectivity

We have adopted the reverse genetics technology developed for OW LCMV by our collaborator Dr. Juan Carlos de la Torre (Scripps Research Institute, CA) to study the functional assembly of arenavirus particles (95, 96). This study involved co-transfection of each of four plasmids encoding the viral proteins (L, N, Z and GP-C) along with a plasmid from virus minigenome (MG) RNA, capable of replicating in cells, is transcribed. The following are the critical elements of a prototype minigenome: A murine Pol-1 promoter (60) for proper transcription initiation, the 5` untranslated (UTR) and intergenic hairpin regions of the LCMV genomic S RNA, a luciferase gene in antisense orientation, and the 3` UTR of the LCMV S RNA, followed by the hairpin ribozyme to generate a 3` end in the upstream RNA that corresponds to the precise LCMV S RNA 3` terminus. Transduction of VLPs that package the MG RNA into target cells expressing the nucleoprotein N and the RNA Dependent RNA polymerase (RDRP) L allows for replication and expression of the MG- encoded luciferase gene from the viral 3` UTR.

Infectious VLPs containing the MG RNA were generated as follows. BHK-21 cells were transfected with the following LCMV plasmids: pC-Lv2, pC-NP, pC-Z and pC-GPC that express the respective viral proteins under the control of nuclear promoter of pCAGGS (125) and, the pol-1MG luc plasmid (60) which is transcribed using a murine pol1 promoter to generate a replication competent MG RNA containing an antisense luciferase reporter gene. These VLPs are then transduced onto human 293T target cells expressing the polymerase (pC-Lv2) and pC-NP (to amplify replication and transcription of the incoming MG). After 24 hours target cells are lysed and luciferase activity was

determined using Luc Screen reagents (Tropix) and a microplate luminometer. Preliminary studies showed that JUNV GP-C can substitute for LCMV GP-C in transduction of the luciferase reporter (Fig. 33). Furthermore, proteolytic processing of JUNV GP-C is essential for the formation of infectious VLPs, as VLPs formed with cd JUNV GP-C are not capable of transducing the luciferase reporter into target cells (Fig. 33).

The RG system was utilized to investigate the importance of GP-C myristoylation (using the G2A mutant of GP-C) in arenavirus morphogenesis and infectivity. We hypothesized if SSP myristoylation were important in GP-C interaction with the matrix protein Z, VLPs formed in the cells expressing G2A GP-C under the influence of matrix protein Z will be particularly diminished in GP-C and hence be defective in virus entry. To investigate this hypothesis the G2A mutant was examined for its ability to form infectious VLPs. As shown in the Fig. 33, the luciferase reporter assay indicated that the VLPs containing the G2A mutant exhibit 30% infectivity levels relative to the wild-type GP-C. Since cell-cell fusion levels of G2A mutant was also 30% of the wild type GP-C (188), it was difficult to attribute the decrease in infectivity to deficiency in GP-C incorporation. To further explore this observation, metabolically labeled VLPs assembled from cells expressing GP-C and G2A mutant were purified by centrifugation in 20% sucrose cushion , lysed in cold 1% Tx-100 and immunoprecipitated using a G1Mab BE08. We were unable to biochemically detect the GP-Cs from purified VLPs. Pilot studies to improve VLPs yield were tried but without success. Studies from LCMV reverse-genetic system have not been successful in detection of LCMV GP-C (96). These studies conclude that there is a precious amount of VLPs that are not sensitive to

biochemical detection, but are successful in transducing the luciferase signal to the target cells. The strict requirement for the LCMV Z to support the packaging of VLPs containing the LCMV RNP, has limited the use of Junin Z in the system. Furthermore, the unavailability of a functional clone of the Junin polymerase protein L makes the establishment of a homologous reverse-genetic system for assembling Junin VLPs impossible.

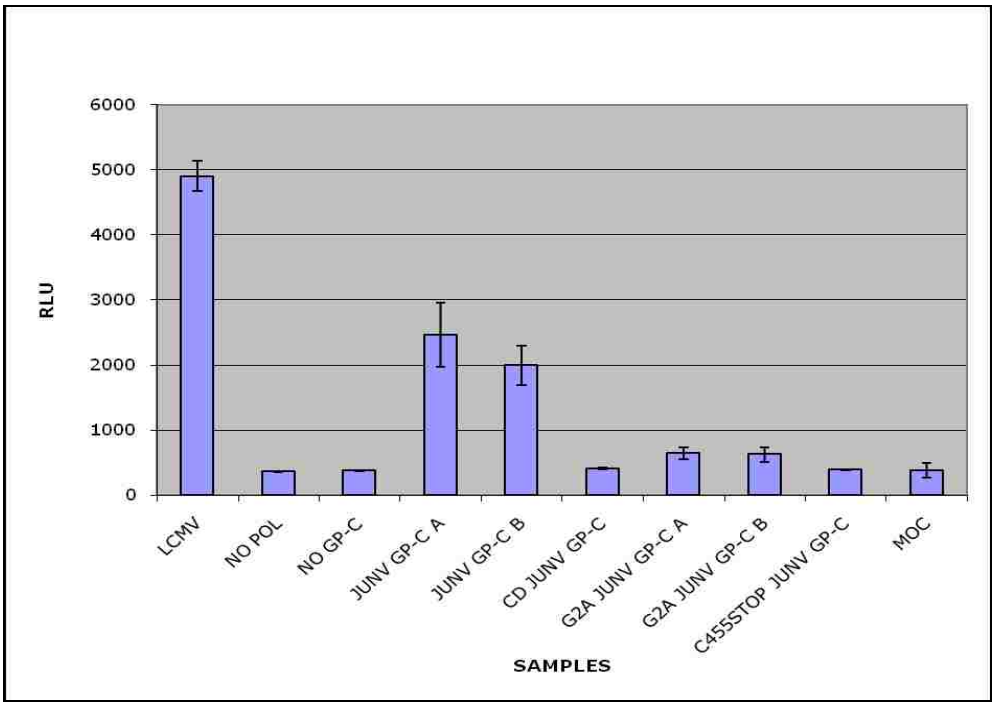

Figure 33. JUNV GP-C can substitute for LCMV GP-C in forming VLPs that transduce of MG luc into the target cells.

BHK-21 cells were tranfected with the following plasmids MG luc , L ,N, Z and GP-C in a 6 well plate. 48 hours post transfection, cell culture supernatants were harvested and spun at 1000 rpm for 5 mins to pellet dead cells and membrane fragments. The supernatants containing VLPs were transduced on to target HEK 293T cells expressing the nucleoprotein N and RDRP L, to support the transcription and replication of the incoming minigenome. The target cells were lysed 24 hrs post transduction and the luciferase activity was measured using LucScreen reagents (Tropix) and a Tropix TR717 microplate luminometer. Duplicate cultures were employed for wild type GP-C (JUNV GP-C) and the myristoylation mutant (G2A JUNV GP-C). The cleavage defective GP-C and the C455STOP (GP-C mutant that does not associate with SSP and hence not expressed on cell surface) are indicated.

To address these constraints, specificity and compatibility between the Old and New world viral proteins, a collaboration has also been initiated with Dr. Nora Lopez (CEVAN-CONICET, Buenos Aires, Argentina), to develop a New world arenavirus reverse genetic system. A plasmid-based system using Tacaribe virus (TCRV) N and L for replication of a TCRV MG and expression of the chloramphenicol acetyl transferase (CAT) reporter gene has been described by Dr. Lopez (107, 108). This replicon system has been recently extended by Dr. Lopez to include Z and GP-C proteins of TCRV (80) and also JV (Fig. 34). Expression of viral proteins is driven by plasmid encoded T7 polymerase and VLPs comprising TCRV L, N and MG with JUNV Z and GP-C are able to transduce CAT activity into target cells. Entry is again dependent upon functional GP-C (Fig. 34, top panel).

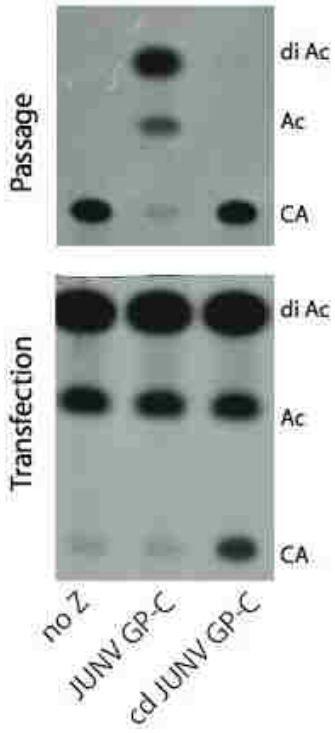

Figure 34. Passage of New World VLPs.

Plasmids in the complete reverse-genetics system are TCRV MG, L, N, Z and JUNV GP-C (2, 1, 2, 0.15 and 2 µg, respectively per 12-well culture) with 1µg pT7. CAT activity in the transfected cells and on transduction with passage was determined using ^{14}C-chloramphenicol (CA) and mono- and di-acetylated (Ac, di Ac) forms are resolved by TLC. This image was kindly provided by Dr. Nora Lopez.

4. Discussion

The critical roles played by the SSP in pH dependent membrane fusion, assembly and intracellular trafficking of arenavirus glycoprotein complex makes it as an essential subunit of the mature glycoprotein complex. SSP might be involved in several other stages of arenavirus lifecycle including assembly and budding. Viral proteins encode sorting signals that allow them to be targeted to the site of virus assembly, where they can interact with other viral components to mediate budding of the progeny virions (30). We hypothesized that SSP myristoylation may target GP-C to lipid rafts on the plasma membrane where the cytoplasmic face of GP-C may interact with the matrix protein Z to mediate arenavirus assembly and budding. Studies described in this chapter address several questions including the contribution of SSP myristoylation in lipid raft association of GP-C, pattern of GP-C distribution on the plasma membrane and finally describes a reverse-genetic system to study the role of GP-C in arenavirus morphogenesis and infectivity.

We have identified that lipid rafts or DRMs does not play a role in arenavirus assembly and morphogenesis. GP-C from Junin virus infected cells show no evidence of distribution in DRMs and all of the GP-C expressed from the Junin virus including the precursor and the proteolytically mature G2 subunit partition to the detergent soluble compartments (Fig. 26). Although recombinantly expressed GP-C shows association with DRMs, the molecular species of GP-C that are relevant for inclusion into Junin virions , partition to the detergent soluble compartments in these cells. The higher molecular weight species of GP-C associated with DRMs may indicate any of the post-translationally modified forms (e.g., ubiqutination, sumoylation etc.,) that may arise as a

result of protein misfolding. Ubiquitination has been shown to play a major role in endoplasmic reticulum-associated protein degradation pathway (ERAD) (89) where misfolded proteins are ubiquitinated and degraded through the ERAD pathway. Over expression of proteins might result in a proportion of proteins being misfolded and degraded via ERAD pathway, which could occur in the case of GP-C over-expression from a nuclear promoter. GP-C associated with DRMs might be misfolded and be destined for degradation. This possibility was supported by the observation that DRMs from BHK-21 cells transfected with the CD4spGPC (G1-G2 precursor with CD4 signal peptide, described in chapter 3) contained the same higher molecular weight forms of the precursor and G2 subunit as found in case of GP-C and G2A, where as the soluble fraction contained only the lower molecular weight precursor and no G2. The precursor is retained in the ER in the absence of SSP and does not undergo proteolytic maturation by SKI/S1-P protease in the Golgi compartment to yield G2 subunit of 35kDa. Hence, the higher molecular weight forms in the DRMs could represent GP-C that is not processed by SKI/S1P protease, but modified by other enzymes (e.g., ubiquitin ligases) to be destined for degradation. Since these proteins were not relevant in terms of budding virions, we decided not to proceed with further investigations with regard to the recombinantly expressed GP-C.

Organization of proteins into membrane microdomains facilitates protein-protein interactions that are important for a variety of cellular processes including receptor-mediated signaling, protein trafficking and apoptosis. For viruses, this phenomenon holds high significance in the context of assembly and budding. Budding of new progeny virions is mediated by interactions between structural proteins of the virus at the site of

assembly, a process that is facilitated by their organization into membrane microdomains. In viruses that bud from plasma membrane, the interaction of the transmembrane envelope glycoprotein with the matrix protein may be promoted by their localization to microdomains on the plasma membrane. We have shown that GP-C clusters into membrane microdomains of 120 nm on the plasma membrane independent of other viral proteins. GP-C on the plasma might represent the species found in detergent-soluble fraction of cell lysates, since the higher molecular weight forms associated with DRMs represent intracellular GP-C, as shown by the characterization of CD4sp-GPC (Fig. 28, Panel D). This finding concludes that lipid rafts are not involved in assembly of Junin virus and detergent-soluble microdomains containing GP-C might serve as arenavirus budding sites. Myristoylation of GP-C does not play a role in clustering of GP-C, since the G2A mutant was found to cluster similar to the wild type GP-C (Fig. 31). These results argue that the observed 30% fusogenicity of the G2A mutant relative to the wild-type GP-C (188) could be due to an intrinsic defect (e.g., conformational defects) in the ability of G2A mutant to mediate pH dependent membrane fusion, and not due to a defect in its membrane organization. These observations conclude that myrsitoylation of SSP is dispensable for clustering of GP-C on the plasma membrane.

Co-localization analysis point out that the distribution of Z is random with respect to GP-C, and they are not localized to the same microdomains on the plasma membrane. This observation hints a possibility that arenavirus budding may not be initiated by Z GP-C interactions in localized microdomains, but instead clustering of proteins and lipids on the plasma membrane may bring Z and GP-C together to form arenavirus budding sites. Specific protein-protein interactions between Z and GP-C at the budding site might allow

the incorporation of GP-C into budding virions. A similar mechanism has been described recently in the case of Vesicular Stomatitis Virus where the matrix protein M and the G protein are organized into separate microdomains, and they come together at the site of virus budding (167). Membrane reorganization is a dynamic process and could result due to clustering of oligomeric proteins, as has been proposed in the case of HIV-1 Gag. This process may bring together the proteins localized on different microdomains, where interactions between them could be spontaneous during virus budding. We anticipate such a mechanism to underlie arenavirus budding, where membrane reorganization during virus budding may lead to clustering of microdomains containing Z and GP-C. This process might allow spontaneous interactions between Z and GP-C, leading to incorporation of GP-C into the budding virions. The occurrence of such an event can be examined by immunogold labeling of GP-C and Z from cells infected with Junín virus. This experiment might capture budding sites where Z and GP-C might co-localize, thereby illustrating the above mentioned mechanism. The unavailability of a monoclonal antibody to the Z protein limits such an investigation, and the absence of a homologous reverse genetic system confines the ability to label Z in the context of a whole virion.

Although the results described here are interpretations from recombinantly expressed proteins, the clustering analysis samples GP-C expressed on the cell surface, which represents a small proportion of GP-C expressed in the cell. Since majority of the recombinant GP-C stays intracellular and is not expressed on cell surface, as shown by DRM-associated species of GP-C in CD4spGPC (Fig. 28, Panel D and Fig. 12, Panel B), we reason that the fraction of GP-C expressed on the cell surface may be relevant to what is found in detergent-soluble fraction of Junin virus infected cells. Nonetheless, the

immunogold electron microscopy studies describe here offer new insight into membrane organization of GP-C and Z, which may underlie arenavirus assembly and budding. Future studies examining the determinants in GP-C responsible for its clustered organization may further unveil the role of SSP or ectodomain ort TM domains of G2 in membrane trafficking of GP-C.

Reverse genetic system is a powerful tool to genetically manipulate RNA viruses and identify viral determinants essential for replication, assembly, budding and infectivity. Reverse genetics studies have contributed greatly in basic understanding of virus life cycle of several viruses including coronaviruses (55, 172), bunyaviruses (109), and bornadisease viruses (37). A reverse genetic system has been established for the OW arenaviruses, using the prototype arenavirus LCMV (38). Rapid progress has been made in identifying minimal elements essential for viral replication (141), viral proteins essential for replication (96), viral proteins that inhibit replication (36) and development of reverse genetic system containing virions pseudotyped with other viral glycoproteins. The study of the new world arenaviruses awaits a development of reverse genetic system and less information is available about the role of glycoprotein in the virus life cycle. We have adopted the reverse-genetic system for the OW arenaviruses and have extended it to study the determinants in GP-C essential for arenavirus infectivity. We have shown that JUNV GP-C can substitute for LCMV GP-C in packaging the RNP of the OW LCMV and is successful in transducing the luciferase signal on to the 293T target cells expressing the nucleoprotein N and RNA dependent RNA polymerase L, which support replication and transcription of the incoming minigenome. Proteolytic processing of GP-C is essential for mediating virus entry, which is consistent with the observation that cd

GP-C does not mediate cell-cell fusion (1). These results validate the successful establishment of the system with proper controls. Although the VLPs formed under the influence of G2A mutant exhibit 30% infectivity relative to the wild type GP-C, it is difficult to attribute this difference to deficiency in GP-C incorporation, since G2A mutant exhibits 30% cell-cell fusion relative to the wild type GP-C. Our inability to biochemically detects GP-C in VLP preparations limits experiments to measure GP-C incorporation. Future studies will be aimed at identification of determinants in GP-C essential for arenavirus morphogenesis and infectivity.

5. Materials and Methods

Cells, molecular reagents and monoclonal antibodies

The pCAGGS vector containing the modified RNA polymerase II promoter (125) was a kind gift from Dr. Juan Carlos de la Torre (Scripps Research Institute, CA). The cDNA inserts encoding for wild type Junin GP-C and its derivatives, and the Z-Speptide were cloned from the mammalian expression vector pCDNA3.1+ (1) into the pCAGGS vector. The restriction sites used for GP-C and N cloning were Sst and Xho1 in the pCDNA 3.1+, and Sac1 and Xho1 in the pCAGGS vector. For Z-Speptide, the sites used in the pcDNA 3.1+ were SSt and XbaI and the sites used in the pCAGGS were SSt and Xba 1. These plasmids were designated as pC followed by the name of the protein (e.g., pc GP-C, pC Zspep), and were used in the density gradient flotation analysis and the reverse-genetic system. The plasmids used in the Immunogold electron microscopy studies contained the GP-C coding regions in the vector pcDNA3.1+, where GP-C expression was driven by the bacteriophage T7 promoter, as described previously (1).

BHK-21 cells were cultured in DMEM (Invitrogen, cat no: 11996065) 10% FCS (GIBCO), 1% antibiotic (penicillin and streptomycin) with 1% minimal non-essential amino acids (NEAA, GIBCO). HEK 293T cells were cultured in DMEM 10% FCS with 1% antibiotic.

Mouse monoclonal antibody F106G3SC2 directed against the ecto domain of the fusion subunit G2 was provided by Dr. Jody Berry, National Microbiology Laboratory, Public Health Agency of Canada. The mouse monoclonal antibody against the S-Peptide tag (Affinity Bioreagents cat no: MA1981), Rabbit polyclonal antibody (Abcam, cat no: ab 18199), Biotinylated S-protein probe (Novagen, cat no: 69218-3), 12 nm colloidal gold antimouse IgG (Jackson Immunoresearch), 6 nm gold coupled streptavidin (Electron Microscopy Sciences), Benzonase (Novagen, cat no: 70746-3) were used in the experiments described in this chapter.

Immunogold electron microscopy and Confocal laser scanning microscopy.

Vero cells grown in a 6 cm dish in DMEM 10% FCS were incubated with 10µM ara-c for 2 hrs. Cells in each dish were then infected with 500µl of a recombinant vaccinia virus vTF7-3 (1) in DMEM 2% FCS 10µM ara-c for 30 min at 37 degrees with swirling for every 7 min. Infected cells were then washed twice with serum free media and transfected with 8µg of GP-C expression plasmid in 1ml of optimem containing 20µl lipofectamine (Invitrogen), in 2.5 ml of SFM containing 10µM. 3 hrs later 2.5 ml of 20 % FCS with 10µM ara-c was added to bring the concentration of the media to 10% FCS. Twenty hours post tranfection, the media was aspirated and the cells were washed with 3 ml of ice-cold phosphate buffered saline two times. Cells were fixed 2ml of 2% cold formaldehyde in 1x PBS (freshly prepared before the experiment) for 1hr on ice. The

cells were then quenched with 2 ml of ice cold 50mM TrisCl for 15 min on ice. Plasma membrane of the cells were then permeabilized with 2.5 ml of 5µg/ml digitonin (1µg/µl fresh stock of frozen digitonin thawed and heated at 95 degrees for 4 min before diluted in buffer) in cytoplasmic ionic buffer (20 mM HEPES buffer, 110 mM potassium acetate, 5 mM sodium chloride, 2 mM magnesium chloride, and 5 mM EGTA, pH 7.3) (2) for 20 min on ice. Excess digitonin was washed twice with ice-cold cytoplasmic ionic buffer. Non-specific protein binding sites were blocked with 2.5 ml of ice-cold block buffer (5% dialyzed FCS in cytoplasmic ionic buffer) for 1 hr on ice. Cells were then stained with MAb BE08 - to stain G1 (3:500) and biotinylated-S-protein to stain Z (1:1000) in block buffer, for 1 hr on ice. Unbound antibodies were removed by washing 3 times for 10 min each time with ice-cold block buffer. Secondary antibody staining was performed using 1ml volume of ice cold block buffer containing 12 nm colloidal gold anti-mouse IgG (1:3 dilution), 6 nm gold coupled streptavidin (1:3 dilution) for 1 hour. The dishes were placed on a rocker and swirled every 15 min to ensure even distribution of the secondary antibody. Excess antibodies were removed by washing 3 times with ice cold block buffer (10 min washes), followed by a quick wash with ice cold cytoplasmic ionic buffer to remove any serum proteins prior to fixation. The cells were then scraped in 1ml of cytoplasmic ionic buffer using a plastic scrapper, and then transferred to 2 ml screw-capped, eppendorf using a transfer pipette. Any residual cells were scrapped further in an additional 500µl volume of the cytoplasmic ionic buffer, added to the cell suspension, spun down at 1000 rpm at 4 degrees. The buffer was then aspirated and 1ml of 2.5% EM grade glutaraldehyde fixative (sent by Dr. Douglas Lyles) was added to fix the antibodies. The cells were then shipped to Wake Forest University School of Medicine

where the post processing of the cells for electron microscopy were carried out as described (18, 167). For parallel studies using confocal microscopy, staining for Z and GP-C were performed on vero cells expressing GP-C on chambered coverslips, except the secondary antibody staining was done using fluorescent antibodies Alexa Fluor 488-conjugated F (ab`) $_2$ anti-mouse (1:1000) and an Alexa Fluor 568 conjugated Streptavidin (1:800) in block buffer, and the cells were then viewed in the microscope in slow fade antifade gold.

Density gradient flotation analysis of cells expressing GP-C

2.7 x10^6 BHK-21 cells grown in DMEM 2% FCS 1% NEAA were transfected with 24 µg of pc plasmids encoding GP-C in 3 ml optimem containing 60µl of lipofectamine. Forty eight hours post transfection, cells were washed twice with ice cold phosphate buffered saline, scrapped and pelleted down at 1000 rpm at 4 degrees for 5 min and cells were lysed as follows. PBS was aspirated and 450 µl of ice cold PBS containing 1mM EDTA, 1mM EGTA was added along with 50 µl of ice-cold 10% TX-100 in PBS, to bring the concentration to 1% TX-100. The lysates were transferred to a 1.5 ml eppendorf, vortexed and placed on ice for 1 hr to facilitate complete lysis of lipid membranes. Aliquot of total lysate was removed at this stage for biochemical analysis in experiments described in results section. The lysates were then spun for 11,000 rpm for 30 min at 4 degrees to pellet the detergent-resistant membranes (DRMs). The supernatant (detergent-soluble fraction) was removed and aliquots were biochemically analyzed for GP-C and Z expression, wherever indicated in results section. The DRMs were then resuspended in 180 µl of cold Buffer B (38mM each of the K salts of aspartic acid, glutamic acid and gluconic acid, 20mM MOPS pH 7.1, 10mM potassium bicarbonate, 0.5mM magnesium

carbonate, 1mM EDTA, 1mM EGTA) containing protease, phosphatase inhibitors and glutathione and 20 µl of 10% TX-100 was added to bring the concentration to 1% TX-100. Benzonase was then added to digest any nucleic acids in DRM preparations, and incubated for 30 min on ice. 90µl of the DRM suspension was aliquoted separately in a polyallomer tube and mixed with 408µl of 60% Optiprep (SIGMA) to make it to 49% Optiprep. This suspension was overlaid with a mixture of 48% and 15% Optiprep in Cold Buffer B, to set up a final gradient of 48-15% Optiprep. The samples were then subjected to ultracentrifugation for 18 hrs in a Beckmann Coulter Optima ultracentrifuge, in a SW 55Ti rotor. The DRMs were noted visually on the top of the gradient while the samples were being removed from the centrifuge. Twenty three fractions of ~ 200µl each were then collected from the bottom of the tube using a manual fraction collector, and 800µl of 13% ice-cold trichloroacetic acid (TCA) was added to each tube and incubated overnight to precipitate proteins. The tubes were then spun at 15,000 X g for 20 mins at 4 degrees, and the precipitated proteins were then washed with 800µl of ice cold acetone, and air dried. The samples were then dissolved in 50µl of 7M urea sample buffer containing 0.1mM DTT (7M urea, 125mM Tris pH 6.95, 2% SDS, 1mM EDTA, 0.1% Bromophenol blue) vortexed well and heated at 55 degrees for 15 mins and resolved on a 10% Bis-Tris Gel at 12mA for 14 hours in SDS gel running buffer. Molecular weight was determined by using biotinylated protein ladder (Cell Signaling Technologies. cat no 7727) and a prestained protein marker (Cell Signaling Technologies, cat no 7720). Proteins were then transferred on to a nitrocellulose membrane in ice-cold transfer buffer (400mA for 4 hrs). The membrane was stained in 2.5% Ponceau in 13% TCA to identify the transferred proteins, washed with wash buffer (PBS with 0.1% Tween 20), blocked in blateau (5%

nonfat dry milk in wash buffer), stained with F106G3SC2 (1:200 dilution in blateau buffer) for GP-C and mouse monoclonal antibody against S-peptide (Affinity Bioreagents, cat no MA1981, 1µg/ml diln) for Z and an HRP conjugated anti- mouse IgG (1:2000 diln in blateau) secondary antibody. Proteins were visualized using Super Signal West Pico (Pierce, cat no 34079) chemilumiscence system.

For analyzing the DRMs from candid infected cells, vero cells infected with candid-1 strain of Junin virus were lysed 5 days after infection and the DRMs were prepared, floated in the optiprep density gradient. Gradient fractions were collected, density determined by refractometer and the gradient fractions were examined as described above for GP-C distribution using a G2 Ab. In some experiments (data not shown), cell culture supernatants (4 ml) were centrifuged at 34,000 rpm for 90 mins at 4degrees through 400 20% sucrose cushion to pellet down the virions. The virions were then lysed in cold PBS containing 1% TX-100, adjusted to 49% optiprep and overlaid with a mixture of 48 and 15% optiprep in cold Buffer B, to set up a final gradient of 48-15% Optiprep in a polyallomer tube. The samples were then ultracentrifuged and the gradient fractions were collected and analyzed for GP-C staining as described above.

Reverse genetic system

BHK-21 cells (producer cells) were seeded in a 6 well plate at 0.7 x 10^6cells per well in DMEM 10% FCS 1% NEAA. The cells were then transfected in 2% FCS 1% NEAA with a plasmid mixture (total 4µg) containing the following plasmids. pC GP-C LCMV or pC GP-C (JUNIN) 0.571 µg, pC N (LCMV) 1.14 µg , pC L (LCMV) 1.42 µg , pC Z (LCMV) 0.142 µg and a MG-Luc plasmid 0.714 µg, in 500µl of optimem containing

10µl of Lipofectamine 2000. Six hours later, the media was replaced with DMEM 10% FCS 1% NEAA. Twelve hours post transfection of producer cells, $3x10^6$ HEK 293T (target cells)/6 cm dish seeded in DMEM 10% FCS were transfected with 8µg plasmid mixture (4µg of pC N + 4µg pC L in 1ml optimem containing 20µl of lipofectamine) in serum free media. Six hours later the serum free media was replaced with DMEM 10% FCS. Twenty four hours post transfection of target cells, they were reseeded on to 6 well plates 2.4 $x10^6$ cells/well in DMEM 10% FCS. At forty eight hours post transfection of producer cells, cell culture supernatants from producer cells were collected in a 15 ml falcons tube, spun at 4 degrees at 1000 rpm to pellet dead cells. 3ml of the sups were diluted with 1ml of serum free media per sample, and then added on to target HEK 293T cells after aspiration of the media in which the target cells were grown. The target cells were then incubated with the virions for six hours to allow efficient binding and entry, supernatants were aspirated and DMEM 10% FCS was added on to target cells. The cells were then incubated for twenty four hours. The producer cells were then pelleted in 500µl of cold PBS and quadreplicates of 100µl cell suspension were added to a well of opaque 96-well microtiter plate. 50µl of solution I and 50µl of solution II from Luc Screen Assay kit (Tropix) was added to each well, incubated for 10 mins in dark and analyzed in and a Tropix TR717 microplate luminometer for luciferase activity. The target cells were lysed at 24 hours post transduction and analyzed for luciferase activity as described here. For biochemical studies, the producer cells were metabolically labeled 36 hrs post transfection with 250µci of label/well and the supernatants were purified by ultracentrifugation in 20% sucrose cushion and analyzed for GP-C detection by immunoprecipation using BEO8 Ab. In some experiments, lysed virions were denatured

in NUPAGE sample buffer and resolved using 4-12% Bis-Tris gels. Phosphorimages were analyzed for presence of viral proteins.

CHAPTER SIX

CONCLUSION

My dissertation research has employed genetic tools to understand the structure and function of the GP-C complex and its role in virus life cycle. Virus membrane fusion is an important step in mediating viral entry, and for enveloped viruses the transmembrane envelope glycoproteins mediate this step. Chapter 2 summarizes results from genetic studies that have identified arenavirus GP-C as a Class I fusion protein (183). These findings have contributed significantly to the research field in understanding the mechanism of membrane fusion in arenaviruses (57). An unusual future of the arenavirus GP-C is the presence of 58 amino acid stable signal peptide (SSP), that remains attached non-covalently in the mature glycoprotein complex, and is included as a part of the mature glycoprotein complex in the virion (52, 188). Signal peptides are usually 20 to 30 amino acids in length and target the nascent protein to the endoplasmic reticulum and get cleaved off thereafter. The inclusion of an unusually long stable signal peptide in the mature glycoprotein complex suggests its significance in virus life cycle. Prior to the start of my dissertation research, literature studies using the old world Lassa virus had identified SSP as a *trans* acting factor required for proteolytic maturation of the G1-G2 precursor (50). No further evidence was available about the functions of SSP subunit, in particular in the case of New World arenaviruses. My dissertation research was the first to describe that SSP subunit is required for the transport of G1-G2 precursor form the ER to the Golgi complex for proteolytic maturation. In the absence of SSP, the precursor is retained to ER through the dibasic retrieval signals in the cytoplasmic tail of G2, which may be masked upon SSP association with the cytoplasmic tail of G2 thereby enabling

the transit of GP-C through the Golgi to the surface. We propose this assembly-dependent control of intracellular trafficking by SSP as a quality control mechanism evolved in the arenaviruses to ensure that the fully assembled GP-C complex is transported to the cell surface for virion assembly (1). These findings decipher the role of SSP in intracellular trafficking of GP-C, a critical step in virus life cycle.

Studies that have identified the bitopic membrane topology of SSP are instrumental in understanding how the membrane orientation of SSP in the GP-C complex allows it to contribute towards a variety of functions of the GP-C complex (2). SSP assumes a bitopic membrane topology with the hydrophobic regions spanning the membrane twice and its N and C termini residing the cytosol. The short ectodomain loop of SSP that harbors the critical lysine (K33) side chain is exposed in the outer side of the membrane. This orientation allows the SSP to interact with the cytoplasmic tail of G2 and control the intracellular trafficking of GP-C whereas the ectodomain loop of SSP interacts with the ectodomain of G2 and modulates the pH at which the membrane fusion is activated (187). Previous reports attempting to identify the membrane topology of SSP in the OW arenaviruses Lassa and LCMV describe results that are different from ours and these studies do not account for the functional integrity of GP-C complex (51, 62). The topology of SSP described in my dissertation research is supported by strong genetic evidence that relates the membrane orientation of SSP to the function of GP-C complex (2). Furthermore, the model of GP-C complex derived from the topology studies has benefited the understanding of the mechanism of action of newly discovered small molecule inhibitors of arenavirus entry (184). Taken together, these studies have aided us in understanding how the organization of SSP in the GP-C complex allows it to

contribute in the function of GP-C complex including pH-dependent membrane fusion and intracellular trafficking.

Knowledge about the role of GP-C in arenavirus assembly and budding is less clear and my dissertation research has contributed significantly in understanding concepts about membrane trafficking of GP-C that may underlie arenavirus assembly and budding. GP-C clusters into membrane microdomains on the plasma membrane (Fig. 30) and this pattern of membrane organization is independent of SSP myristoylation or co-expression of the matrix protein Z. The observation that Z is randomly distributed on the plasma membrane in correlation to GP-C, hints that arenavirus budding may be mediated by clustering of proteins and lipids on the plasma membrane. These clustering events may bring Z and GP-C together to form arenavirus budding sites, where interactions between Z and GP-C might allow the incorporation of GP-C into the budding virions. Biochemical evidence described in Chapter 5 argues that the GP-C on the plasma membrane possibly represents the molecular species found in detergent-soluble fractions of the cell lysates, arguing that lipid rafts are not involved in arenavirus assembly and budding. The development of a reverse genetic system (Fig. 33) where JUNV GP-C can substitute for LCMV GP-C in transduction of the luciferase reporter, introduces a good experimental platform to investigate genetic determinants in Junin GP-C that are essential for arenavirus morphogenesis and infectivity. In the absence of a homologous reverse-genetic system for Junin virus, studies described in my dissertation research are promising in use of this system to identify GP-C determinants for virion infectivity. This system will serve as a powerful genetic tool to tool to understand the role of GP-C in arenavirus life cycle.

Taken together, my dissertation research has identified several basic concepts about the structure-function of GP-C complex with particular emphasis on the role of SSP in biogenesis assembly and membrane trafficking of GP-C complex. Future studies will elucidate the determinants in the unusual cytoplasmic face of GP-C including SSP in arenavirus morphogenesis and entry.

Abbreviations

1. LCMV - Lymphocytic choriomeningitis virus
2. LAFV - Lassa fever virus
3. JUNV - Junin virus
4. OW - Old world
5. NW - New world
6. SSP - Stable signal peptide
7. GP-C - Junin virus glycoprotein complex
8. RDRP - RNA dependent RNA polymerase
9. MGLuc - Minigenome luciferase
10. VLPs - Virus-like particles

Bibliography

1. **Agnihothram, S. S., J. York, and J. H. Nunberg.** 2006. Role of the stable signal peptide and cytoplasmic domain of G2 in regulating intracellular transport of the Junin virus envelope glycoprotein complex. J Virol **80:**5189-98.
2. **Agnihothram, S. S., J. York, M. Trahey, and J. H. Nunberg.** 2007. Bitopic membrane topology of the stable signal peptide in the tripartite Junín virus GP-C envelope glycoprotein complex. J Virology **81:**4331-7.
3. **Ali, A., R. T. Avalos, E. Ponimaskin, and D. P. Nayak.** 2000. Influenza virus assembly: effect of influenza virus glycoproteins on the membrane association of M1 protein. J Virol **74:**8709-19.
4. **Ali, A., and D. P. Nayak.** 2000. Assembly of Sendai virus: M protein interacts with F and HN proteins and with the cytoplasmic tail and transmembrane domain of F protein. Virology **276:**289-303.
5. **Allison, S. L., J. Schalich, K. Stiasny, C. W. Mandl, C. Kunz, and F. X. Heinz.** 1995. Oligomeric rearrangement of tick-borne encephalitis virus envelope proteins induced by an acidic pH. J Virol **69:**695-700.
6. **Anderson, R. G., and K. Jacobson.** 2002. A role for lipid shells in targeting proteins to caveolae, rafts, and other lipid domains. Science **296:**1821-5.
7. **Awe, K., C. Lambert, and R. Prange.** 2008. Mammalian BiP controls posttranslational ER translocation of the hepatitis B virus large envelope protein. FEBS Lett **582:**3179-84.
8. **Balzarini, J.** 2007. Targeting the glycans of glycoproteins: a novel paradigm for antiviral therapy. Nat Rev Microbiol **5:**583-97.
9. **Bavari, S., C. M. Bosio, E. Wiegand, G. Ruthel, A. B. Will, T. W. Geisbert, M. Hevey, C. Schmaljohn, A. Schmaljohn, and M. J. Aman.** 2002. Lipid raft microdomains: a gateway for compartmentalized trafficking of Ebola and Marburg viruses. J Exp Med **195:**593-602.
10. **Beyer, W. R., D. Popplau, W. Garten, D. von Laer, and O. Lenz.** 2003. Endoproteolytic processing of the lymphocytic choriomeningitis virus glycoprotein by the subtilase SKI-1/S1P. J Virol **77:**2866-72.
11. **Bhattacharya, J., P. J. Peters, and P. R. Clapham.** 2004. Human immunodeficiency virus type 1 envelope glycoproteins that lack cytoplasmic domain cysteines: impact on association with membrane lipid rafts and incorporation onto budding virus particles. J Virol **78:**5500-6.
12. **Bhattacharya, J., A. Repik, and P. R. Clapham.** 2006. Gag regulates association of human immunodeficiency virus type 1 envelope with detergent-resistant membranes. J Virol **80:**5292-300.
13. **Blobel, G., P. Walter, C. N. Chang, B. M. Goldman, A. H. Erickson, and V. R. Lingappa.** 1979. Translocation of proteins across membranes: the signal hypothesis and beyond. Symp Soc Exp Biol **33:**9-36.
14. **Bolken, T. C., S. Laquerre, Y. Zhang, T. R. Bailey, D. C. Pevear, S. S. Kickner, L. E. Sperzel, K. F. Jones, T. K. Warren, S. Amanda Lund, D. L. Kirkwood-Watts, D. S. King, A. C. Shurtleff, M. C. Guttieri, Y. Deng, M. Bleam, and D. E. Hruby.** 2006. Identification and characterization of potent small molecule inhibitor of hemorrhagic fever New World arenaviruses. Antiviral Res **69:**86-9.
15. **Borrow, P., and M. B. A. Oldstone.** 1994. Mechanism of lymphocytic choriomeningitis virus entry into cells. Virology **198:**1-9.

16. **Brown, D. A., and E. London.** 1998. Functions of lipid rafts in biological membranes. Annu Rev Cell Dev Biol **14:**111-36.
17. **Brown, D. A., and E. London.** 1997. Structure of detergent-resistant membrane domains: does phase separation occur in biological membranes? Biochem Biophys Res Commun **240:**1-7.
18. **Brown, E. L., and D. S. Lyles.** 2003. A novel method for analysis of membrane microdomains: vesicular stomatitis virus glycoprotein microdomains change in size during infection, and those outside of budding sites resemble sites of virus budding. Virology **310:**343-58.
19. **Brown, M. S., and J. L. Goldstein.** 1999. A proteolytic pathway that controls the cholesterol content of membranes, cells, and blood. Proc Natl Acad Sci U S A **96:**11041-8.
20. **Buchmeier, M. J.** 2002. Arenaviruses: protein structure and function. Curr Top Microbiol Immunol **262:**159-73.
21. **Buchmeier, M. J., M. D. Bowen, and C. J. Peters.** 2001. Arenaviruses and their replication, p. 1635–1668. *In* D. M. Knipe and P. M. Howley (ed.), Fields Virology, vol. 2. Lippincott, Williams & Wilkins, Philadelphia.
22. **Burns, J. W., and M. J. Buchmeier.** 1991. Protein-protein interactions in lymphocytic choriomeningitis virus. Virology **183:**620-9.
23. **Candurra, N. A., and E. B. Damonte.** 1997. Effect of inhibitors of the intracellular exocytic pathway on glycoprotein processing and maturation of Junin virus. Arch Virol **142:**2179-93.
24. **Cao, W., M. D. Henry, P. Borrow, H. Yamada, J. H. Elder, E. V. Ravkov, S. T. Nichol, R. W. Compans, K. P. Campbell, and M. B. A. Oldstone.** 1998. Identification of alpha-dystroglycan as a receptor for lymphocytic choriomeningitis virus and Lassa fever virus. Science **282:**2079-81.
25. **Capul, A. A., M. Perez, E. Burke, S. Kunz, M. J. Buchmeier, and J. C. de la Torre.** 2007. Arenavirus Z-GP association requires Z myristoylation but not functional RING or L domains. J Virol **e print 20 June 2007**.
26. **Castilla, V., and S. E. Mersich.** 1996. Low-pH-induced fusion of Vero cells infected with Junin virus. Arch Virol **141:**1307-1317.
27. **Castilla, V., S. E. Mersich, N. A. Candurra, and E. B. Damonte.** 1994. The entry of Junin virus into Vero cells. Arch Virol **136:**363-74.
28. **Centers for Disease Control and Prevention.** 2005. Lymphocytic choriomeningitis virus infection in organ transplant recipients--Massachusetts, Rhode Island, 2005. MMWR Morb Mortal Wkly Rep **54:**537-9.
29. **Chazal, N., and D. Gerlier.** 2003. Virus entry, assembly, budding, and membrane rafts. Microbiol Mol Biol Rev **67:**226-37, table of contents.
30. **Chazal, N., and D. Gerlier.** 2003. Virus entry, assembly, budding, and membrane rafts. Microbiol Mol Biol Rev **67:**226-37.
31. **Chen, B. J., and R. A. Lamb.** 2008. Mechanisms for enveloped virus budding: can some viruses do without an ESCRT? Virology **372:**221-32.
32. **Chen, J., J. J. Skehel, and D. C. Wiley.** 1999. N- and C-terminal residues combine in the fusion-pH influenza hemagglutinin HA(2) subunit to form an N cap that terminates the triple-stranded coiled coil. Proc Natl Acad Sci U S A **96:**8967-72.
33. **Clegg, J. C. S.** 2002. Molecular phylogeny of the arenaviruses. Curr Top Microbiol Immunol **262:**1-24.

34. **Clegg, J. C. S., M. D. Bowen, M. J. Buchmeier, J.-P. Gonzalez, I. S. Lukashevich, C. J. Peters, R. Rico-Hesse, and V. Romanowski.** 2000. Arenaviridae, p. 633-40. *In* M. H. V. van Regenmortel, C. M. Fauquet, D. H. L. Bishop, E. B. Carstens, M. K. Estes, S. M. Lemon, J. Maniloff, M. A. Mayo, D. J. McGeoch, C. R. Pringle, and R. B. Wickner (ed.), Virus Taxonomy: Seventh Report of the International Committee on Taxonomy of Viruses. Academic Press, San Diego.
35. **Cocquerel, L., A. Op de Beeck, M. Lambot, J. Roussel, D. Delgrange, A. Pillez, C. Wychowski, F. Penin, and J. Dubuisson.** 2002. Topological changes in the transmembrane domains of hepatitis C virus envelope glycoproteins. EMBO J **21:**2893-902.
36. **Cornu, T. I., and J. C. de la Torre.** 2001. RING finger Z protein of lymphocytic choriomeningitis virus (LCMV) inhibits transcription and RNA replication of an LCMV S-segment minigenome. J Virol **75:**9415-26.
37. **de la Torre, J. C.** 2006. Reverse-genetic approaches to the study of Borna disease virus. Nat Rev Microbiol **4:**777-83.
38. **de la Torre, J. C.** 2008. Reverse genetics approaches to combat pathogenic arenaviruses. Antiviral Res.
39. **DeBose-Boyd, R. A., M. S. Brown, W. P. Li, A. Nohturfft, J. L. Goldstein, and P. J. Espenshade.** 1999. Transport-dependent proteolysis of SREBP: relocation of site-1 protease from Golgi to ER obviates the need for SREBP transport to Golgi. Cell **99:**703-12.
40. **Deen, K. C., J. S. McDougal, R. Inacker, G. Folena-Wasserman, J. Arthos, J. Rosenberg, P. J. Maddon, R. Axel, and R. W. Sweet.** 1988. A soluble form of CD4 (T4) protein inhibits AIDS virus infection. Nature **331:**82-84.
41. **Delgado, P., and B. Alarcon.** 2005. An orderly inactivation of intracellular retention signals controls surface expression of the T cell antigen receptor. J Exp Med **201:**555-66.
42. **Di Simone, C., and M. J. Buchmeier.** 1995. Kinetics and pH dependence of acid-induced structural changes in the lymphocytic choriomeningitis virus glycoprotein complex. Virology **209:**3-9.
43. **Di Simone, C., M. A. Zandonatti, and M. J. Buchmeier.** 1994. Acidic pH triggers LCMV membrane fusion activity and conformational change in the glycoprotein spike. Virology **198:**455-65.
44. **Dolganiuc, V., L. McGinnes, E. J. Luna, and T. G. Morrison.** 2003. Role of the cytoplasmic domain of the Newcastle disease virus fusion protein in association with lipid rafts. J Virol **77:**12968-79.
45. **Doms, R. W., R. A. Lamb, J. K. Rose, and A. Helenius.** 1993. Folding and assembly of viral membrane proteins. Virology **193:**545-6.
46. **Donzella, G. A., D. Schols, S. W. Lin, J. A. Este, K. A. Nagashima, P. J. Maddon, G. P. Allaway, T. P. Sakmar, G. Henson, E. De Clercq, and J. P. Moore.** 1998. AMD3100, a small molecule inhibitor of HIV-1 entry via the CXCR4 co-receptor. Nature Medicine **4:**72-7.
47. **Earp, L. J., S. E. Delos, H. E. Park, and J. M. White.** 2005. The many mechanisms of viral membrane fusion proteins, p. 25-66. *In* M. Marsh (ed.), Membrane Trafficking in Viral Replication, vol. 285. Springer Verlag, New York.
48. **Eckert, D. M., and P. S. Kim.** 2001. Mechanisms of viral membrane fusion and its inhibition. Annual Review of Biochemistry **70:**777-810.

49. **Eckert, D. M., V. N. Malashkevich, L. H. Hong, P. A. Carr, and P. S. Kim.** 1999. Inhibiting HIV-1 entry: discovery of D-peptide inhibitors that target the gp41 coiled-coil pocket. Cell **99:**103-115.
50. **Eichler, R., O. Lenz, T. Strecker, M. Eickmann, H. D. Klenk, and W. Garten.** 2003. Identification of Lassa virus glycoprotein signal peptide as a trans-acting maturation factor. EMBO Rep **4:**1084-8.
51. **Eichler, R., O. Lenz, T. Strecker, M. Eickmann, H. D. Klenk, and W. Garten.** 2004. Lassa virus glycoprotein signal peptide displays a novel topology with an extended ER-luminal region. J Biol Chem **279:**12293-9.
52. **Eichler, R., O. Lenz, T. Strecker, and W. Garten.** 2003. Signal peptide of Lassa virus glycoprotein GP-C exhibits an unusual length. FEBS Lett **538:**203-6.
53. **Elagoz, A., S. Benjannet, A. Mammarbassi, L. Wickham, and N. G. Seidah.** 2002. Biosynthesis and cellular trafficking of the convertase SKI-1/S1P: ectodomain shedding requires SKI-1 activity. J Biol Chem **277:**11265-75.
54. **Ellgaard, L., and A. Helenius.** 2003. Quality control in the endoplasmic reticulum. Nat Rev Mol Cell Biol **4:**181-91.
55. **Enjuanes, L., I. Sola, S. Alonso, D. Escors, and S. Zuniga.** 2005. Coronavirus reverse genetics and development of vectors for gene expression. Curr Top Microbiol Immunol **287:**161-97.
56. **Enria, D. A., A. M. Briggiler, N. J. Fernandez, S. C. Levis, and J. I. Maiztegui.** 1984. Importance of dose of neutralising antibodies in treatment of Argentine haemorrhagic fever with immune plasma. Lancet **2:**255-6.
57. **Eschli, B., K. Quirin, A. Wepf, J. Weber, R. Zinkernagel, and H. Hengartner.** 2006. Identification of an N-terminal trimeric coiled-coil core within arenavirus glycoprotein 2 permits assignment to class I viral fusion proteins. J Virol **80:**5897-907.
58. **Flanagan, M. L., J. Oldenburg, T. Reignier, N. Holt, G. A. Hamilton, V. K. Martin, and P. M. Cannon.** 2008. New world clade B arenaviruses can use transferrin receptor 1 (TfR1)-dependent and -independent entry pathways, and glycoproteins from human pathogenic strains are associated with the use of TfR1. J Virol **82:**938-48.
59. **Flatz, L., A. Bergthaler, J. C. de la Torre, and D. D. Pinschewer.** 2006. Recovery of an arenavirus entirely from RNA polymerase I/II-driven cDNA. Proc Natl Acad Sci U S A **103:**4663-8.
60. **Flatz, L., A. Bergthaler, J. C. de la Torre, and D. D. Pinschewer.** 2006. Recovery of an arenavirus entirely from RNA polymerase I/II-driven cDNA. Proc Natl Acad Sci U S A **103:**4663-8.
61. **Follis, K. E., S. J. Larson, M. Lu, and J. H. Nunberg.** 2002. Genetic evidence that interhelical packing interactions in the gp41 core are critical for transition to the fusion-active state of the HIV-1 envelope glycoprotein. J Virol **76:**7356-7362.
62. **Froeschke, M., M. Basler, M. Groettrup, and B. Dobberstein.** 2003. Long-lived signal peptide of lymphocytic choriomeningitis virus glycoprotein pGP-C. J Biol Chem **278:**41914-20.
63. **Fuerst, T. R., E. G. Niles, F. W. Studier, and B. Moss.** 1986. Eukaryotic transient-expression system based on recombinant vaccinia virus that synthesizes bacteriophage T7 RNA polymerase. Proc Natl Acad Sci U S A **83:**8122-6.
64. **Gallaher, W. R., C. DiSimone, and M. J. Buchmeier.** 2001. The viral transmembrane superfamily: possible divergence of Arenavirus and Filovirus glycoproteins from a common RNA virus ancestor. BMC Microbiol **1:**1.

65. **Garoff, H., R. Hewson, and D. J. Opstelten.** 1998. Virus maturation by budding. Microbiol Mol Biol Rev **62:**1171-90.
66. **Garoff, H., R. Hewson, and D. J. Opstelten.** 1998. Virus maturation by budding. Microbiol Mol Biol Rev **62:**1171-90.
67. **Gassmann, M., C. Haller, Y. Stoll, S. A. Aziz, B. Biermann, J. Mosbacher, K. Kaupmann, and B. Bettler.** 2005. The RXR-type endoplasmic reticulum-retention/retrieval signal of GABAB1 requires distant spacing from the membrane to function. Mol Pharmacol **68:**137-44.
68. **Gaudin, Y.** 2000. Reversibility in fusion protein conformational changes. The intriguing case of rhabdovirus-induced membrane fusion. Subcell Biochem **34:**379-408.
69. **Gerrard, S. R., and S. T. Nichol.** 2002. Characterization of the Golgi retention motif of Rift Valley fever virus G(N) glycoprotein. J Virol **76:**12200-10.
70. **Ghildyal, R., D. Li, I. Peroulis, B. Shields, P. G. Bardin, M. N. Teng, P. L. Collins, J. Meanger, and J. Mills.** 2005. Interaction between the respiratory syncytial virus G glycoprotein cytoplasmic domain and the matrix protein. J Gen Virol **86:**1879-84.
71. **Ghiringhelli, P. D., R. V. Rivera-Pomar, M. E. Lozano, O. Grau, and V. Romanowski.** 1991. Molecular organization of Junin virus S RNA: complete nucleotide sequence, relationship with other members of the Arenaviridae and unusual secondary structures. J Gen Virol **72:**2129-41.
72. **Gibbons, D. L., A. Ahn, P. K. Chatterjee, and M. Kielian.** 2000. Formation and characterization of the trimeric form of the fusion protein of Semliki Forest Virus. J Virol **74:**7772-80.
73. **Guo, Q., H.-T. Ho, I. Dicker, F. L, N. Zhou, J. Friborg, T. Wang, B. V. McAuliffe, H. G. Wang, R. E. Rose, H. Fang, H. T. Scarnati, D. R. Langley, N. A. Meanwell, R. Abraham, R. J. Colonno, and P. F. Lin.** 2003. Biochemical and genetic characterizations of a novel human immunodeficiency virus type 1 inhibitor that blocks gp120-CD4 interactions. J Virol **77:**10528-36.
74. **Haferkamp, S., L. Fernando, T. F. Schwarz, H. Feldmann, and R. Flick.** 2005. Intracellular localization of Crimean-Congo Hemorrhagic Fever (CCHF) virus glycoproteins. Virol J **2:**42.
75. **Han, X., J. H. Bushweller, D. S. Cafiso, and L. K. Tamm.** 2001. Membrane structure and fusion-triggering conformational change of the fusion domain from influenza hemagglutinin. Nat Struct Biol **8:**715-20.
76. **Hill, C. P., D. Worthylake, D. P. Bancroft, A. M. Christensen, and W. I. Sundquist.** 1996. Crystal structures of the trimeric human immunodeficiency virus type 1 matrix protein: implications for membrane association and assembly. Proc Natl Acad Sci U S A **93:**3099-104.
77. **Hobman, T. C., L. Woodward, and M. G. Farquhar.** 1992. The rubella virus E1 glycoprotein is arrested in a novel post-ER, pre-Golgi compartment. J Cell Biol **118:**795-811.
78. **Hruby, D. E., D. L. Lynn, and J. R. Kates.** 1980. Identification of a virus-specified protein in the nucleus of vaccinia virus-infected cells. J Gen Virol **47:**293-9.
79. **Hughson, F. M.** 1997. Enveloped viruses: a common mode of membrane fusion? Curr. Biol. **7:**R565-R569.
80. **Iapalucci, S., N. Lopez, O. Rey, M. M. Zakin, G. N. Cohen, and M. T. Franze-Fernandez.** 1989. The 5' region of Tacaribe virus L RNA encodes a protein with a potential metal binding domain. Virology **173:**357-61.

81. **Ji, H., C. Bracken, and M. Lu.** 2000. Buried polar interactions and conformational stability in the simian immunodeficiency virus (SIV) gp41 core. Biochemistry **39:**676-685.
82. **Kentsis, A., E. C. Dwyer, J. M. Perez, M. Sharma, A. Chen, Z. Q. Pan, and K. L. Borden.** 2001. The RING domains of the promyelocytic leukemia protein PML and the arenaviral protein Z repress translation by directly inhibiting translation initiation factor eIF4E. J Mol Biol **312:**609-23.
83. **Khalil, H., A. Brunet, I. Saba, R. Terra, R. P. Sekaly, and J. Thibodeau.** 2003. The MHC class II beta chain cytoplasmic tail overcomes the invariant chain p35-encoded endoplasmic reticulum retention signal. Int Immunol **15:**1249-63.
84. **Kielian, M.** 2006. Class II virus membrane fusion proteins. Virology **344:**38-47.
85. **Kielian, M., and F. A. Rey.** 2006. Virus membrane-fusion proteins: more than one way to make a hairpin. Nat Rev Microbiol **4:**67-76.
86. **Kilby, J. M., S. Hopkins, T. M. Venetta, B. DiMassimo, G. A. Cloud, J. Y. Lee, L. Alldredge, E. Hunter, D. Lambert, D. Bolognesi, T. Matthews, M. R. Johnson, M. A. Nowak, G. M. Shaw, and M. S. Saag.** 1998. Potent suppression of HIV-1 replication in humans by T-20, a peptide inhibitor of gp41-mediated virus entry. Nature Medicine **4:**1302-7.
87. **Kilby, J. M., J. P. Lalezari, J. J. Eron, M. Carlson, C. Cohen, R. C. Arduino, J. C. Goodgame, J. E. Gallant, P. Volberding, R. L. Murphy, F. Valentine, M. S. Saag, E. L. Nelson, P. R. Sista, and A. Dusek.** 2002. The safety, plasma pharmacokinetics, and antiviral activity of subcutaneous enfuvirtide (T-20), a peptide inhibitor of gp41-mediated virus fusion, in HIV-infected adults. AIDS Res Hum Retroviruses **18:**685-93.
88. **Kim, J.-S., and R. T. Raines.** 1993. Ribonuclease S-peptide as a carrier in fusion proteins. Protein Science **2:**348-356.
89. **Kostova, Z., Y. C. Tsai, and A. M. Weissman.** 2007. Ubiquitin ligases, critical mediators of endoplasmic reticulum-associated degradation. Semin Cell Dev Biol **18:**770-9.
90. **Kunz, S., K. H. Edelmann, J.-C. de la Torre, R. Gorney, and M. B. A. Oldstone.** 2003. Mechanisms for lymphocytic choriomeningitis virus glycoprotein cleavage, transport, and incorporation into virions. Virology **314:**168-78.
91. **Laliberte, J. P., L. W. McGinnes, M. E. Peeples, and T. G. Morrison.** 2006. Integrity of membrane lipid rafts is necessary for the ordered assembly and release of infectious Newcastle disease virus particles. J Virol **80:**10652-62.
92. **Lange, Y.** 1991. Disposition of intracellular cholesterol in human fibroblasts. J Lipid Res **32:**329-3.
93. **Lappin, D. F., G. W. Nakitare, J. W. Palfreyman, and R. M. Elliott.** 1994. Localization of Bunyamwera bunyavirus G1 glycoprotein to the Golgi requires association with G2 but not with NSm. J Gen Virol **75:**3441-51.
94. **Larson, R. A., D. Dai, V. T. Hosack, Y. Tan, T. C. Bolken, D. E. Hruby, and S. M. Amberg.** submitted. Identification of a broad-spectrum arenavirus entry inhibitor. JVI00941-08 Version 1.
95. **Lee, K. J., and J. C. de la Torre.** 2002. Reverse genetics of arenaviruses. Curr Top Microbiol Immunol **262:**175-93.
96. **Lee, K. J., M. Perez, D. D. Pinschewer, and J. C. de la Torre.** 2002. Identification of the lymphocytic choriomeningitis virus (LCMV) proteins required to rescue LCMV RNA analogs into LCMV-like particles. J Virol **76:**6393-7.
97. **Lee, M. C., E. A. Miller, J. Goldberg, L. Orci, and R. Schekman.** 2004. Bi-directional protein transport between the ER and Golgi. Annu Rev Cell Dev Biol **20:**87-123.

98. **Lenz, O., J. ter Meulen, H. Feldmann, H.-D. Klenk, and W. Garten.** 2000. Identification of a novel consensus sequence at the cleavage site of the Lassa virus glycoprotein. J Virol **74:**11418-21.
99. **Lenz, O., J. ter Meulen, H.-D. Klenk, N. G. Seidah, and W. Garten.** 2001. The Lassa virus glycoprotein precursor GP-C is proteolytically processed by subtilase SKI-1/S1P. Proc Natl Acad Sci U S A **98:**12701-5.
100. **Leser, G. P., and R. A. Lamb.** 2005. Influenza virus assembly and budding in raft-derived microdomains: a quantitative analysis of the surface distribution of HA, NA and M2 proteins. Virology **342:**215-2.
101. **Letourneur, F., S. Hennecke, C. Demolliere, and P. Cosson.** 1995. Steric masking of a dilysine endoplasmic reticulum retention motif during assembly of the human high affinity receptor for immunoglobulin E. J Cell Biol **129:**971-8.
102. **Li, F., and C. Wild.** 2005. HIV-1 assembly and budding as targets for drug discovery. Curr Opin Investig Drugs **6:**148-54.
103. **Li, X., and M. Donowitz.** 2008. Fractionation of subcellular membrane vesicles of epithelial and nonepithelial cells by OptiPrep density gradient ultracentrifugation. Methods Mol Biol **440:**97-110.
104. **Lindwasser, O. W., and M. D. Resh.** 2001. Multimerization of human immunodeficiency virus type 1 Gag promotes its localization to barges, raft-like membrane microdomains. J Virol **75:**7913-24.
105. **Linstedt, A. D., M. Foguet, M. Renz, H. P. Seelig, B. S. Glick, and H. P. Hauri.** 1995. A C-terminally-anchored Golgi protein is inserted into the endoplasmic reticulum and then transported to the Golgi apparatus. Proc Natl Acad Sci U S A **92:**5102-5.
106. **Linstedt, A. D., and H. P. Hauri.** 1993. Giantin, a novel conserved Golgi membrane protein containing a cytoplasmic domain of at least 350 kDa. Mol Biol Cell **4:**679-93.
107. **Lopez, N., and M. T. Franze-Fernandez.** 2007. A single stem-loop structure in Tacaribe arenavirus intergenic region is essential for transcription termination but is not required for a correct initiation of transcription and replication. Virus Res **124:**237-44.
108. **Lopez, N., R. Jacamo, and M. T. Franze-Fernandez.** 2001. Transcription and RNA replication of tacaribe virus genome and antigenome analogs require N and L proteins: Z protein is an inhibitor of these processes. J Virol **75:**12241-51.
109. **Lowen, A. C., A. Boyd, J. K. Fazakerley, and R. M. Elliott.** 2005. Attenuation of bunyavirus replication by rearrangement of viral coding and noncoding sequences. J Virol **79:**6940-6.
110. **Lu, Y., T. I. R, A. Bragin, K. Carveth, A. S. Verkman, and W. R. Skach.** 2000. Reorientation of aquaporin-1 topology during maturation in the endoplasmic reticulum. Mol Biol Cell **11:**2973-85.
111. **Lumb, K., and P. Kim.** 1995. A buried polar interaction imparts structural uniqueness in a designed heterodimeric coiled coil. Biochemistry **34:**8642-8.
112. **Luo, Z., and S. R. Weiss.** 1998. Roles in cell-to-cell fusion of two conserved hydrophobic regions in the murine coronavirus spike protein. Virology **244:**483-94.
113. **Maddon, P. J., A. G. Dalgleish, J. S. McDougal, P. R. Clapham, R. A. Weiss, and R. Axel.** 1986. The T4 gene encodes the AIDS virus receptor and is expressed in the immune system and the brain. Cell **47:**333-348.
114. **Margeta-Mitrovic, M.** 2002. Assembly-dependent trafficking assays in the detection of receptor-receptor interactions. Methods **27:**311-7.
115. **Margeta-Mitrovic, M., Y. N. Jan, and L. Y. Jan.** 2000. A trafficking checkpoint controls GABA(B) receptor heterodimerization. Neuron **27:**97-106.

116. **Martinez, M. G., S. M. Cordo, and N. A. Candurra.** 2008. Involvement of cytoskeleton in Junin virus entry. Virus Res.
117. **Martoglio, B., and B. Dobberstein.** 1998. Signal sequences: more than just greasy peptides. Trends in Cell Biology **8:**410-415.
118. **Marty, A., J. Meanger, J. Mills, B. Shields, and R. Ghildyal.** 2004. Association of matrix protein of respiratory syncytial virus with the host cell membrane of infected cells. Arch Virol **149:**199-210.
119. **McBride, C. E., J. Li, and C. E. Machamer.** 2007. The cytoplasmic tail of the severe acute respiratory syndrome coronavirus spike protein contains a novel endoplasmic reticulum retrieval signal that binds COPI and promotes interaction with membrane protein. J Virol **81:**2418-28.
120. **McCallus, D. E., K. E. Ugen, A. I. Sato, W. V. Williams, and D. B. Weiner.** 1992. Construction of a recombinant bacterial human CD4 expression system producing a bioactive CD4 molecule. Viral Immunol **5:**163-72.
121. **McCormick, J. B., and S. P. Fisher-Hoch.** 2002. Lassa fever. Curr Top Microbiol Immunol **262:**75-109.
122. **McCormick, J. B., P. A. Webb, J. W. Krebs, K. M. Johnson, and E. S. Smith.** 1987. A prospective study of the epidemiology and ecology of Lassa fever. J Infect Dis **155:**437-44.
123. **McGinnes, L. W., J. N. Reitter, K. Gravel, and T. G. Morrison.** 2003. Evidence for mixed membrane topology of the Newcastle disease virus fusion protein. J Virol **77:**1951-1963.
124. **Michelsen, K., H. Yuan, and B. Schwappach.** 2005. Hide and run. Arginine-based endoplasmic-reticulum-sorting motifs in the assembly of heteromultimeric membrane proteins. EMBO Rep **6:**717-22.
125. **Miyazaki, J., S. Takaki, K. Araki, F. Tashiro, A. Tominaga, K. Takatsu, and K. Yamamura.** 1989. Expression vector system based on the chicken beta-actin promoter directs efficient production of interleukin-5. Gene **79:**269-77.
126. **Monne, M., I. Nilsson, M. Johansson, N. Elmhed, and G. von Heijne.** 1998. Positively and negatively charged residues have different effects on the position in the membrane of a model transmembrane helix. J Mol Biol **284:**1177-83.
127. **Monto, A. S., D. P. Robinson, M. L. Herlocher, J. M. Hinson, Jr., M. J. Elliott, and A. Crisp.** 1999. Zanamivir in the prevention of influenza among healthy adults: a randomized controlled trial. Jama **282:**31-5.
128. **Murphy, F. A., P. A. Webb, K. M. Johnson, S. G. Whitfield, and W. A. Chappell.** 1970. Arenoviruses in Vero cells: ultrastructural studies. J Virol **6:**507-18.
129. **Muster, T., F. Steindl, M. Purtscher, A. Trkola, A. Klima, G. Himmler, F. Rüker, and H. Katinger.** 1993. A conserved neutralizing epitope on gp41 of human immunodeficiency virus type 1. J Virol **67:**6642-6647.
130. **Nakai, K., T. Okamoto, T. Kimura-Someya, K. Ishii, C. K. Lim, H. Tani, E. Matsuo, T. Abe, Y. Mori, T. Suzuki, T. Miyamura, J. H. Nunberg, K. Moriishi, and Y. Matsuura.** 2006. Oligomerization of Hepatitis C Virus Core Protein Is Crucial for Interaction with Cytoplasmic Domain of E1 Envelope Protein. J Virol **[Epub ahead of print]**.
131. **Nguyen, D. H., and J. E. Hildreth.** 2000. Evidence for budding of human immunodeficiency virus type 1 selectively from glycolipid-enriched membrane lipid rafts. J Virol **74:**3264-72.
132. **Nussbaum, O., C. C. Broder, and E. A. Berger.** 1994. Fusogenic mechanisms of enveloped–virus glycoproteins analyzed by a novel recombinant vaccinia virus-based assay quantitating cell fusion–dependent reporter gene activation. J Virol **68:**5411-22.

133. **Ono, A., and E. O. Freed.** 2001. Plasma membrane rafts play a critical role in HIV-1 assembly and release. Proc Natl Acad Sci U S A **98:**13925-30.
134. **Op De Beeck, A., and J. Dubuisson.** 2003. Topology of hepatitis C virus envelope glycoproteins. Rev Med Virol **13:**233-41.
135. **Oravecz, T., and M. A. Norcross.** 1993. Costimulatory properties of the human CD4 molecule: enhancement of CD3-induced T cell activation by human immunodeficiency virus type 1 through viral envelope glycoprotein gp120. AIDS Research and Human Retroviruses **9:**945-955.
136. **Ostapchuk, P., P. Hearing, and D. Ganem.** 1994. A dramatic shift in the transmembrane topology of a viral envelope glycoprotein accompanies hepatitis B viral morphogenesis. EMBO J **13:**1048-57.
137. **Ott, C. M., and V. R. Lingappa.** 2002. Integral membrane protein biosynthesis: why topology is hard to predict. J Cell Sci **115:**2003-9.
138. **Pantophlet, R., and D. R. Burton.** 2006. GP120: target for neutralizing HIV-1 antibodies. Annu Rev Immunol **24:**739-69.
139. **Perez, M., R. C. Craven, and J. C. de la Torre.** 2003. The small RING finger protein Z drives arenavirus budding: implications for antiviral strategies. Proc Natl Acad Sci U S A **100:**12978-83.
140. **Perez, M., R. C. Craven, and J. C. de la Torre.** 2003. The small RING finger protein Z drives arenavirus budding: implications for antiviral strategies. Proc Natl Acad Sci U S A **100:**12978-83.
141. **Perez, M., and J. C. de la Torre.** 2003. Characterization of the genomic promoter of the prototypic arenavirus lymphocytic choriomeningitis virus. J Virol **77:**1184-94.
142. **Perez, M., D. L. Greenwald, and J. C. de la Torre.** 2004. Myristoylation of the RING finger Z protein is essential for arenavirus budding. J Virol **78:**11443-8.
143. **Peters, C. J.** 2002. Human infection with arenaviruses in the Americas. Curr Top Microbiol Immunol **262:**65-74.
144. **Pollack, P., and J. R. Groothuis.** 2002. Development and use of palivizumab (Synagis): a passive immunoprophylactic agent for RSV. J Infect Chemother **8:**201-6.
145. **Qiu, Z., F. Tufaro, and S. Gillam.** 1995. Brefeldin A and monensin arrest cell surface expression of membrane glycoproteins and release of rubella virus. J Gen Virol **76 (Pt 4):**855-63.
146. **Quirin, K., B. Eschli, I. Scheu, L. Poort, J. Kartenbeck, and A. Helenius.** 2008. Lymphocytic choriomeningitis virus uses a novel endocytic pathway for infectious entry via late endosomes. Virology **378:**21-33.
147. **Radoshitzky, S. R., J. Abraham, C. F. Spiropoulou, J. H. Kuhn, D. Nguyen, W. Li, J. Nagel, P. J. Schmidt, J. H. Nunberg, N. C. Andrews, M. Farzan, and H. Choe.** 2007. Transferrin receptor 1 is a cellular receptor for New World haemorrhagic fever arenaviruses. Nature **446:**92-6.
148. **Radoshitzky, S. R., J. H. Kuhn, C. F. Spiropoulou, C. G. Albariño, D. P. Nguyen, J. Salazar-Bravo, T. Dorfman, A. S. Lee, E. Wang, S. R. Ross, H. Choe, and M. Farzan.** 2008. Receptor determinants of zoonotic transmission of New World hemorrhagic fever arenaviruses. Proc Natl Acad Sci U S A **105:**2664-9.
149. **Rawat, S. S., M. Viard, S. Gallo, A, A. Rein, R. Blumenthal, and A. Puri.** 2003. Modulation of entry of enveloped viruses by cholesterol and sphingolipids. Mol Membr Biol **20:**243-54.
150. **Resh, M. D.** 1999. Fatty acylation of proteins: new insights into membrane targeting of myristoylated and palmitoylated proteins. Biochim Biophys Acta **1451:**1-16.

151. **Rojek, J. M., A. B. Sanchez, N. T. Nguyen, J. C. de la Torre, and S. Kunz.** 2008. Different mechanisms of cell entry by human-pathogenic Old World and New World arenaviruses. J Virol **82:**7677-87.
152. **Salazar-Bravo, J., L. A. Ruedas, and T. L. Yates.** 2002. Mammalian reservoirs of arenaviruses. Curr Top Microbiol Immunol **262:**25-63.
153. **Sanchez, A., D. Y. Pifat, R. H. Kenyon, P. C. J, J. B. McCormick, and M. P. Kiley.** 1989. Junin virus monoclonal antibodies: characterization and cross-reactivity with other arenaviruses. J Gen Virol **70:**1125-32.
154. **Scheiffele, P., A. Rietveld, T. Wilk, and K. Simons.** 1999. Influenza viruses select ordered lipid domains during budding from the plasma membrane. J Biol Chem **274:**2038-44.
155. **Scott, M., G. Lu, M. Hallett, and D. Y. Thomas.** 2004. The Hera database and its use in the characterization of endoplasmic reticulum proteins. Bioinformatics **20:**937-44.
156. **Sha, B., and M. Luo.** 1997. Structure of a bifunctional membrane-RNA binding protein, influenza virus matrix protein M1. Nat Struct Biol **4:**239-44.
157. **Shi, X., D. F. Lappin, and R. M. Elliott.** 2004. Mapping the Golgi targeting and retention signal of Bunyamwera virus glycoproteins. J Virol **78:**10793-802.
158. **Shikano, S., and M. Li.** 2003. Membrane receptor trafficking: evidence of proximal and distal zones conferred by two independent endoplasmic reticulum localization signals. Proc Natl Acad Sci U S A **100:**5783-8.
159. **Simons, K., and E. Ikonen.** 1997. Functional rafts in cell membranes. Nature **387:**569-72.
160. **Smith, D. H., R. A. Byrn, S. A. Marsters, T. Gregory, J. E. Groopman, and D. J. Capon.** 1987. Blocking of HIV-1 infectivity by a soluble, secreted form of the CD4 antigen. Science **238:**1704-1707.
161. **Spiropoulou, C. F., S. Kunz, P. E. Rollin, K. P. Campbell, and M. B. A. Oldstone.** 2002. New World arenavirus clade C, but not clade A and B viruses, utilizes alpha-dystroglycan as its major receptor. J Virol **76:**5140-6.
162. **Stiasny, K., S. L. Allison, C. W. Mandl, and F. X. Heinz.** 2001. Role of metastability and acidic pH in membrane fusion by tick-borne encephalitis virus. J Virol **75:**7392-8.
163. **Stiegler, G., R. Kunert, M. Purtscher, S. Wolbank, R. Voglauer, F. Steindl, and H. Katinger.** 2001. A potent cross-clade neutralizing human monoclonal antibody against a novel epitope on gp41 of human immunodeficiency virus type 1. AIDS Res Hum Retroviruses **17:**1757-65.
164. **Strecker, T., R. Eichler, J. ter Meulen, W. Weissenhorn, K. H. D, W. Garten, and O. Lenz.** 2003. Lassa virus Z protein is a matrix protein and sufficient for the release of virus-like particle. J Virol **77:**10700-5.
165. **Strizki, J. M., S. Xu, N. E. Wagner, L. Wojcik, J. Liu, Y. Hou, M. Endres, A. Palani, S. Shapiro, J. W. Clader, W. J. Greenlee, J. R. Tagat, S. McCombie, K. Cox, A. B. Fawzi, C. C. Chou, C. Pugliese-Sivo, L. Davies, M. E. Moreno, D. D. Ho, A. Trkola, C. A. Stoddart, J. P. Moore, G. R. Reyes, and B. M. Baroudy.** 2001. SCH-C (SCH 351125), an orally bioavailable, small molecule antagonist of the chemokine receptor CCR5, is a potent inhibitor of HIV-1 infection in vitro and in vivo. Proc Natl Acad Sci U S A **98:**12718-23.
166. **Suomalainen, M.** 2002. Lipid rafts and assembly of enveloped viruses. Traffic **3:**705-9.
167. **Swinteck, B. D., and D. S. Lyles.** 2008. Plasma membrane microdomains containing vesicular stomatitis virus M protein are separate from microdomains containing G protein and nucleocapsids. J Virol **82:**5536-47.
168. **Tagawa, A., A. Mezzacasa, A. Hayer, A. Longatti, L. Pelkmans, and A. Helenius.** 2005. Assembly and trafficking of caveolar domains in the cell: caveolae as stable, cargo-triggered, vesicular transporters. J Cell Biol **170:**769-79.

169. **Takeda, M., G. P. Leser, C. J. Russell, and R. A. Lamb.** 2003. Influenza virus hemagglutinin concentrates in lipid raft microdomains for efficient viral fusion. Proc Natl Acad Sci U S A **100:**14610-7.
170. **Tam, R. C., J. Y. Lau, and Z. Hong.** 2001. Mechanisms of action of ribavirin in antiviral therapies. Antivir Chem Chemother **12:**261-72.
171. **Teasdale, R. D., and M. R. Jackson.** 1996. Signal-mediated sorting of membrane proteins between the endoplasmic reticulum and the golgi apparatus. Annu Rev Cell Dev Biol **12:**27-54.
172. **Thiel, V., and S. G. Siddell.** 2005. Reverse genetics of coronaviruses using vaccinia virus vectors. Curr Top Microbiol Immunol **287:**199-227.
173. **Thorp, E. B., J. A. Boscarino, H. L. Logan, J. T. Goletz, and T. M. Gallagher.** 2006. Palmitoylations on murine coronavirus spike proteins are essential for virion assembly and infectivity. J Virol **80:**1280-9.
174. **Vincent, S., D. Gerlier, and S. N. Manie.** 2000. Measles virus assembly within membrane rafts. J Virol **74:**9911-5.
175. **von Heijne, G.** 1985. Signal sequences. The limits of variation. J Mol Biol **184:**99-105.
176. **Wahlberg, J. M., R. Bron, J. Wilschut, and H. Garoff.** 1992. Membrane fusion of Semliki Forest virus involves homotrimers of the fusion protein. J Virol **66:**7309-18.
177. **Wahlberg, J. M., and H. Garoff.** 1992. Membrane fusion process of Semliki Forest virus. I: Low pH-induced rearrangement in spike protein quaternary structure precedes virus penetration into cells. J Cell Biol **116:**339-48.
178. **Weissenhorn, W., A. Dessen, L. J. Calder, S. C. Harrison, J. J. Skehel, and D. C. Wiley.** 1999. Structural basis for membrane fusion by enveloped viruses. Molecular Membrane Biology **16:**3-9.
179. **West, J. T., P. B. Johnston, S. R. Dubay, and E. Hunter.** 2001. Mutations within the putative membrane-spanning domain of the simian immunodeficiency virus transmembrane glycoprotein define the minimal requirements for fusion, incorporation, and infectivity. J Virol **75:**9601-12.
180. **Wharton, S. A., R. B. Belshe, J. J. Skehel, and A. J. Hay.** 1994. Role of virion M2 protein in influenza virus uncoating: specific reduction in the rate of membrane fusion between virus and liposomes by amantadine. J Gen Virol **75:**945-8.
181. **White, S. H., and G. von Heijne.** 2005. Transmembrane helices before, during, and after insertion. Curr Opin Struct Biol **15:**378-86.
182. **Wingfield, W. L., D. Pollack, and R. R. Grunert.** 1969. Therapeutic efficacy of amantadine HCl and rimantadine HCl in naturally occurring influenza A2 respiratory illness in man. N Engl J Med **281:**579-84.
183. **York, J., S. S. Agnihothram, V. Romanowski, and J. H. Nunberg.** 2005. Genetic analysis of heptad-repeat regions in the G2 fusion subunit of the Junin arenavirus envelope glycoprotein. Virology **343:**267-79.
184. **York, J., D. Dai, S. M. Amberg, and J. H. Nunberg.** 2008. pH-INDUCED ACTIVATION OF ARENAVIRUS MEMBRANE FUSION IS ANTAGONIZED BY SMALL-MOLECULE INHIBITORS. J Virol.
185. **York, J., and J. H. Nunberg.** 2006. Distinct requirements for signal peptidase processing and function of the stable signal peptide (SSP) subunit in the Junin virus envelope glycoprotein. Virology **in press**.
186. **York, J., and J. H. Nunberg.** 2004. Role of hydrophobic residues in the central ectodomain of gp41 in maintaining the association between HIV-1 envelope glycoprotein subunits gp120 and gp41. J Virol **78:**4921-26.

187. **York, J., and J. H. Nunberg.** 2006. Role of the stable signal peptide of the Junín arenavirus envelope glycoprotein in pH-dependent membrane fusion. J Virol **80:**7775-80.
188. **York, J., V. Romanowski, M. Lu, and J. H. Nunberg.** 2004. The signal peptide of the Junín arenavirus envelope glycoprotein is myristoylated and forms an essential subunit of the mature G1-G2 complex. J Virol **78:**10783-92.
189. **Zerangue, N., M. J. Malan, S. R. Fried, P. F. Dazin, Y. N. Jan, L. Y. Jan, and B. Schwappach.** 2001. Analysis of endoplasmic reticulum trafficking signals by combinatorial screening in mammalian cells. Proc Natl Acad Sci U S A **98:**2431-6.
190. **Zerangue, N., B. Schwappach, Y. N. Jan, and L. Y. Jan.** 1999. A new ER trafficking signal regulates the subunit stoichiometry of plasma membrane K(ATP) channels. Neuron **22:**537-48.
191. **Zwick, M. B., A. F. Labrijn, M. Wang, C. Spenlehauer, E. O. Saphire, J. M. Binley, J. P. Moore, G. Stiegler, H. Katinger, D. R. Burton, and P. W. Parren.** 2001. Broadly neutralizing antibodies targeted to the membrane-proximal external region of human immunodeficiency virus type 1 glycoprotein gp41. J Virol **75:**10892-10905.